EROSION RATES IN AND AROUND SHENANDOAH NATIONAL PARK, VA, DETERMINED USING ANALYSIS OF COSMOGENIC ^{10}BE

A Masters Thesis Presented

by

Jane Duxbury

to

The Faculty of the Graduate College

of

The University of Vermont

In Partial Fulfillment of the Requirements
for the Degree of Master of Science
Specializing in Geology

February, 2009

Accepted by the Faculty of the Graduate College, The University of Vermont, in partial fulfillment of the requirements for the degree of Master of Science, specializing in Geology.

Thesis Examination Committee:

_____ **Advisor**
Paul R. Bierman, Ph.D.

_____
Gregory Druschel, Ph.D.

_____ **Chairperson**
John Aleong, Ph. D.

_____ **Vice President for Research**
Frances E. Carr, Ph. D   **and Dean of Graduate Studies**

Date: September 5, 2008

Abstract

We use cosmogenic [10]Be analysis of fluvial sediments and bedrock to estimate erosion rates (10^3 – 10^6 year timescale) and to infer the distribution of post-orogenic geomorphic processes in the Blue Ridge Province in and around Shenandoah National Park, VA. Our sampling plan was designed to investigate relationships between erosion rate, lithology, slope, and basin area. Fifty-nine samples were collected from a variety of basin sizes (<1 – 3351 km^2) and average basin slopes (7 - 26°) in each of four different lithologies that crop out in the Park: granite, metabasalt, quartzite, and siliciclastic rocks. The samples include bedrock (n = 5), fluvial sediment from single-lithology basins (n = 43), and fluvial sediment from multilithology basins (n = 11): two of these samples are from rivers draining streams exiting the eastern and western slopes of the Park (Rappahannock and Shenandoah Rivers).

Inferred erosion rates for all lithologies for fluvial samples range from 3.8 to 24 m/My. The mean erosion rate for single-lithology basins in the Park is 11.6 ± 4.8 m/My. Single-lithology erosion rates ranges for fluvial samples are: granite (basin size = ~0.4-40 km^2 and slope = 11-23°), 7.9–22 m/My; metabasalt (basin size = ~1-25 km^2 and slope = 11-19°), 4.8–24 m/My; quartzite (basin size = ~0.1-9 km^2 and slope = 12-23°), 4.7–17 m/My; and siliciclastic rocks (basin size = ~0.3-13 km^2 and slope = 18-26°), 6.2–17 m/My. The mean erosion rate for multilithology basins (basin size = ~1-3351 km^2 and slope = 7-22°) is 10.2 m/My, and individually for the Shenandoah River 7.3 m/My and the Rappahannock River 13.8 m/My. Bedrock erosion rates range from 2.4-13 m/My across all lithologies, with a mean erosion rate of 7.9 ± 5.0 m/My. Grain-size specific [10]Be analysis of four samples showed no consistent trend of concentration with grain size.

These data support Hack's *dynamic equilibrium* model. Slope and erosion rate are not well correlated, and mean erosion rates are similar for different lithologies. Cosmogenically-determined erosion rates in Shenandoah Park are similar to or lower than those reported elsewhere in the Appalachians including those of Matmon and others (2003), 25 to 30 m/My for metaclastic rocks in the steep Great Smoky Mountains, Reuter and others (2004), 4 – 54 m/My in Susquehanna River basin for shale, sandstone, and schist, and Sullivan and others (2006), 6-38 m/My in the micaceous schist and gneiss of the Blue Ridge Escarpment. Cosmogenic erosion rates (integration over 10^4 yrs) in the Blue Ridge province of Shenandoah National Park are consistent with long-term unroofing rates (integration over 10^7 yrs) estimated from U-Th/He measurements (11-18 m/My) in samples collected near the Blue Ridge Escarpment by Spotila and others (2004), and fission tracks (20 m/My) in the Appalachians by Naeser and others (2005). The consistency of denudation rates integrated over very different periods of time suggests steady erosion most likely in balance with, and driving isostatic uplift of rock.

Citation

**Material for this thesis has been submitted for publication to
American Journal of Science on June 12, 2008 in the following form:**

Duxbury, J., Bierman, P. R., Larsen, J., Pavich, M. J., Southworth, S., Miguéns-
Rodríguez, M. and Freeman,S. Erosion Rates in and Around Shenandoah National Park,
Va, Determined Using Analysis of Cosmogenic ^{10}Be. American Journal of Science.

Acknowledgements

Many thanks to all my very dear friends who have supported my through the last three years of this journey: Billy Best, Karen Thompson, Judith Moman, Caroline Shanti and Elizabeth Brassil.

My last big thanks go to my son Dashiell, who presence in my life kept me motivated towards completion.

Table Of Contents

List Of Tables

Chapter 4

List Of Figures

Chapter 4

Chapter 1 – Introduction

Understanding the dynamic nature of the Earth's surface, the form of the land surface, the processes that create it and how the landscape has changed over time are fundamental to geomorphology. Geomorphologists have sought to understand the relationships between erosion rates (both physical and chemical, e.g. Riebe and others, 2001b, 2003), and climate (Harris and Mix, 2002), as well as topography and lithology (Hack, 1960). The Appalachian Mountains have been the subject of intense study because of the interest in understanding the geomorphic processes that occur in mountain ranges following the cessation of orogenic events (Miller and Duddy, 1989; Pazzaglia and Brandon, 1996; Granger and others, 1997; Naeser and others, 2001, 2005; Matmon and others, 2003a, 2003b; Reuter and others, 2003, 2004, 2005; Morgan and others, 2004; Hancock and Kirwin, 2007). Of particular interest in the Appalachian Mountains is the paradox that exists in the continued existence of mountainous topography hundreds of millions of years after orogenic events ceased (Pazzaglia and Brandon, 1996).

In the context of these previous studies, this research investigates millennial scale erosion rates in the vicinity of the Blue Ridge Province in the Shenandoah National Park, Virginia. I estimate such rates over the $10^3 - 10^5$ timescale using 59 ^{10}Be cosmogenic measurements derived from fluvial sediments and bedrock. The spatial scale of my study corresponds to the areas of the sampled drainage basins, the sizes of which are constrained by lithology and the morphology of the range to 0.3 - 3351 km^2.

Motivation and Objectives

The data presented in this thesis represent [10]Be derived erosion rates from 54 drainage basins, underlain by the four lithologies present in or adjacent to the Shenandoah National Park. This sediment was collected from outcrops and basins draining the four predominant lithologies in and around the Park (granite, metabasalt, quartzite, and siliciclastic rocks). These erosion rates characterize landscape transformation of the Blue Ridge over the $10^3 - 10^5$ timescale; thus, my data provide insight into the recent evolution of the Appalachian Mountains. In concert with thermochronologic data sets, my new cosmogenic data allow an improved understanding of erosion since the cessation of orogenic events (Ahnert, 1970; Baldwin and others, 2003). This study examines the relationship between erosion rate, lithology, slope, and basin area via the erosion rates derived from [10]Be measurements made in samples of fluvial sediment and bedrock. I use the data to consider Hack's (1960) model of *dynamic equilibrium* and steady state behavior, which predicts that erosion rates should be independent of lithology; less resistant lithologies will have shallow slopes and more resistant lithologies will have steeper slopes, but all will erode at similar rates. As was considered in the research of Matmon and others, (2003a, 2003b), Brown and others, (1995) and Clapp and others, (1997, 1998, 2001, 2002), this study also investigated the relationship between [10]Be concentrations and grain size. Analysis of different sediment grain sizes is important because erosion rates are directly calculated from the concentration of [10]Be in sediment. If nuclide concentration consistently differs between grain sizes, then one needs to examine the active geomorphic processes that determine

how the sediments are dosed by cosmic rays as they are being transported downslope and downstream. Motivated by the issues considered above, the primary objectives of my study are:

➢ To determine whether average erosion rates differ between the four lithologies cropping out in the Blue Ridge province within the Shenandoah National Park.

➢ To explore the relationships between erosion rates and slope so as to test Hack's (1960) inference of *dynamic equilibrium* and steady state behavior.

➢ To compare the relationships between [10]Be-based erosion rates and slope, basin area and lithology with other Appalachian Mountain range studies such as Matmon and others, (2003a, 2003b); Reuter and others, (Reuter, 2005a); and Sullivan and others, (accepted).

➢ To examine the relationship between [10]Be concentration and grain size in the context of previous research by Matmon and others, (2003b), Brown and others, (1995), Clapp and others (1997, 1998, 2001, 2002), and Sullivan and others (accepted).

Thesis Structure

My research will be presented as a journal-style thesis containing a paper for publication and additional chapters that provide supporting information. A comprehensive literature review is contained within Chapter 2 and includes a survey of pertinent research relating to the use of cosmogenic isotopes to study erosion rates by the analysis of fluvial sediments, weathering as a function of lithology and climate, and structural and tectonic influences on the Shenandoah National Park. Chapter 3 includes a detailed account of the methods used in this study including sampling strategy, field

techniques and analytical procedures. Chapter 4 is a journal article that has been

submitted to the American Journal of Science entitled, *Erosion Rates in and Around*

Shenandoah National Park, Va, Determined Using Analysis of Cosmogenic ^{10}Be.

Chapter 5 contains my conclusions of my research and recommendations for future work.

Chapter 2 – Background and Literature Review

Appalachian Mountain Physiography

The Appalachian Mountain belt stretches from Newfoundland, Canada in the northeast, southwest to Alabama (Rodgers, 1970). The belt is divided into five physiographic provinces: the Coastal Plain, the Piedmont, the Blue Ridge, the Valley and Ridge, and the Appalachian Plateau. The mountain belt was formed in the early Paleozoic Era when a change in plate motion and tectonic setting, from passive plate margin to convergent boundary, set the stage for formation of the proto-Appalachian Mountains. With this transition in plate tectonic setting, the oceanic edge of the Afro-European plate was subducted underneath the North American craton, followed by the continent-to-continent collision of the two plates, which began the formation of the supercontinent Pangaea (Rodgers, 1970).

This convergence spurred a series of orogenic events (Taconic, Acadian and Allegheny) that resulted in the deformation of Paleozoic and Precambrian basement rocks and the formation of the Appalachian Mountains (Rodgers, 1970). The Taconic orogeny, which began in the Ordovician period, represents terrane collisions with North America and is noted for the thrusting and faulting that occurred mainly in the northern portion of the Appalachians (Pavlides and others, 1968). The Devonian-period Acadian orogeny occurred with the closing of the Iapetus Ocean, as the Afro-European plate was thrust up and sutured onto the North American craton (Harris and others, 1990). This orogenic event was centered in New England and southern New York and included thrusting, folding, metamorphism and granitic intrusions. The Allegheny orogeny occurred in the

southern Appalachians during the Pennsylvanian period, and was characterized by folding, thrusting, metamorphism, and intrusions from Pennsylvania south to Alabama.

Shenandoah National Park Physiography

The Shenandoah National Park is situated within the Blue Ridge Mountains between Fort Royal in the north and Rockfish Gap in the south, near Waynesboro, VA (Gathright, 1976). The park covers an area of ~780 km^2 through parts of eight counties, is approximately 110 km in length, and varies between 5 and 10 km in width. The highest point of the Blue Ridge Mountains within the Park boundary is Hawksbill, which stands 1,235 m high above the low-lying Piedmont Province to the East and the Shenandoah Valley to the west (Kiver and others, 1999). The Potomac River crosses the Blue Ridge to the north at Harpers Ferry, and the James and Roanoke Rivers cross to the south. There are also two wind gaps, Thornton and Powell, which mark the path of ancient stream courses (Kiver and others, 1999). Mountaintops and slopes within the Park are heavily vegetated and soil covered.

Climate in Virginia is influenced by three landscape controls. Firstly, the Gulf Stream has a dominant effect on Virginia's precipitation regime. Winter storms tend to track from the west and when in proximity with the coast and the Gulf Stream move northeast, following the boundary between the cold land and the warmth of the Gulf Stream waters. Storms grow rapidly as they cross the coast, and as they track north eastwards, the moisture-laden air precipitates on the eastern slopes and foothills of the

Blue Ridge Mountains.[1]

The climate is also controlled by the high relief of the western Appalachian provinces (Valley and Ridge, Appalachian Plateau) and the Blue Ridge in the context of the Park. A well-developed rainfall pattern can be observed in the Blue Ridge Mountains, whereby as air flows from the east, precipitation is concentrated on the eastern slopes and the western slopes and valleys are in a "rain shadow."[1] When air flows from the west the Shenandoah Valley and the western slopes of the Shenandoah National Park are in the "rain shadow" of the western Appalachian provinces.

Third, there is local control on climate due to the complex systems of rivers that drain the precipitation and alter the pattern of moist airflow. Moist air travels up rivers valleys such as the Rappahannock River bringing precipitation to the eastern slopes of the Blue Ridge.[2] These landscapes controls on climate ensure that northeast-tracking winter storms bring heavy snowfall and ice storms to the Park. Thunderstorms, which can focus on the high terrain, reach a peak in September. Storms and significant run-off can occur year round with precipitation in the park averaging 100 – 150 cm per annum.[3] The mountains in Shenandoah National Park are usually ~6 °C cooler than the valley below, whilst a modified continental climate, with mild winters and warm, humid summers is experienced at lower elevation areas of the Park. The average annual precipitation at Big Meadows is 132 cm, including ~94 cm of snow. At Luray in the lowland area, the mean annual temperature averages 12 °C, and average annual precipitation is 91 cm, with about

---

[1] http://www.climate.virginia.edu/description.htm, accessed 6/14/07.
[2] http://www.climate.virginia.edu/description.htm, accessed 6/14/07.
[3] http://www.nps.gov/shen/pphtml/subenvironmentalfactors21.html, accessed 6/14/07.

43 cm of snow.[3]

The Blue Ridge Mountains are the northward plunging, western limb of an anticlinorium, which was formed as the result of the suturing of the Blue Ridge terrane onto the North American craton during the Taconic orogeny (Morgan and others, 2004). The core of the anticline is composed of igneous, metamorphic, and sedimentary rocks. The end of the Paleozoic Era completed the main faulting and folding connected with the Appalachians. Major thrusting was a feature of the Alleghenian orogeny in the late Paleozoic, when the crystalline rocks of the Blue Ridge were thrust westward over younger sedimentary rocks, creating a linear feature, an overturned anticline. The broad regional area of the Blue Ridge experienced uplift, arching and erosion, which supplied sediment to adjacent Mesozoic basins. The Blue Ridge may have been eroded to near sea level during this period (Morgan and others, 2004).

There are four principal rock types within the Shenandoah National Park: granite, metabasalt, quartzite, and siliciclastic rocks. These rock types are represented by a variety of units of different ages: Precambrian - Old Rag Granite, the Pedlar Formation (granodiorite), Swift Run Formation (quartzites, conglomerates and siliceous slates), the Catoctin Formation (flood basalt); Cambrian – the Chilhowee Group composed of the Weverton Formation (conglomerate, sandstone and phyllite), the Hampton (Harpers) Formation (phyllite) and the Erwin (Antietam) Formation (quartzite) (Gathright, 1976). These are all overlain by lower Cambrian Tomstown Dolomite (Morgan and others, 2004).

---

[3] http://www.nps.gov/shen/pphtml/subenvironmentalfactors21.html, accessed 6/14/07.

Understanding the evolution of mountain belts – techniques for estimating erosion rates

There are currently several techniques that allow an understanding of landscape change through quantification of erosion rates and sediment export. These techniques include cosmogenic nuclides, thermochronology and sediment yields measured over different time-scales.

Sediment yield data allow the assessment of contemporary sediment mobility using geomorphic tools such as sediment traps and stream flow monitoring measuring stations (Gellis and others, 2004). These direct measures of sediment flux are only usually applicable or available over yearly to decadal timescales (Kirchner and others, 2001). Trimble (1977) and Kirchner and others, (2001) suggest that interpreting sediment fluxes as erosion rates, even over the short-term is fraught with difficulties. Trimble, in his study of 10 large drainage basins in the southeastern United States, suggests that sediments yields are not adequate proxies for denudation rates because of the mismatch between upland erosional processes and sediment yield measurements due to storage of sediment in rivers. He also suggests that southeastern U.S. streams and rivers have not been in steady state since European settlement, thus equating denudation rates derived from sediment yields with a rate of erosion is a misnomer. Kirchner and others research, comparing short-term sediment fluxes with long-term sediment generation rates via cosmogenic ^{10}Be and apatite fission track analysis suggests that in the Idaho batholith, short-term sediment yield measurements grossly underestimate long-term average rates of sediment delivery. Both Trimble and Kirchner and others research suggests that due to processes of sediment storage there is the potential in some places for

9

a disconnect in timescales between erosion (long-term sediment generation rates) and short-term sediment loads.

Pazzaglia and Brandon (1996) utilized a different technique to estimate sediment yields or offshore sediment flux, via deconvolution of the offshore sedimentary record at Baltimore Canyon Trough (BCT), in order to understand the post-Triassic geomorphic evolution of the Appalachian Mountains. Offshore cores collected in the BCT provide a robust offshore sedimentary record from which to reconstruct the central/northern Appalachian landscape by restoring denuded sediments back to the originating drainages. This was achieved via an elevation-dependent mechanical erosion law where the mean rate of mechanical erosion is proportional to the mean elevation above any given base level. This erosional law was used to evaluate a model that could best describe the geomorphic evolution of the Appalachians.

Thermochronology allows the estimate of the rates at which deeply buried rocks approach the surface as exhumation proceeds (Reiners and Brandon, 2006). Noble gas and fission-track thermochronometric systems have a range of closure temperatures, which make them sensitive to exhumation through a range of crustal depths (1 -10 km, Reiners and Brandon, 2006). Knowing the geothermal gradient and the closure temperature sets a beginning point from which to calculate erosion/unroofing rates. An erosion rate can be calculated because the depth of unroofing can be estimated by assuming a geothermal gradient, and time since passing the closure isotherm can be measured. Three thermochronological methods currently in use include $^{40}Ar/^{39}Ar$, (U-Th)/He, and fission-track (FT) dating. These techniques are based on thermally

controlled retention of nuclear decay products such as isotopes or radiation damage and are normally integrated over a time scale of $10^5 - 10^8$ years (Reiners, 2002).

$^{40}Ar/^{39}Ar$ ages are determined by gas source mass spectrometry, and are based on the decay rate of ^{40}K to radiogenic ^{40}Ar (McDougall and Harrison, 1988). (U-Th)/He dating is based on the accumulation of ^4He by the α decay of Uranium and Thorium (Reiners, 2002). Apatite, titanite and zircon are common minerals used in the (U-Th)/He dating technique. Fission-tracks occur as the spontaneous fission of ^{238}U atoms causes highly charged nuclei to create zones of damage in a crystal (Reiners, 2002). The age of a mineral, or the time the mineral crossed the closure isotherm at some depth below Earth's surface, can be determined by quantifying uranium content and by counting the increase in the number of tracks over time (Naeser and others, 2005). The primary uncertainties in such calculations are a lack of detailed knowledge of the P-T-t paths of the analyzed rocks and minerals as well as paleogeothermal gradients.

Cosmogenic isotopes produced in near-surface rock and sediment, primarily ^{10}Be and ^{26}Al, have been used to estimate rates of rock erosion (e.g. Nishiizumi and others, 1986; Small and others, 1997; Kirwan, 2002a, 2002b; Phillips and others, 2006; Hancock and others, 2007) and sediment generation (Brown and others, 1995; Bierman and others, 1996; Granger and others, 1996) for two decades. When the measured concentrations of these isotopes are interpreted using steady-state models, the resulting information suggests the rate at which the landscape has changed over timescales of 10^3 to 10^5 years (Bierman and others, 2004).

Of specific utility for this study is the cosmogenic isotope [10]Be because it is the longest-lived of the radioactive isotopes and is easily measured in quartz (Bierman and others, 2002). [10]Be measured in quartz is commonly applied as a geomorphic tracer because quartz is widely distributed on Earth's surface and can separated with relative ease from other minerals because of its low reactivity with most acids (Kohl and others, 1992).

[10]Be is produced *in situ* as a result of spallation, the splitting of target nuclei by incoming, high-energy, fast cosmic ray neutrons (Bierman, 1994; Lal, 1998). The nuclear transformations caused by the interaction of cosmic rays with minerals within rock attenuate with depth and therefore [10]Be concentrations in rock decrease exponentially with depth. The abundance of *in situ* produced [10]Be in rocks is proportional to the amount of time the rock has been at or near the Earth's surface. Nuclide concentrations in rock are also dependent and on latitude and altitude (Nishiizumi and others, 1989). The utility of [10]Be-derived erosion rates is that they are averaged over long enough timescales to allow interpretations of geomorphic change.

Lal and Peters (1967) first suggested that [10]Be could be a functional label for sediment transport processes and erosion because of its physical and chemical properties. In this context then, [10]Be can be used to estimate erosion rates in two different materials: in sediment (Bierman & Steig, 1996, Brown and others, 1995, Granger and others, 1996) or rock (Nishiizumi and others, 1989, Bierman and others, 1999, Bierman and Caffee, 2001, 2002). In eroding landscapes, as rock that is transitioning to sediment approaches the surface, it is accumulating [10]Be. In simple terms when utilizing [10]Be in sediment to

estimate erosion rates, quartz grains in basins that are eroding slowly have a high concentration of ^{10}Be because they have been exposed to cosmic-ray bombardment longer than quartz grains in rapidly eroding basins from which regolith is rapidly removed. Sediment gathered in streams is therefore an averager of ^{10}Be concentration and sediment production for a whole basin, rather than for a particular point on the landscape as are bedrock samples.

For estimating erosion rates for bedrock, samples collected from large, flat lying surfaces afford the easiest interpretation (Bierman and Caffee, 1994, 2001; Gosse and others, 1995). Calculation of neutron fluxes is necessary in surfaces that are spherical or not flat lying (Bierman, 1994). For the purpose of modeling erosion rates from ^{10}Be concentrations for bedrock, cosmogenic nuclide production rates are dependent on latitude and altitude (Nishiizumi and others, 1989); thus, correction schemes have been developed (Lal, 1991; Lifton, 2000; Desilets and Zreda, 2000; Dunai, 2000) .

Several assumptions underlie the translation of measured isotopic abundances into erosion rates via conceptual and mathematical models (Bierman, 1994). For both sediment and bedrock it is assumed that the cosmic ray flux (and thus nuclide production rates) is constant over time (the concentration of cosmogenic nuclides within surficial rock is related to the time over which the surface was exposed, convolved with the intensity of cosmic-ray dosing); there is no inheritance from prior cosmogenic dosing; no shielding from soil, snow, water or vegetation; the system is in steady state (isotopic equilibrium within basins for sediments and underlying rock column for bedrock (Bierman and Nichols, 2004); and that the nuclide production rate is known.

Appalachian Climate and Erosion

Although the role of climate, and in particular the role of precipitation, remains uncertain with regards to erosion rates, some links have been established between precipitation and weathering/erosion (Kneller and Peteet, 1999; Reiners and others, 2003; Bookhagen and others, 2005). In the context of this research it is reasonable to investigate the paleoclimate of the Appalachian Mountains in order to understand the role that climate has in the weathering of the rocks within the Shenandoah National Park. Initially I will discuss the role/effects of climate in the Appalachian Mountain Belt and then more specifically address the issues of weathering with regards to the four main lithologies found within the Park boundaries (granite, quartzite, metabasalt, and siliciclastic rocks).

Climate and Geography

The geomorphic evolution of the Appalachian Mountains reflects interactions between drainage evolution, climate and tectonics (Barron, 1989). A large role in the geomorphic evolution of the Appalachians has been attributed to tectonics (Gardner, 1989; Poag and Sevon, 1989; Slingerland and Furlong, 1989; Gilchrist and Summerfield, 1991; Pazzaglia and Gardner, 1994; Pazzaglia and Brandon, 1996; Bishop, 2007) and a lesser one to climate. Many studies have sought to point out the importance of climate change when considering the geomorphic evolution of mountain ranges (Parrish and Curtis, 1982; Parrish and others, 1982; Barron, 1989; Barron and Washington, 1982, 1984; Delcort and Delcourt, 1984; Kutzbach and others, 1998; Bard, 2003; Leigh and Webb, 2006; Hebbeln and others, 2007). The relationship of climate to Appalachian

geomorphology and hence erosion rates can be divided into two categories; long-term and short-term climate change.

Regionally, climate is influenced by global circulation patterns, proximity to moisture sources and topography. Reconstructions of climate during the Late Carboniferous to Late Permian by Parrish and others, (1982) envisioned the Appalachian Mountains as part of the super continent Pangaea, positioned at latitudes between the equator and 15° S. This climate reconstruction presents high pressure in the southern hemisphere during winter (arid), transitioning to low pressure in the summer (increasing precipitation).

During the late Permian, the climate transitioned to a pattern of seasonally wet conditions on the eastern margin of the Appalachians, which was curtailed by the early Mesozoic due to the northward movement of Pangaea to a latitude of ~15° N, where the Appalachian climate became subtropical and arid (Parrish and Curtis, 1982). The rifting of Pangaea, beginning in the Jurassic, placed a large moisture source adjacent to the Appalachian Mountain Belt and initiated the formation of a new paleogeographic configuration, which was dominated by the Tethys, a zonal subtropical ocean bordered by a North American-Greenland-Eurasia continent, within the subtropics (Barron, 1989).

A series of general Circulation Model experiments by Barron and Washington (1982, 1984) suggest that during the Cretaceous the zonal nature of the Tethys encouraged geographically influenced regions of high precipitation on its northern (Appalachians) and southern margins during the winter months. The models of Parrish and Curtis (1982) also support the idea of increased precipitation over the Appalachian

Mountains specifically and the northern hemisphere generally during the Cretaceous. This is evidenced by the abundance of northern hemisphere bauxites, kaolinites, smectities and extensive coal formation (Tourtelot, 1983; Chamley, 1989; Beeson, 1984; Hallam, 1985). The Appalachian Mountains remained at a latitude of ~ 40° N from the late Cretaceous to present, with the main geographic changes being a decrease in eustatic sea level and the development of the Atlantic Ocean.

Ice advances into the Appalachian Mountains, grossly equivalent to the late Wisconsinin glacial period, have been documented via marine ^{18}O records beginning in the Pliocene ~2.4 Ma (Ruddiman and McIntyre, 1982; Zimmerman and others, 1984). Intermittent glacial and periglacial activity occurred in the northern Appalachians until ~0.85 Ma, followed by, in the mid to late Pleistocene, several glaciations that covered the northern Appalachians and also brought periglacial conditions to the southern Appalachians (Braun, 1989). Pliocene-Pleistocene glacial activity is thought to account for the large volume of sediment deposited in offshore canyons such as the Baltimore Canyon Trough during this epoch (Braun, 1989).

Driese and others research (2005) in southwestern Virginia, documents a late Pleistocene cooler full-glacial paleoclimate from paleosols and floodplain soils, followed by an interglacial period in the early Holocene. Clark and Kiolcosz (1988) confirm the presence of periglacial conditions such as seasonally frozen ground and sporadic permafrost from field relations of large-scale microfeatures such as grèzes litées, block fields and block slopes. They also suggest that paleoperiglacial processes may have had geomorphic importance at high elevations in the Quaternary.

During the early Holocene interglacial period, Leigh and Webb (2006) suggest that increased sedimentation rates in the southern Blue Ridge were due to changes in global paleoclimate that ushered in higher rates and frequency of precipitation in the form of floods, and tropical/thunderstorms. Kutzbach and others (1998) and Bard (2003) suggest that sea temperatures increased in the North Atlantic during this period, which may have favored tropical storms that are more frequent and precipitation during late summer and fall in the Appalachian Mountains. Hebbeln and others (2007) research in the Chilean Andes suggests that increased sedimentation rates are correlated with increased precipitation and are due to glacial/interglacial climate variability and during the late Quaternary through into the Holocene.

The research of Delcort and Delcourt (1984) focuses on eastern North American and the western Atlantic Ocean using palynological records and marine Foraminifera. They note that the glacial/interglacial climate variability saw periods of increased seasonality of temperatures during the early Holocene, and during the Hypisthermal Interval (8000-4000 B.P.) prevailing westerlies increased the mid-continental region of warmth and aridity. This has been replaced in the last 4000 years by increased meridian flow in eastern North America, which reflects the influence of Arctic, Pacific and Maritime tropical air masses.

Long-term changes in climate are primarily due to changes in geography (as discussed previously) and CO_2 concentrations. The geochemical models of Berner and others, (1983) and Lasaga and others, (1986) suggest that paleo CO_2 levels could have been as much as 10x present day levels during the Cretaceous due to plate tectonic

processes e.g. volcanic eruptions, and the rates of chemical weathering of continental crust (dependent on precipitation, temperature and continental area). Glacial and interglacial periods during the Pleistocene and Holocene have significantly contributed to the geomorphic processes that have sculpted the Appalachian Mountains during the late Cenozoic, but there is little data to indicate how such changes were manifested in basin-scale rates of erosion.

Geomorphic Models of Appalachian Landscape Evolution

Several researchers have proffered geomorphic models in order to understand and explain landscape evolution in the Appalachian Mountains. William Morris Davis and John Hack have proposed two of the most prominent models. Davis' *Geographic Cycle* (1899), developed from observations in the Susquehanna River and the Appalachian Mountains, describes how topography changes over time. Davis' model is based on the peneplain concept where in an unperturbed landscape, topography will diminish over time, until only the flat, low relief peneplain exists. Alternatively, Hack's model (1960) of *dynamic equilibrium* describes where landscape morphology is adjusted to the erosional resistance of the underlying rock over the long-term. In Hack's schema, differences in erosional resistance or rock strength are compensated for by slope; less resistant lithologies have shallow slopes and more resistant lithologies have steeper slopes. Hack's model in particular can be used as a framework within which to assess the landscape evolution of the Blue Ridge Province within the Shenandoah National Park.

How Does Appalachian Type Climate Affect Weathering and the Erosion of the

Lithologies in the Shenandoah National Park

Understanding the relationship between climate's effects on weather patterns, weathering, and in turn its effects on erosion, may help the investigation into Hack's (1960) theory of *dynamic equilibrium* and steady state behavior, which predicts that erosion rates should be independent of lithology. The sampling plan and cosmogenic nuclide analyses reported in this thesis examine the relationship between the lithologies in terms of erosion rates and slope. Hack's model is therefore important to consider. In order to do this, it is useful to understand the dynamics of weathering on the various lithologies (granite, metabasalt quartzite, and siliciclastic rocks). In terms of Hack, (1960, 1979) [10]Be concentration in drainage basin sediment is a proxy for rock resistance.

Other researchers have also investigated Hack's idea that less resistant lithologies will have shallow slopes and more resistant lithologies will have steeper slopes. Research by Clayton and Shamoon (1998) used km squares of the National Grid to study topography and geology and created a six-part classification of rock resistance. The classification attempts to relate rock resistance to relief, where lower altitude is equated with less resistant rocks, and the local relative relief is attributed to differences in rock resistance.

In terms of utilizing slope as an attribute that describes rock resistance, Grender (1973) used gridded elevation data of southwest Virginia to differentiate slope variation in various rock units. He associated lower slopes with less resistant lithologies, e.g. shales, and higher slopes with sandstones. Similarly, Mills (2003) used digital elevation models (DEM'S) to calculate measures of local relief, regional relief and slope, and from

these measures he calculated an erosional resistance index (ERI), the higher the ERI, the more resistant the rock. In the Valley and Ridge and Blue Ridge Province in Tennessee he found that coarse to intermediate clastic and metaplutonic rocks had higher ERI values and that shales, limestone and fine clastic rocks had low ERI values. He also found that there was a strong correlation between regional relief and slope (R^2 value = 0.8), which may be explained by the fact that mountains with high elevations tend to have steeper slopes. He concludes unit thickness, outcrop area, or age of bedrock have little effect on the ERI, streams tend to flow on units with low ERI values, and that the greatest lithologic control is on small streams.

In order to further investigate the validity of Hack's theories, it may be useful to understand something about rock resistance or erodability. How do rocks behave under certain climate conditions? White and others, (2001) studied granitic regolith in the Piedmont Province in Georgia to understand how different weathering regimes affected feldspar weathering. From their results they developed a weathering model that describes the sequential weathering environments of granitic rock, beginning with water infiltration of pristine rock, through weathering via fluid dynamics of plagioclase and k-spar and ending with a high permeability zone where both plagioclase and k-spar weathering are kinetically controlled. Pavich and others (1985, 1995) work on the Virginia Piedmont at Davis Run suggested that there was little weathering of feldspars in bedrock; much of the weathering occurred in the overlying saprolite sequences. Pavich and others conclude that a warmer, wetter climate, and a high content of anorthite and disseminated calcite increased bedrock permeability, which increased the weathering rate of feldspars and of

the bedrock generally.

Typically, weathering of joint blocks in granitic rocks starts at joint planes and moves inwards towards the center of the block (Ollier, 1971), causing rounding of edges and resulting in spheroidal weathering. Spheroidal weathering of granitic rocks, or "rindlet systems", is the basis of research by Turner and others (2003) in the Rio Icacos Basin in Puerto Rico. They suggest that at a watershed scale, weathering fronts move down through the porous zones of bedrock in a "conveyor belt" fashion, equal to that of the denudation rate. At an outcrop scale, "parallel" weathering fronts move up and down from joint planes towards the center of the rock. Ultimately, rock that tends to exfoliate will weather faster than rock that does not.

Many studies have investigated the controls on silicate weathering, both physical and chemical, including, temperature, rainfall and lithology (Raymo and Ruddiman, 1992; Bluth and Klump, 1994; White and Blum, 1995; Gaillardet and others, 1999). More recently, the role of mechanical erosion on weathering rates has been considered, (Riebe and others, 2001a, 2001b, 2004; Millot et al., 2002), but this alone does not account for climate-dependent weathering in some settings. Recent work by West et al. (2005) attempts to differentiate and quantify the influence of erosion rate, runoff and temperature on chemical weathering rates. They conclude that at higher erosion rates there is plentiful material, but climatic and kinetic factors limit weathering, and at lower erosion rates mineral supply limits weathering.

Studies on basalt weathering have been carried out in both Hawaii and Iceland (Gíslason and others, 1996; Moulton and Berner, 1998; Stefánsson and Gíslason, 2001;

Stewart and others, 2001). Stewart and others (2001) investigated the impact of rainfall

on the weathering of basalt in Hawaii based on strontium isotopes. In their study,

chemical weathering rates increase with an increase in mean annual precipitation (MAP),

supported by the increase in strontium in the soil silicate residues, also linked to

increased amounts of exogenous eolian material at high MAP sites. Moulton and Berner

(1998) examined the role of plants in weathering of basalts in Iceland by measuring the

chemistry of waters in streams draining areas adjacent to basalt outcrops. Their study

area chose areas that would maximize vegetational differences and the results suggest

that the rate of weathering release of Ca and Mg to streams is 2 to 5 times higher in

vegetated as opposed to non-vegetated areas, and also that vascular plants such as trees

play and important role in accelerating weathering. Conversely, Gíslason and others,

(1996) in their study in Iceland found that chemical weathering rates are independent of

vegetative cover, where vegetation slows down mechanical denudation rates by

stabilizing soils, decreasing the exposure of rock to incoming solutions. They suggest

that weathering rates are also dependent on the age of the rocks, the relative mobility of

elements within the rock and run-off, where the dependence of chemical denudation on

run-off is lower in older rocks than younger ones.

Stefánsson and Gíslason's (2001) study in southwest Iceland examines the effect of

rock crystallinity and secondary minerals on chemical fluxes to the ocean via the

chemical weathering of basalts. They sampled dissolved solids in water, and determined

the proportions of the solids derived from precipitation, air and rock weathering. They

found that certain elements are more dependent on run-off (Si, Ca, F, S, Al, K, Mg, and

B) and that fully crystallized basaltic rock dissolves slower than basaltic glass.

Appalachian Cosmogenic Studies

In order to put the results of this research into a broader context, I review previously published cosmogenic nuclide analyses from sample sites in the Appalachian Mountains. Cosmogenic isotope analysis has become a powerful geomorphological tool to assess landscape change, in terms of drainage-wide erosion, movement of sediment off hillslopes, and calculation of bedrock incision rates. Erosion rates are quantified using models that are subject to various assumptions including homogeneous quartz distribution, thorough mixing of sediment, constant rates of erosion, and minimal sediment storage (Bierman and Steig, 1996; Granger and others, 1996).

Lal and others, (1996) measured *in situ* produced cosmogenic ^{14}C and ^{10}Be from quartz chips chiseled from a quartz vein of a soil profile near Reston, Virginia. Model erosion rates of ~30m/My for ^{14}C and 3 m/My for ^{10}Be were estimated. The order of magnitude difference in erosion rates between these two cosmogenic isotopes can be resolved by considering the isotopes as a ratio and by utilizing a model where the quartz vein eroded at the slower of the two rates, followed by an abrupt burial or slow soil covering of the surface, followed by another period of erosion at the pre-burial rate. In terms of the general erosion of the Piedmont, these data suggests that there may have been short-term cycles of rapid deposition followed by soil wash erosional processes that re-exhumed the sampled surface.

Granger and others (2001) used cosmogenic isotope analysis (^{26}Al and ^{10}Be) to examine Pliocene-Pleistocene incision of the Green River, Kentucky. The cosmogenic

[26]Al and [10]Be were extracted from river sediments washed into Mammoth Cave, Kentucky, and they record the 3.5 My incision history of the water table position contingent on the incision and aggradation of the Green River. The incision history of the Green River occurred synonymously with drainage reorganizations and major climate changes. Measurement of the cosmogenic isotopes suggest that the sandstone uplands have been denuding at a rate of 2-7m/My over the last 3.5 million years, with increased river incision rates during the Pleistocene of ~ 30 m/My.

Matmon and others, (2003a, 2003b) investigated erosion rates utilizing cosmogenic isotopes in the Great Smoky Mountains National Park. The Great Smoky Mountains are the highest range in the humid southern Appalachians and are located between Tennessee and North Carolina. The topography of the region is composed of medium grade, metamorphosed quartz-rich sedimentary rocks and gneiss that form steep, soil-covered and vegetated slopes. The mean annual rainfall is 1400-2300 mm. Cosmogenic nuclide concentrations were measured in bedrock, alluvial sediments and colluvium. The similarity of erosion rates (25-30 m/My) amongst the samples suggests that the whole range is being lowered at a similar rate.

Cosmogenic isotope analysis has also been used to investigate rates of bedrock incision in the Appalachians. Using two rivers that drain the Atlantic passive margin, the Susquehanna and Potomac rivers, Reusser and others, (2004) sought to measure the rate and timing of bedrock incision commencing 35,000 years ago, prior to the last glacial period. Both the Susquehanna and the Potomac River valleys exhibit long-term lowering into the Piedmont Province, which reflects an amalgamation of late Cenozoic sea-level

fall, slow flexural uplift due to offshore sediment loading and isostatic response to denudation.

In order to examine the effects of rapidly changing climate on river incision, they sampled fluvially eroded bedrock surfaces that were exposed as the rivers incised to lower levels, from Holtwood Gorge on the Susquehanna and Great Falls/Mather Gorge on the Potomac. Low [10]Be concentrations in modern bank Potomac samples allowed modeling of [10]Be concentrations directly as terrace abandonment ages (Reusser and others, 2004).

Results suggest that rates of downcutting on both rivers increased markedly post 35,000 years ago (600-800 m/My), which was evidenced by abandonment and exposure of bedrock terraces defining gorges on the Susquehanna and Potomac Rivers (Reusser and others, 2004). The data suggest that the rivers draining the Atlantic passive margin are capable of periodic rapid incision. The incision rates measured are 1 to 2 orders of magnitude higher than the long-term incision rates. Reusser and others suggest that this period of rapid incision occurred concurrent with a period of cold, stormy and unstable climate, and that incision rates slowed with the transition to the warmer, more stable, Holocene climate.

Reuter and others, (2005) research focused on the central Appalachians, specifically the rates and patterns of erosion in the Susquehanna River Basin of Maryland, Pennsylvania and New York. Fluvial sediments were collected in three Appalachian Provinces comprising four distinct lithologies mapped as single lithologies: the Appalachian Plateau (sandstone), the Valley and Ridge (sandstone and shale), and the

Piedmont (schist). In this study, erosion rates correlate well with slope, and lithology does not affect basin-scale erosion rates. The results suggest that the small basins sampled are eroding on the order of 4-54 m/My, implying that steep slopes are eroding more rapidly than shallower ones and that valleys lower faster than ridges. An erosion rates increase towards the Susquehanna headwaters (Piedmont (9 ± 2 m/My), Valley and Ridge (13 ± 6 m/My), Appalachian Plateaus (22 ± 12 m/My) suggests that the system is not in steady state, but is exhibiting a transient response to drainage network perturbation (Reuter and others, 2005).

Ward and others, (2005) examine the incision history of the New River, Virginia using cosmogenic [10]Be exposure dating. The New River drains to the Gulf of Mexico whilst incising through the Blue Ridge (crystalline metasedimentary and metaigneous rocks), Valley and Ridge (carbonates) and the Cumberland Plateau (clastic and carbonate rocks) of the Appalachian Mountains. The New River is wider and shallower through more resistant units (Tuscarora sandstone), and incises deeply through less resistant Cumberland Plateau units (sandstones and shales). Samples were collected from terrace soils and bedrock at four sites along the New River.

The incision and aggradation history of the New River over the last few million years was inferred from cosmogenic radionuclide dating of the terrace soil and bedrock samples. This dating allows some understanding of how river incision is affected by variables such as bedrock lithologies, climate and drainage network organization. Starting at ~955 ka, the incision rates for the New River through alluvial fill and bedrock average 43m/My, with periodic episodes where downcutting rates reached ~100 m/My. These

intermittent periods of incision were punctuated. In between erosion events, there were

extensive times of aggradation, during which extensive terraces were formed. These

results imply short periods of disequilibrium where incision rates exceed the rates of

erosion of surrounding landforms.

The geomorphologic evolution of the Blue Ridge Escarpment (BRE) has also

been quantified using cosmogenic isotope analysis. Sullivan and others, (accepted)

utilized ^{10}Be in order to constrain and understand how this feature has changed over time.

Fluvial and bedrock samples (schist) were collected along four transects normal to the

BRE in order to investigate variables that may have an effect on the evolution of this

landform (basin slope, relative position of the Brevard Fault Zone and landscape

position). The data gives basin averaged erosion rates of 6.5-38 m/My, which suggests

that most of the erosion that shaped the BRE occurred following rifting in the Mesozoic

(~200Ma). There is a positive relationship between slope and erosion rate, and the

erosion rates infer that the BRE has been retreating and lowering at very slow rates.

Hancock and Kirwan (2007) modeled erosion rates measured using ^{10}Be from

high elevation exposed bedrock surfaces in Dolly Sods, West Virginia, and the

Appalachian paleoperiglacial plateau. Dolly Sods is a broad, gently rolling upland

situated ~300 km south west of the late Wisconsinin glacial maximum, with a topography

composed of quartz conglomerates and sandstones. Bedrock samples were collected from

bedrock blocks, tors and outcrops and the concentration of ^{10}Be was measured from

quartz in the rock. Quartz clasts were also collected from the conglomerate in order to

ascertain the erosional history of the rock in which they were weathered.

The mean average erosion rate from the bedrock outcrops was 5.7 m/My and 5.9 m/My from the clasts, interpreted as an average erosion rate. These results suggest that erosion at Dolly Sods is slow, even though it was exposed to the rigors of a periglacial regime during at least some of the last 2.4 My. These bedrock rates are much lower than those fluvial rates obtained throughout the Appalachians previously outlined. Hancock and Kirwan suggest that this is due to a disequilibrium in the Appalachian landscape, and topographic relief is increasing at a rate of ~10-790 m/My. Their observation of increasing relief is inconsistent with Hack's theory of *dynamic equilibrium,* and they suggest that the Dolly Sods landscape is one that is in transition to equilibrium state, adjusting to climate driven increases in rates of fluvial incision, which results in relief generation.

These previous studies have utilized cosmogenic isotope analysis as a technique to improve the understanding of the landscape evolution of the Appalachian Mountain belt. This technique can estimate erosion rates via sediments or bedrock to ascertain denudation rates of mountains or bedrock incision rates. The overarching themes drawn from these studies are that the Appalachian Mountains are a dynamic system where long-term erosion rates, both fluvial and bedrock, are slow (~4-54 m/My), and are punctuated by periods of rapid bedrock incision by rivers as they drain the passive margin to the east (43-800 m/My).

Chapter 3 – Methods

This chapter provides a detailed account of the methods used for data collection in and around the Shenandoah National Park, in the laboratories of the University of Vermont, and in the Glasgow University - Cosmogenic Nuclide Laboratory at the Scottish Universities Environmental Research Centre in East Kilbride, Scotland. These methods include: sampling strategy incorporating GIS analysis, field methods, laboratory techniques and experimental design for analysis of erosion rate data.

Sampling Strategy – Basin Selection

One of the interesting features of the geology of the Shenandoah National Park region is that within the Park boundary there are four distinct lithologies: granite, metabasalt, quartzite, and siliciclastic rocks. In order to determine whether there is a relationship between lithology and erosion rate, we sampled sediment originating from 54 single lithology basins and 5 outcrops. During the first field effort in November, 2005, four initial sample sites were chosen, one for each lithology using 1:24000 USGS topographic maps and 1:62,500-scale geologic maps of the Park. At these first four sample sites grain size splits (0.25 – 0.85 mm, 0.85 – 2 mm, 2 – 10 mm, and >10 mm) were collected and later processed separately in order to test the relationship between [10]Be concentrations and grain size (Brown and others, 1995; Clapp and others, 1997, 1998, 2001. 2002; Matmon and others, 2003a, 2003b; von Blanckenburg, 2005; Belmont and others, 2006; Duxbury and others, 2006; Sullivan and others, 2006).

Prior to two subsequent field efforts in late May/early June 2006 and December, 2006, sample sites were selected using ArcGIS to generate a list of single-lithology

drainage basins that also considered criteria such as basin size, location, mean slope, and elevation range. These basins were delineated using several GIS layers including: USGS 10 m DEM's (Digital Elevation Models) of the Park; bedrock geology shape files that provided an overall characterization of the physiography and principal bedrock formations; National Hydrography Datasets (NHD) provided the stream layer; digital contour maps (DRG) were overlayed to provide a visual confirmation of streams, and a digitalized layer of the National Park Boundary. Once the basins were delineated, and the desired criteria were established, I chose sample sites of sufficient basin size to allow for adequate mixing of sediments within the basin (about a km^2), while sampling basins that represented a variety of average slopes, basin sizes, elevations, and lithologies. These maps and data became useful field tools that enabled me to choose alternate basins if field conditions, such as access limitations, prevented me from sampling preselected basins.

Field Sampling Methods

With the help of Colleen Sullivan, Corey Coutu, and Luke Reusser over three field efforts I collected the 54 sediment and 5 bedrock samples. In the fall of 2005, I collected 4 samples (split into four grain size splits: 0.25 – 0.85 mm, 0.85 – 2 mm, 2 - 10 mm, > 10 mm), followed by 36 samples in the summer of 2006 and in the winter of 2006 a further 14 sediment and 5 bedrock samples. The sediment samples were gathered from active river or stream channels within or near to the boundaries of the park. The amount of sediment I collected in the summer and winter of 2006 was based on the results of the lab-processed samples that had been collected in the fall of 2005. For all the quartz-rich

30

lithologies ~ 0.5 - 1 kg of sample was sufficient to carry out the lab processes to isolate

^{10}Be. Where possible, the majority of samples were wet sieved in the field to the 0.25 –

0.85 mm size fraction, which is a suitable size for processing in the lab. Digital

photographs were taken of each sample site and samples were labeled and stored for

transport in gallon zip-lock bags. On return to the University of Vermont samples were

oven dried, and where necessary re-sieved to isolate the 0.25-0.85mm size fraction using

a rotational tapping device.

During the winter of 2006, I collected bedrock samples that were not accessible in

the summer due to heavily vegetated outcrops. Five bedrock samples were randomly

collected using a hammer and chisel, based on accessibility and occurrence, from each of

the four lithologies and from Massanutten Ridge (sandstone) in the Valley and Ridge

Province adjacent to the Shenandoah National Park. The Massanutten Ridge was

sampled in order to compare the Valley and Ridge bedrock erosion rates with bedrock

erosion rates in the Park. At the time of collection the samples were taken from non-

vegetated outcrops with flat lying surfaces and were ~2-5 cm in thickness. The bedrock

samples were crushed and ground and sieved to the 0.25-0.85 mm size fraction in the

University of Vermont rock preparation lab for processing.

Laboratory Work

Samples were processed according to standard techniques developed by Bierman

and Caffee (2001). Quartz was isolated at in the Mineral Separation Lab at UVM using

protocols[1] established by P. Bierman.   A brief synopsis of the process is as follows: the

quartz was initially cleaned via a process of ultrasonic etching in heated 6N HCl. The

samples that had high iron content, such as the metabasalt, received two 24-hour 6N HCl

etches.   This was followed by three 1.5%HF/ 1%HNO$_3$ etches of 8, 14 and 24 hours (for

high yield samples such as granite, quartzite, siliciclastic rocks), or three 2%HF/

2.5%HNO$_3$ etches of 24 hours on hot dog rollers for those samples with low quartz yields

(metabasalt). Samples were then placed in an oven and burned at 500°C to remove

organic material including coal. A density separation using LST (lithium polytungstate)

was performed to remove heavy minerals such as magnetite and ilmenite.   The final step

of the processes was a 48 hour etch in 1.5%HF/ 1%HNO$_3$.

The clean quartz was tested for its purity and recleaned until Al, Ti and Fe levels

were generally below 150 ppm. Jennifer Larsen isolated ^{10}Be on four initial samples

using standard lab procedures developed by Bierman and Caffee (2001)[1]. Process blanks

were run with every seven samples and average blank ^{10}Be/^{9}Be ratios were subtracted

from measured ratios of samples. The ^{10}Be isolated from the initial samples (SH-01

through SH-04 including grain-size splits) was then measured using accelerator mass

spectrometry (AMS) at the Lawrence Livermore National Laboratory (LLNL)[2]. The

remaining samples were processed to isolate ^{10}Be at the GU-SUERC Cosmogenic Isotope

Laboratory (Glasgow University- Scottish Universities Environmental Research Centre) [3]

---

[1] http://www.uvm.edu/cosmolab/?Page=methods.html
[2] https://cams.llnl.gov/
[3] http://web.ges.gla.ac.uk/~dfabel/CN_intro.html

at the Scottish Universities Environmental Research Centre (SUERC)[1] in East Kilbride, Scotland. The ^{10}Be isolated from the remaining samples was then measured using accelerator mass spectrometry (AMS) at the SUERC Accelerator Mass Spectrometry Laboratory[2]. Process blanks at SUERC were run with every fifteen samples and average blank ^{10}Be/^{9}Be ratios were subtracted from measured ratios of samples.

For LLNL-analyzed samples, ^{10}Be concentrations were normalized using standards developed by Nishiizumi (1986), assuming a ^{10}Be half-life of 1.5 My (KNSTD 3110, $^{10/9}$Be ratio standard of 3.15 x 10^{12}). Samples analyzed at SUERC followed procedures based on methods modified from Kohl and Nishiizumi (1992) and Child and others, (2000), using the standard NIST (SRM4325) (National Institute of Standards and Technology) and a $^{10/9}$Be ratio standard of 3.06 x 10^{11}. The data obtained from samples processed from both facilities are directly comparable, and given the values assigned to the standards are best interpreted with production rates also derived from these standards prior to standard value revision. This is in the light of new data suggesting a change in the accepted value of the ^{10}Be half-life (Nishiizumi and others, 2007).

Calculation of erosion rates from ^{10}Be and analysis

Measured ^{10}Be concentrations were corrected for basin latitude and altitude based on the polynomials of Lal (1988) for neutrons only. Basin hypsometry (elevation interval = 100 m), for use in the interpretive model, was calculated using ArcGIS. Basin-scale erosion rates were modeled using the interpretive model of Bierman and Steig (1996)

---

[1] http://www.gla.ac.uk/surrc/
[2] http://www.gla.ac.uk/suerc/ams/index.html

with a normalized sea level, high latitude ^{10}Be production rate of 5.2 atoms g quartz^{-1} yr^{-1}, an attenuation depth of 165 g cm^{-2}, and assuming a rock density of 2.7 g cm^{-3} considering only neutron spallation. Bedrock erosion rates were calculated using procedures developed by Lal (1988). Erosion rates and ^{10}Be concentrations have been analyzed with respect to lithology, slope, basin size, aspect and grain-size using simple/multiple regression analysis, descriptive statistics, analysis of covariance, one-way ANOVA tests to a 95% confidence level. The erosion rate data were transformed using a square root transformation of the model erosion rate.

Chapter 4: Paper submitted to the *American Journal of Science*

Erosion Rates in and Around Shenandoah National Park, Va, Determined Using Analysis of Cosmogenic [10]Be.

Jane Duxbury
Geology Department, University of Vermont, Burlington, Vermont 05405

Paul R. Bierman
Geology Department and School of Natural Resources, University of Vermont, Burlington, Vermont 05405

Jennifer Larsen
Geology Department, University of Vermont, Burlington, Vermont 05405

Milan J. Pavich
U.S. Geological Survey, Reston, Virginia 20192

Scott Southworth
U.S. Geological Survey, Reston, Virginia 20192

María Miguéns-Rodríguez
Glasgow University-Scottish Universities Environmental Research Centre, Cosmogenic Nuclide Laboratory, East Kilbride, Scotland

Stewart Freeman
Accelerator Mass Spectrometry Laboratory, SUERC, East Kilbride, Scotland

Abstract

We use cosmogenic [10]Be analysis of fluvial sediments and bedrock to estimate erosion rates ($10^3 - 10^6$ year timescale) and to infer the distribution of post-orogenic geomorphic processes in the Blue Ridge Province in and around Shenandoah National Park, VA. Our sampling plan was designed to investigate relationships between erosion rate, lithology, slope, and basin area. Fifty-nine samples were collected from a variety of basin sizes (<1 – 3351 km^2) and average basin slopes (7 - 26°) in each of four different lithologies that crop out in the Park: granite, metabasalt, quartzite, and siliciclastic rocks. The samples include bedrock (n = 5), fluvial sediment from single-lithology basins (n = 43), and fluvial sediment from multilithology basins (n = 11): two of these samples are from rivers draining streams exiting the eastern and western slopes of the Park (Rappahannock and Shenandoah Rivers).

Inferred erosion rates for all fluvial samples from all lithologies range from 3.8 to 24 m/My. The mean erosion rate for single-lithology basins in the Park is 11.6 ± 4.8 m/My. Single-lithology erosion rates ranges for fluvial samples are: granite (basin size = ~0.4-40 km^2 and slope = 11-23°), 7.9–22 m/My; metabasalt (basin size = ~1-25 km^2 and slope = 11-19°), 4.8–24 m/My; quartzite (basin size = ~0.1-9 km^2 and slope = 12-23°), 4.7–17 m/My; and siliciclastic rocks (basin size = ~0.3-13 km^2 and slope = 18-26°), 6.2–17 m/My. The mean erosion rate for multilithology basins (basin size = ~1-3351 km^2 and slope = 7-22°) is 10.2 m/My, and individually for the Shenandoah River 7.3 m/My and the Rappahannock River 13.8 m/My. Bedrock erosion rates range from 2.4-13 m/My across all lithologies, with a mean erosion rate of 7.9 ± 4.4 m/My. Grain-size specific [10]Be analysis of four samples showed no consistent trend of concentration with grain size.

These data support Hack's *dynamic equilibrium* model slope and erosion rate are not well correlated and mean erosion rates are similar for different lithologies. Cosmogenically-determined erosion rates in Shenandoah Park are similar to or lower than those reported elsewhere in the Appalachians including those of Matmon and others (2003), 25-30 m/My for metaclastic rocks in the steep Great Smoky Mountains, Reuter and others (2005), 4 – 54 m/My in Susquehanna River basin for shale, sandstone, and schist,

and Sullivan and others (2006), 6-38 m/My in the micaceous schist and gneiss of the Blue Ridge Escarpment. Cosmogenic erosion rates (integration over 10^4 yrs) in the Blue Ridge province of Shenandoah National Park are consistent with long-term unroofing rates (integration over 10^7 yrs) estimated from U-Th/He measurements (11-18 m/My) in samples collected near the Blue Ridge Escarpment by Spotila and others (2004), and fission tracks (20 m/My) in the southern Appalachians by Naeser and others (2005). The consistency of denudation rates integrated over very different periods of time suggests steady erosion most likely in balance with, and driving isostatic uplift of rock.

Introduction

Understanding the dynamic nature of the Earth's surface and the rate at which the landscape has changed over time are fundamental to geomorphology. Geomorphologists have long sought to understand the relationships between erosion (both physical and chemical, e.g. Riebe and others, 2001b; Riebe and others, 2003), climate (Harris and Mix, 2002), topography, and lithology (Hack, 1960). Over the last decade, the development and widespread application of cosmogenic and thermochronologic techniques capable of quantitatively estimating rates of erosion has revolutionized our understanding of Earth's dynamic surface (Bierman and Nichols, 2004; Reiners and Brandon, 2006; Bishop, 2007).

The Appalachian Mountains have been the subject of intense study for more than a century (Davis, 1899; Hack, 1960; Barron, 1989; Pavich, 1990; Pazzaglia and Gardner, 1994; Granger and others, 1997; Eaton and others, 2003a; Ward and others, 2005; Hancock and Kirwan, 2007). These mountains are of particular interest because they are an easily accessible natural laboratory in which to understand better the geomorphic processes that occur at passive margin mountain ranges following the cessation of orogenesis (Pazzaglia and Brandon, 1996). Of particular interest in the Appalachian

Mountains is the apparent paradox of mountainous topography existing hundreds of

millions of years after the cessation of convergent orogenic activity (Rodgers, 1970).

In the broader context of this interest in aging orogens, and as part of a series of

cosmogenic studies of the Appalachian Mountains (Matmon and others, 2003a; Matmon

and others, 2003b; Reuter, 2005; Sullivan and others, accepted), this research investigates

millennial scale erosion rates of the Blue Ridge Province in and around the Shenandoah

National Park region, Virginia using 59 [10]Be cosmogenic measurements derived from

fluvial sediments and bedrock. Using these data, we test for relationships between erosion

rates and lithology, slope, basin area and aspect. The sizes of sampled drainage basins

are constrained by the lithology of the area and range from <1-3351 km^2. Our findings

can be compared with the several hundred cosmogenic nuclide analyses made along the

length of the Appalachian Mountains, including two regional rivers, the Rappahannock

(13 km^2) and the South Fork of the Shenandoah (3351 km^2).

Background

Appalachian Mountain Physiography and History

The Appalachian Mountains (fig. 1) extend from Newfoundland, Canada in the

northeast, southwest to Alabama (Rodgers, 1970). The belt is divided into five

physiographic provinces. From west to east, these are: the Appalachian Plateau, the

Valley and Ridge, the Blue Ridge, the Piedmont, and the Coastal Plain (Gathright, 1976).

The Appalachian Plateau lies to the northwest of the Valley and Ridge Province and it

is separated from the Valley and Ridge by the Allegheny structural front, an escarpment

at the transition from the tight folds of the Valley and Ridge to the low-amplitude folds

and flat lying, gently folded strata of the Plateau (sandstones, conglomerates, shales and

coal). The Valley and Ridge consists of linear, parallel ridges and valleys with the

Shenandoah Valley being the easternmost limestone valley of the Valley and Ridge. This

topography is thought to be the result of differential weathering and erosion of the

heavily faulted and folded rocks (Kiver and others, 1999).

The Blue Ridge Province is a highland that abruptly rises hundreds of meters above

sea level and is situated between the Piedmont to its east and the Shenandoah Valley to

its west. It is an allochthonous anticlinorium with a core of Mesoproterozoic crystalline

rocks flanked by metamorphosed sedimentary and volcanic rocks (Kiver and others,

1999).

The Piedmont Province is a low-relief area to the east of the Blue Ridge Province. It

is characterized by gently rolling topography, few outcrops and deeply weathered and

saprolitized bedrock (Pavich, 1985). The Piedmont is underlain by a variety of Paleozoic

to Mesozoic igneous, metamorphic, and sedimentary rocks. Low-relief interior basins of

the Piedmont contain diabase dikes, basalt flows, and isolated sedimentary rocks, which

are located in half-graben basins formed during the early stages of rifting associated with

the opening of the Atlantic Ocean (Pavich, 1985; Kiver and others, 1999).

The Coastal Plain is east of the Piedmont Province and Fall Zone, and extends to the

Atlantic Ocean. The Coastal Plain is characterized by Cretaceous and Tertiary sediments

that overly the igneous and metamorphic bedrock of the Piedmont (Kiver and others,

1999).

Cenozoic drainage capture and erosion rate variation

In the Miocene, the ancestral Potomac River drainage breached the Blue Ridge and

captured the then westward flowing drainage (Naeser and others, 2006a). The re-

orientation of Appalachian drainages (Potomac and Susquehanna Rivers) to the east

accompanied increases of relief and topography (Pazzaglia and Brandon, 1996).

Pazzaglia and Brandon (1996) attribute the increased relief to four factors: two

aesthenopheric flow and magmatism events in the Cretaceous, subsequent post-rift

thermal relaxation and aesthenopheric flow, and development of dynamically supported topography in the Miocene.

On the basis of the offshore sediment record and interpretive models, Pazzaglia and Gardner (1994) and Pazzaglia and Brandon (1996) suggest that after the Alleghenian orogeny, Appalachian erosion rates have varied between ~12 and 44 m/My over the last ~ 200 my. They posit that flexural isostatic deformation, which is a continual uplift process with variable rates modulated by eustatic sea-level variations, drove Cenozoic erosional sediment delivery to offshore basins (Pazzaglia and others, 2006). In the central Appalachians, U-Th/He thermochronologic data and existing apatite fission track (AFT) thermochronology reveal a shift in the drainage divide linked to the accumulation of Miocene sediments on the Coastal Plain. U-Th/He and AFT closure ages are practically indistinguishable over the last ~200 My, suggesting moderate amounts of unroofing (Pazzaglia and others, 2006). This is in contrast to Blue Ridge and Piedmont Provinces. The U-Th/He ages are younger than the AFT ages in these areas, inferring increased and continuous unroofing during Alleghenian orogenesis and Mesozoic rifting. Long-term average continental denudation rates based on offshore sediment accumulation are likely between ~ 10-20 m/My (Pazzaglia and others, 2006), which is in good agreement with

AFT data from the Blue Ridge. Together these datasets indicate that the Appalachian

Mountain landscape has been eroding at ~20 m/My since the Miocene (Naeser and

others, 2004).

Geology and Physiography of the Shenandoah National Park Region

Shenandoah National Park Region physiography

Shenandoah National Park (fig. 1) is situated along the Blue Ridge, a highland

area between Front Royal to the north and Rockfish Gap to the south, near Waynesboro,

VA (Kiver and others, 1999). The highlands contain mostly forested uplands; adjacent

lowlands are privately held and largely cleared for agriculture. The highest elevation

within the ridge containing the Park is Hawksbill, which stands 1,235 m, rising above the

low-lying Piedmont Province to the east and the Shenandoah Valley to the west (Kiver

and others, 1999). The Potomac River crosses the Blue Ridge to the north at Harpers

Ferry, West Virginia, and the James and Roanoke Rivers cross to the south. There are

also two major wind gaps, Thornton and Powell, which are thought to mark the path of

ancient stream courses (Kiver and others, 1999). Mountaintops and slopes within and

near the Park are heavily vegetated and mostly covered by residuum. Unvegetated

outcrops are scarce.

Shenandoah National Park region geology

The geology of the Shenandoah National Park region, and the rocks we have sampled

both directly and in river sediments, have been well studied by King (1950), Reed (1955),

Gathright (1976), and Southworth (2008). This part of the Blue Ridge province (figs. 1

and 2A and B), consists of Mesoproterozoic to early Cambrian rocks that record the

earliest history of eastern North America. Mesoproterozoic granitic gneisses were

emplaced, metamorphosed and deformed about one billion years ago during the

Grenvillian orogeny (Tollo and others, 2006). Neoproterozoic granites were emplaced,

and sediments were deposited prior to the extrusion of flood basalts from 575-560 Ma

associated with extensional tectonics and continental breakup (Bailey and others, 2006).

As the Laurentian sea opened, coastal plain deposits covered the subsiding landmass. The

rocks were buried, metamorphosed, folded, faulted, and tectonically transported

westward to their current geographic position in the late Paleozoic Alleghenian orogeny,

forming the Blue Ridge-South Mountain anticlinorium (Southworth and others, 2006).

The western limb of this anticlinorium is composed of the lithologies we sampled;

granite, metabasalt, quartzite, and siliciclastic rocks (metasiltstone, sandstone, and

phyllite).

Following the Alleghenian orogeny, erosional events during the late Permian and

early Triassic periods transported sediment to the Appalachian foreland basin to the west.

The extensional separation of North America and Africa ~ 200 Ma, resulted in the

opening of the Atlantic Ocean in the early Jurassic, and led to the development of the

Atlantic passive margin. This rifting likely caused renewed uplift on the rift shoulders

and increased relief (Pazzaglia and Brandon, 1996).

Stratigraphy

There are four principal rock types within and adjacent to the Shenandoah National

Park: (1) Mesoproterozoic granitic gneisses underlie the highlands along Blue Ridge and

the lowlands to the east. There are at least 30 different sub-varieties of granitic gneisses

that have been mapped (Southworth, 2008) (2) Neoproterozoic metabasalt and

metasedimentary rocks also underlie the highlands along Blue Ridge and the lowlands to

the east. The metabasalt is the dominant rock in the Catoctin Formation (Badger and

Sinha, 1988), and the underlying Swift Run Formation consists of local accumulations of

sandstone and phyllite. (3) Cambrian quartzite and metasiltstone are restricted to the

boundary of the Blue Ridge and the Valley and Ridge and they underlie distinctive ridges

and swales that have lower altitude and relief than the adjacent highlands. The quartzite

and metasiltstone constitutes the Chilhowee Group, comprised of the Weverton, Harpers, and Antietam Formations. (4) Cambrian and Ordovician carbonate rocks are restricted to the Valley and Ridge province west of the quartzite ridges and are mostly covered by extensive alluvial fans derived from the quartzite of the Cambrian Chilhowee Group. The carbonate rocks that overly the Antietam Formation in the Valley and Ridge are the Tomstown, Waynesboro, Elbrook, and Conococheaque formations.

The landforms within and surrounding the area provide insight into the erosional history of the area. The alluvial fans on the west side of the Shenandoah National Park are long-term accumulations of coarse clastic debris transported by water. The 100 m thickness of these deposits is in part a function of the setting, which is a trap for sediment (Hack, 1965; Kochel and Johnson, 1984; Whittecar, 1992). The coarse material has only locally been eroded by modern drainage systems, whereas the carbonate substrate has been lowered by chemical weathering over an extended period. Manganese deposits in the underlying clay residuum, as well as lignitic material, interpreted as Tertiary (Stose and others, 1919) and (or) late Cretaceous (Pierce, 1965) in age, suggests the chemical lowering of the valley substrate has been active for at least 65 My.

To the east of the Park, broad alluvial plains with strath terraces (Morgan and others, 2004) are incised into granitic gneisses, but extensive alluvial or fan deposits are not preserved. The tributaries that drain these plains head in the highlands where basins and hollows are underlain by large boulder deposits related to ancient debris flows and perhaps more recent periglacial processes (Morgan and others, 2004). Modern high rainfall events have resulted in debris flows east of the Park that flushed the coarse debris out of the hollows and deposited them on the adjacent lowland valley floor (Morgan and others, 1999; Bierman and others, 2002b; Eaton and others, 2003a; Eaton and others, 2003b). The highlands are underlain in places by a thick mantle of stratified slope deposits (slope wash processes) probably relict from an earlier periglacial climate; these deposits are not affected by modern storm-driven erosion (Litwin and others, 2001; Smoot, 2004). Scree slopes, block fields, and colluvium occur at the high elevations (Gathright, 1976) and locally overlie the older stratified slope deposits (Smoot, 2004).

There is evidence of periglacial climate in the high elevations of the Blue Ridge region characterized by mass wasting and freeze-thaw processes (Washburn, 1973; Washburn, 1980). Mountaintop detritus and colluvial deposits found throughout the region are thought to be associated with periglacial activity such as ice wedging. This

detritus takes the form of quartzite block fields, talus sheets, rock streams and tors at summits and along ridgelines (Morgan and others, 2004). These periglacial processes may affect rock strength and stability. Galloway (1961) and Hills (1969) found that in periglacial conditions in Scotland, both granite and quartzite were subjected to frost-shattering which led to the formation of characteristic landforms such as tors (Eaton and others, 2003a). Driese and others (2005) research inn southwestern Virginia, documents a cooler late Pleistocene full-glacial paleoclimate from paleosols and floodplain soils, followed by an interglacial period in the early Holocene. Clark and Kiolcosz (1988) also confirm the presence of periglacial conditions such as seasonally frozen ground and sporadic permafrost from field relations of large-scale microfeatures such as grèzes litées, block fields and block slopes. They also suggest that paleoperiglacial processes may have had geomorphic importance at high elevations in the Quaternary. Kutzbach and others (1998) and Bard (2003) suggest that sea temperatures increased in the North Atlantic during the early Holocene, which may have favored more frequent tropical storms and precipitation during late summer and fall in the Appalachian Mountains. Also during this period, Leigh and Webb (2006) suggest that increased sedimentation rates in the southern Blue Ridge were due to changes in global paleoclimate that ushered in

higher rates and frequency of precipitation in the form of floods and tropical

thunderstorms.

Shenandoah National Park Region Climate

There are several major influences on climate in Virginia. A well-developed,

orographically-induced rainfall pattern exists, where winter storms generally track from

west to east, and move northeastward paralleling the Gulf Stream and the coast. As moist

air rises and condenses, the eastern slopes and foothills of the Blue Ridge receive this

precipitation (http://www.climate.virginia.edu/description.htm, accessed 6/14/07).

Regional climate is also controlled by the high relief of the Appalachian Plateau, and the

Blue Ridge. The Shenandoah River valley is one of the driest areas in the state resulting

from the rain shadow effect of both the Appalachian Plateau and the Blue Ridge when air

flow is from the west or east respectively

(http://www.climate.virginia.edu/description.htm, accessed 6/14/07). A more local

control on climate is the complex systems of rivers and valleys that drain the precipitation

from the Blue Ridge highlands underlying the Park and modify the pattern of moist

airflow. Thunderstorms, which can focus on the high terrain, reach a peak in September,

but storms and significant run-off can occur year round with precipitation in the park

averaging 100 – 150 cm per annum

(http://www.nps.gov/shen/pphtml/subenvironmentalfactors21.html, accessed 6/14/07).

There are significant temperature and precipitation gradients in the park both of

which are related to elevation. The mountains in the Shenandoah National Park are

usually ~6° C cooler than the valley below, where mild winters and warm humid

summers are the norm. The average annual precipitation at Big Meadows (elevation

1067 m, mean annual temperature is 9° C) is 132 cm, including ~20 cm of snow/water

equivalent (http://www.nps.gov/shen/pphtml/subenvironmentalfactors21.html, accessed

6/14/07).

At Luray in the lowland, the mean annual temperature is 12° C, and average annual

precipitation is 91 cm, with <10 cm of snow/water equivalent

(http://www.nps.gov/shen/pphtml/subenvironmental factors21.html, accessed 6/14/07).

Cosmogenic Nuclides in Erosion Rate Studies

Cosmogenic isotopes produced in near-surface rock and sediment, primarily ^{10}Be

and ^{26}Al, have been used to estimate rates of rock erosion (Nishiizumi and others, 1986;

Small and others, 1997; Kirwan, 2002; Kirwan and others, 2002; Phillips and others,

2006; Hancock and Kirwan, 2007) and sediment generation (Brown and others, 1995;

Bierman and Steig, 1996; Granger and others, 1996; Clapp and others, 1999; Clapp and others, 2000; von Blanckenburg, 2005) for two decades. When the measured concentrations of cosmogenic isotopes are interpreted using steady-state models, the resulting information suggests the rate at which the landscape has changed over timescales of 10^3 to 10^7 years depending on the rate of erosion and the isotope employed (Bierman and Nichols, 2004).

Of specific utility for this study is the cosmogenic isotope [10]Be because it is the longest-lived of the cosmogenic radioactive isotopes and is easily measured in quartz (Gosse and Phillips, 2001; Bierman and others, 2002a). Quartz is widely distributed on Earth's surface and can be separated from other minerals because of its low reactivity with various acids (Kohl and Nishiizumi, 1992) . [10]Be is produced in situ as a result of spallation, the splitting of target nuclei by incoming, high-energy, fast cosmic ray neutrons (Lal, 1998). The cosmic ray flux is attenuated by rock thus, [10]Be concentrations decrease nearly exponentially with depth. Cosmogenic nuclide production rates are dependent on latitude and altitude (Lal and Peters, 1967): normalization schemes have been developed (Lal, 1991; Desilets and Zreda, 2000; Dunai, 2000; Lifton, 2000) to account for this effect.

In eroding landscapes, the abundance of ^{10}Be in outcropping rock and soil is proportional to the transit time of rock from depth to surface, allowing erosion rates to be inferred from nuclide concentrations (Lal, 1988). In humid landscapes, rock transitions first to saprolite and then to soil and sediment with the material approaching the lowering surface, all the while accumulating ^{10}Be (Pavich, 1990). As a result, quartz grains in basins that are eroding slowly have a high concentration of ^{10}Be because they have been exposed to cosmic-ray bombardment longer than quartz grains in rapidly-eroding basins. Sediment gathered from streams spatially averages ^{10}Be concentration and thus allows calculation of an average or virtual sediment production rate for the entire basin, rather than for a particular point on the landscape as with bedrock samples (Brown and others, 1995; Bierman and Steig, 1996; Granger and others, 1996). The great utility of ^{10}Be-derived erosion rates is that they are integrated over millennia, thus masking short-term variance and allowing robust interpretations of geomorphic change over longer time-scales than contemporary data allow.

Several assumptions underlie the translation of measured isotopic abundances into erosion rates via conceptual and mathematical models (Bierman, 1994). For both sediment and bedrock it is assumed that the cosmic ray flux is constant over time, that

there has been no ephemeral shielding from soil, snow, or sediments (Bierman and

Nichols, 2004), and that the nuclide production rate is known. For sediment, additional

assumptions include constant or minimal sediment storage in the sampled basin, steady

rates of erosion, adequate mixing of sediment, and homogenous quartz distribution.

Methods

Sampling Strategy – Basin Selection

The region around and including Shenandoah National Park is ideal for testing the

effect of lithology on erosion rates because four distinct lithologies crop out: granite,

metabasalt, quartzite, and siliciclastic rocks. In order to determine whether a relationship

between lithology and erosion rate exists, we sampled sediment originating from 41

single-lithology basins and two temporal replications, 11 multilithology basins, and 5

bedrock outcrops. Four initial sample sites were chosen, one for each lithology using

1:24,000 USGS topographic maps and 1:62,500-scale geologic maps of the Park. At

these first four sample sites grain-size splits (0.25 – 0.85 mm, 0.85 – 2 mm, 2 – 10 mm,

and >10 mm) were collected (11/2005) and later processed separately in order to test the

relationship between ^{10}Be concentrations and grain size (Brown and others, 1995; Clapp

and others, 1997; Clapp and others, 1998; Clapp and others, 2001; Clapp and others,

2002; Matmon and others, 2003a; Matmon and others, 2003b; von Blanckenburg, 2005;

Belmont and others, 2006; Duxbury and others, 2006; Sullivan and others, 2006; Sullivan

and others, accepted).

Sample sites (figs. 2A and 2B) were subsequently selected using ArcGIS to

generate a list of single-lithology drainage basins that also considered criteria such as

basin size, location, mean slope, and elevation range. These basins were delineated using

several GIS layers including: USGS 10 m DEM's (Digital Elevation Models) (Chirico

and Tanner, 2004) along with bedrock geology that provided an overall characterization

of the physiography and principal bedrock formations within the park; National

Hydrography Datasets (NHD) provided the stream layer; digital contour maps (DRG)

were overlaid to provide a visual confirmation of streams and a digitalized layer of the

National Park Boundary. Once the basins were delineated, and the desired criteria were

established, we chose specific sample sites so that basins would be of sufficient size to

allow for adequate mixing of sediments within the basin (about a km^2).   The basins we

selected represented a variety of average slopes, basin sizes, elevations, and lithologies.

The sample sites (figs. 2A and 2B) were chosen as single lithology basins where

possible. However, in some cases subordinate amounts of other rock types crop out. To

deal with this we developed a series of rules that provided upper limits for the surface

area of other lithologies in a "single" lithology basin. These rules were based on quartz

yields we obtained from sediment as we purified quartz using repeated, dilute HF/HNO_3

etching. We find the following average quartz yields in fluvial sediment from what we

know to be single lithology basins: granite (43%), metabasalt (25%), quartzite (63%),

siliciclastic rocks (24%). Basins were identified as single-lithology based on the

following rules: metabasalt basins contain ≤ 10% granite or ≤ 20% siliciclastic rocks by

area and granite basins contain ≤ 20% metabasalt by area. These cutoffs were chosen in

order to ensure that at least 90% of the quartz comes from the dominant lithology in the

basin.

Field Sampling Methods

Sediment samples were gathered in November 2005, and May and December

2006, from active river or stream channels within or near to the boundaries of the park.

Basin size and slope of the sampled basins are a function of geographical location of each

lithology (table 1). The total area represented by the sampled basins is ~355 km^2 (~44%)

of the ~810 km^2 area of the Park (http://www.nature.nps.gov/stats/acreagemenu.cfm).

For all the quartz-rich lithologies, < 0.5 kg of sample was sufficient to carry out the lab processes to isolate ^{10}Be. Metabasalt, which contained less quartz and more hard-to-remove mafic material, required several times as much sample. Most samples were wet sieved in the field to the 0.25-0.85 mm size fraction, the most suitable size for processing in the lab. Digital photographs were taken of each sample site and samples were labeled and stored for transport in gallon zip-lock bags. At the University of Vermont, samples were oven dried and if necessary re-sieved using a rotational tapping device to the 0.25-0.85 mm size fraction.

During a subsequent field season (12/2006), we collected bedrock samples that were not accessible in the summer due to heavy vegetation hiding outcrops. Five bedrock samples were collected using a hammer and chisel, based on accessibility and occurrence, from each of the four lithologies and from Massanutten Mountain (Silurian sandstone) in the Valley and Ridge Province to the west. The bedrock samples were taken from non-vegetated outcrops with flat lying surfaces and were ~2-5 cm in thickness. The bedrock samples were crushed, ground, and sieved to the 0.25-0.85 mm size fraction at the University of Vermont.

Laboratory Methods

Quartz was purified in the mineral separation lab at the University of Vermont by ultrasonic and heated roller etching of samples in hot 6N HCl for two 24-hour periods, followed by three 24-hour etches in dilute HF/ HNO_3. After the samples were dry, density separation removed heavy minerals such as magnetite and ilmenite, before a final 48-hour etch in dilute HF/ HNO_3. For quartz purification purposes, ~60 g of quartzite, ~120 g of granite and siliciclastic rocks and ~180-240 g of metabasalt was etched to obtain a 20 to 40 g sample of pure quartz in order to isolate ^{10}Be. The initial four samples with grain-size splits were extracted at the University of Vermont using standard techniques (Bierman and Caffee, 2001). The ^{10}Be isolated from the initial samples was measured using accelerator mass spectrometry (AMS) at the Lawrence Livermore Laboratory, with one process blank per seven samples; the average of the UVM blanks from the LLNL run was subtracted from the measured ^{10}Be ratios. The remaining samples were processed to isolate ^{10}Be following procedures based on methods modified from Kohl and Nishiizumi (1992) and Child and others (2000), at the GU-SUERC Cosmogenic Nuclide Laboratory (CNL) (http://web.ges.gla.ac.uk/~dfabel/CN_intro.html) at the Scottish Universities Environmental Research Centre (SUERC)

(http://www.gla.ac.uk/suerc/index.html) in East Kilbride, Scotland. The ^{10}Be isolated

from the remaining samples was then measured using accelerator mass spectrometry

(AMS) at the SUERC Accelerator Mass Spectrometry Laboratory. Process blanks were

run with every fifteen samples and average blank ^{10}Be/^{9}Be ratios were subtracted from

measured ratios of samples.

Calculation of Erosion Rates from ^{10}Be and Analysis

^{10}Be concentrations of the initial four samples with grain-size splits were

normalized using standards developed by Nishiizumi at LLNL assuming a ^{10}Be half life

of 1.5 My (KNSTD 3110, $^{10/9}$Be ratio standard of 3.15 x 10^{12}). The remaining samples

analyzed at CNL using the standard NIST (SRM4325) (National Institute of Standards

and Technology) and a $^{10/9}$Be ratio standard of 3.06 x 10^{11} analogous to the original value

of the LLNL standard prior to the recent recalculation of the ^{10}Be half-life (Nishiizumi

and others, 2007). The ^{10}Be concentrations of all the samples were then corrected for

latitude-altitude based on the polynomials of Lal (1988) for neutrons only. Basin

hypsometry was calculated using ArcGIS. Basin-scale erosion rates were modeled using

the interpretive model of Bierman and Steig (1996) with a normalized sea level, high

latitude ^{10}Be production rate of 5.2 atoms g^{-1} quartz yr^{-1}, an attenuation depth of 165 g

cm^{-2}, and assuming a rock density of 2.7 g cm^{-3}. Bedrock erosion rates were calculated

using procedures developed by Lal (1988). Erosion rates and ^{10}Be concentrations were

analyzed with respect to lithology, slope, basin size, basin location and grain-size. The

data were transformed using a square root transformation of the model erosion rate, and

simple/multiple regression analysis, descriptive statistics, analysis of covariance, and

one-way ANOVA tests to a 95% confidence level, were applied.

Data

Bedrock Samples: ^{10}Be Concentrations and Erosion Rates

The four bedrock samples have an averaged ^{10}Be concentration of 8.30 ± 5.1 x

10^5 atoms (g quartz)$^{-1}$ (one standard deviation), and a range of normalized ^{10}Be

concentrations from 4.44 ± 0.12 x 10^5 to 16.9 ± 0.44 x10^5 atoms (g quartz)$^{-1}$ across the

lithologies. Sandstone from Massanutten Mountain has a ^{10}Be concentration of 13.5 ±

0.36 x 10^5 atoms (g quartz)$^{-1}$.   The erosion rates for these samples range from 2.4-13.0

m/My (table 3).

Fluvial Samples
^{10}Be concentrations and erosion rates: grain-size analysis

Grain-size specific ^{10}Be analysis of four samples showed no reproducible trend of

concentration with grain size (table 4, fig. 4). The ^{10}Be concentrations (table 4) for these

grain-size splits indicate that within each lithology there are similar average dosing

histories. ^{10}Be concentrations (table 4) in granite and metabasalt samples exhibit

monotonic decreases with increasing grain-size (figs. 4A and B). Quartzite samples

exhibit a monotonic decrease through increasing grain-size except for >10 mm fraction

(fig. 4C). Sediment from siliciclastic basins has no discernable pattern (fig. 4D). Grain-

size specific erosion rates calculated from the grain-size splits (table 4) are lowest in

quartzite (5.7 – 8.5 m/My) and metabasalt (4.1 – 5.4 m/My), and higher for siliciclastic

(8.7 – 13.2 m/My) and granite (14.6 – 22.4 m/My).

^{10}Be concentrations and erosion rates

Fluvial samples (n = 54) (tables 2 and 4), collected from streams draining the

highlands contain significant concentrations of ^{10}Be, ranging from 2.11-11.5 x 10^5 atoms

(g quartz)$^{-1}$ (table 3). Within each lithology, ^{10}Be concentration ranges were: granite,

2.11–5.42 x 10^5 atoms (g quartz)$^{-1}$; metabasalt, 2.55–11.5 x 10^5 atoms (g quartz)$^{-1}$;

quartzite, 2.88–9.55 x 10^5 atoms (g quartz)$^{-1}$ and siliciclastic rocks, 3.03–7.68 x 10^5

atoms (g quartz)$^{-1}$ (table 4). Multilithology samples (larger basins containing mixed

sediment derived from more than one lithology) have ^{10}Be concentrations similar (2.52-

9.22 x 10^5 atoms (g quartz)$^{-1}$) to average ^{10}Be concentration for all lithologies (2.11-11.5

x 10^5 atoms (g quartz)$^{-1}$).

The inferred erosion rates for the basins sampled range from 3.8 ± 0.5 to 23.6 ±

3.0 m/My for all lithologies (table 4). The mean erosion rate for single-lithology basins

is 11.3 ± 4.8 m/My (n = 43). By lithology, the erosion rate ranges are: granite, 7.9–21.8

m/My; metabasalt, 4.8– 23.6 m/My; quartzite, 4.7–16.8 m/My; and siliciclastic rocks,

6.2–16.7 m/My. The mean erosion rate for multilithology basins (n = 11) is 10.2 ± 4.6

m/My, with a range of 3.8-17.6 m/My. Erosion rates for the Shenandoah and

Rappahannock Rivers are 7.3 ± 0.9 m/My and 13.8 ± 1.8 m/My, respectively. Temporal

replicates SH-18 and SH-41 (SH-02, metabasalt and SH-36, quartzite - samples collected

~6 months apart) fall within 2 sigma in terms of ^{10}Be concentration and erosion rate

(table 4) indicating low variance in isotope concentration over this time period.

When data from the sampled basins are considered by lithology, a positive

correlation exists between erosion rate and slope for all lithologies, but the only

statistically significant regression (p ≤ 0.05) relationships between slope and erosion rate

are for siliciclastic rocks (p = 0.05, R^2 = 0.49) (table 5, fig. 5C) and all fluvial samples (p

= 0.02, R^2 = 0.10). Quartzite exhibits a relatively strong correlation between erosion rate

and slope ($R^2 = 0.45$), but is not statistically significant ($p \leq 0.07$). There is no significant

relationship between erosion rate and basin area for any lithology, except for all fluvial

samples (table 5, figs. 6A-D), indicating that the sediments are well mixed. The only

statistically significant regression ($p \leq 0.05$) correlating slope and basin area is for

metabasalt ($p = 0.03$, $R^2 = 0.57$) (table 5, figs. 7A-D), where there is a positive linear

relationship, as slope increases, basin area increases. This is perhaps from larger

metabasalt basins closer to the ridgeline incorporating the summit flat. The lack of

significant relationships between basin area and slope among the other lithologies is

likely the result of the study area's morphology, which is a sloping highland, excepting a

metabasalt dominated summit flat. Even the largest sampled basins, with the exception

of the Shenandoah River watershed, did not contain significant lowland areas.

Discussion

New cosmogenic nuclide data clearly indicate that over millennial time scales,

outcrops and drainage basins in the Blue Ridge around Shenandoah National Park are

eroding slowly, on the order of meters to a few tens of meters per million years. This

finding is in good agreement with other cosmogenic (Matmon and others, 2003a;

Matmon and others, 2003b; Reuter, 2005; Ward and others, 2005; Sullivan and others,

accepted) and thermochronologic studies (Naeser and others, 2004; Spotila and others, 2004; Naeser and others, 2005; Naeser and others, 2006a; Naeser and others, 2006b) in the Appalachian Mountains.

Comparing Erosion Rates

Bedrock

The range of bedrock (2.4-13 m/My, n = 5) and single lithology, basin-scale erosion rates (4.7 to 24 m/My, n = 42) overlap (fig. 8). Although the number of bedrock samples is limited and the variability in erosion rates too great to provide much statistical power, bedrock outcrops are eroding more slowly on average ($\mu = 7.9 \pm 4.4$ m/My, n = 5, p = 0.001) than single-lithology drainage basins ($\mu = 11.5 \pm 4.7$ m/My, n = 42). This discrepancy between bedrock and fluvial erosion rates has been noted elsewhere (Bierman and Caffee, 2001; Clapp and others, 2001; Clapp and others, 2002; Reuter, 2005) and likely reflects the increased efficacy of bedrock to saprolite conversion under a soil mantle (Heimsath and others, 1999; Heimsath and others, 2000; Heimsath and others, 2001). Sampling bedrock outcrops near and along ridgelines biases sample collection toward the most high-standing topography, and thus perhaps some of the most stable elements of the landscape.

Grain-size

Grain-size specific cosmogenic analysis of four sediment samples showed no consistent trend of concentration but did indicate ~26 to 34 % differences on average between the sand-fraction (250-850 mm) we analyzed and larger grain sizes. Such differences may in part account for the variability in calculated erosion rates we observe between basins and may reflect different source areas or processes delivering different grain sizes to the channels (Brown and others, 1995; Matmon and others, 2003a; Matmon and others, 2003b). Because the differences in nuclide concentrations between grain-sizes are not systematic and in most cases are not large, they may add noise but do not bias the results.

Lithology

In the Shenandoah National Park area, there are few statistically significant relationships between landscape-scale metrics and fluvial erosion rates. Of the four lithologies tested, only quartzite was significantly different from granite when comparing erosion rates ($p = 0.001$) (fig. 8). The stability or resistance to weathering of quartzite is well known. Goudie (1995) suggests that its resistance is due in part to higher silica content of rock, and this is confirmed by field studies (Merschat, 1997) and at the

landscape scale using cosmogenic nuclides by Bierman and others, (1998). The lack of a

definitive relationship between basin-scale erosion rates and lithology echoes previous

work in Namibia (Bierman and Caffee, 2001), the Great Smoky Mountains (Matmon and

others, 2003a; Matmon and others, 2003b), and the Susquehanna River Basin (Reuter,

2005).

Hack (1982) suggested that the lower altitude of the Chilhowee Group rocks is

indicative of less resistance than the metabasalt (Catoctin Formation) and granite (Pedlar

Formation). Given the similar erosion rates for different lithologies measured in this

study, it is more likely that the altitude of the Chilhowee Group is due to geologic

controls, rather than any difference in erosional resistance.

In contrast to findings elsewhere in the Appalachians (Matmon and others, 2003a;

Matmon and others, 2003b; Reuter, 2005; Sullivan and others, accepted) where slope and

basin-scale erosion rate were positively and significantly correlated, in the Shenandoah

National Park area, siliciclastic rocks are the only lithology for which there is a

significant correlation between erosion rate and slope ($p = 0.05$, $R^2 = 0.49$, fig. 5A and

tables 4 and 5). Although there is a significant relationship between cosmogenically-

estimated erosion rates and basin area for all samples, the relationship is very weak ($R^2 =$

0.07). The variability of erosion rates appears to decrease with increasing basin area,

similar to results elsewhere in the Appalachian Mountains and consistent with fluvial

mixing downstream (Matmon and others, 2003a; Matmon and others, 2003b; Reuter,

2005; Sullivan and others, accepted). The consistency of erosion rates over varying basin

sizes are indicative of well-mixed sediments, which received the bulk of their cosmic-ray

dosing on the hillslopes before entering the fluvial system.

Erosion rates appear to be different on either side of the drainage divide (figs. 9

and 10, table 6). The ultimate cause of this significant difference ($p \leq 0.004$ – single-

lithology basins, $p \leq 0.001$ – all basins) is uncertain, but basin erosion rates on the eastern

side of the divide are faster ($\mu = 13.9 \pm 4.0$ m/My) than those on the west ($\mu = 10.0 \pm 4.7$

m/My) ($p = 0.001$). These east-west variations in erosion rates are mirrored by the

erosion rates obtained from two of the major rivers draining the Park, the Rappahannock

River to the east (13.8 m/My) and the Shenandoah River to the west (7.3 m/My). The

Shenandoah River drainage on the west has lower erosion rates and higher base-level

than the Rappahannock River that drains the eastern margin of the Blue Ridge. This east-

west dichotomy may be a function of rock type. Weathered metagranites with more rapid

erosion rates underlie the lowlands to the east. To the west, resistant members of the

Chilhowee Group rocks largely underlie the Page Valley, and the Shenandoah River

flows over them (not carbonate rocks).

The east-west dichotomy in erosion rates could be the result of different landscape

history. Perhaps westward migration of the drainage system since pre-Miocene time,

promoted faster erosion rates, and subsequently, Miocene drainage capture diverted

drainages from the west to the east (Naeser and others, 2001; Pazzaglia and others, 2006).

In this scenario, the Great Valley to Blue Ridge crest relief has remained relatively

unchanged since the Miocene, unlike the Piedmont which may have been lowered

significantly since drainage capture, due to very rapid incision of Atlantic slope

drainages. Pazzaglia and Gardner (1994, 2000) suggest that epierogenic uplift, change in

climate and/or rapid change in the size of the Atlantic slope drainage basin may be

responsible for the removal of regolith during the middle Miocene. Spotila and others,

(2004) thermochronometry data suggests that the Piedmont experienced increased

exhumation throughout the Cenozoic. The topography was higher than at present, and

subsequent late Cenozoic erosion of this topography may be equated with the increased

sedimentation rates observed in the Baltimore Canyon Trough (Pazzaglia, 1993;

Pazzaglia and Gardner, 1994). Reusser and others, (2004) identified late Pleistocene rapid

bedrock incision in the Susquehanna and Potomac Rivers, suggesting both climate

change and flexural upwarping of the Atlantic passive margin, steepening river gradients,

as catalysts for this increased incision.

The effect of climate and periglacial processes on erosion rates

While others have noted evidence consistent with the effects of climate change

and periglacial processes on landforms in the Blue Ridge region (Clark and Ciolkosz,

1988; Kutzbach and others, 1998; Bard, 2003; Driese and others, 2005; Leigh and Webb,

2006), it is not at all clear how and even if changing climate regimes affect

cosmogenically-determined bedrock and basin-scale erosion rates found in this and other

studies. Three lines of evidence argue against any significant climatic effect on erosion

rates: 1) the similarity between Appalachian Mountain erosion rates calculated from both

thermochronometry and sediment accumulation integrated over 10^7 years and

cosmogenically-determined erosion rates integrated over much shorter glacial-interglacial

time scales where significant climate swings (Barron, 1989; Kutzbach and others, 1998;

Driese and others, 2005) and periglacial activity occurred (Clark and Ciolkosz, 1988;

Barron, 1989; Braun, 1989; Kutzbach and others, 1998; Driese and others, 2005). 2)

Riebe and others (2001a, 2004) inability to detect basin-scale erosion rate differences

related to differences in temperature and precipitation in drainages underlain by crystalline rocks. 3) The stability (measured by ^{10}Be accumulation) of quartz conglomerate and sandstone bedrock surfaces exposed to periglacial activity at Dolly Sods, West Virginia (Hancock and Kirwan, 2007). At Dolly Sods, where significant periglacial activity occurred, average erosion rates are (5.7 m/My) similar to erosion rates we measure in bedrock (7.9 ± 4.4 m/My) cropping out at lower elevations and farther from the glacial margin where periglacial activity was presumably less.

Highland vs. lowland erosion rates

Comparison of erosion rates in the highlands with those of the adjacent lowlands and of the Blue Ridge further to the south is illustrative. Despite the presence of easily dissolved carbonate rocks in the Valley and Ridge to the west, the Shenandoah Blue Ridge is lowering (μ = ~11.4 m/My, granite, metabasalt, quartzite, siliciclastic rocks) at a rate within the range of prior estimates for the Valley and Ridge, 8-30 m/My, (carbonates, White, 1984; White and White, 1991; White, 2000). However, the Shenandoah Blue Ridge is eroding somewhat faster, 4.4 to 26 m/My, (granite, metabasalt, quartzite, siliciclastic rocks) than the low-lying Piedmont province to the east, 4.5-8 m/My, (metapelite, metagraywacke, granite, diabase, serpentine, Pavich, 1985); 10

m/My, (Stanford and others, 2002 , reconstruction); 9.7 m/My, (micaceous schist and

gneiss, Sullivan and others, accepted). Together these data suggest that relief between the

Blue Ridge and the adjacent piedmont is slowly decreasing, mirroring findings by

Sullivan and others (accepted) farther to the south.

Placing Shenandoah Region Erosion Rates in Context

Cosmogenically determined bedrock and basin-scale erosion rates for the

Shenandoah National Park region are in general consistent with those estimated

elsewhere in the Appalachian Mountains (Matmon and others, 2003a; Matmon and

others, 2003b; Reuter, 2005; Ward and others, 2005; Hancock and Kirwan, 2007;

Sullivan and others, accepted). Erosion rates for Shenandoah National Park region with

its mixed lithologies (~11 m/My) are indistinguishable from basin-scale erosion rates

measured in schist and gneiss (12.5 m/My) for the Blue Ridge just above the Blue Ridge

Escarpment (Sullivan and others, accepted), ~300 km to the south.

There are however, some differences between the Shenandoah region and other

areas of the southern and central Appalachian Mountains. Average basin-scale rates in

the Shenandoah region (~11 m/My) are in general half as fast as those in the Great

Smoky Mountains (27 ± 6 m/My; Matmon and others, 2003a; Matmon and others,

2003b). The Shenandoah basin-scale erosion rates are similar to those in the Valley and

Ridge of the Susquehanna River (13 m/My; Reuter, 2005). The average bedrock erosion

rates around Shenandoah (7.9 ± 5.0 m/My) are similar to the sandstone on the

Appalachian Plateau at Dolly Sods, West Virginia (5.7 m/My) (Hancock and Kirwan,

2007) and that of the granite that underlies Panola Mountain in the Georgia Piedmont (7

m/My; Bierman, 1993).

Both the bedrock (7.8 m/My) and basin-scale erosion rates (~11 m/My)

determined in the Shenandoah National Park area are consistent with those measured

around the world in diverse tectonically stable areas, independent of climate. Average

bedrock erosion rates have been measured in arid environments such as Australia,

Namibia, and Nevada (~0.7-4 m/My), and in humid-temperate regions such as Puerto

Rico and Hawaii (2-25 m/My) (Kurz, 1986; Bierman and Turner, 1995; Shepard and

others, 1995; Small and others, 1997; Cockburn and others, 1999; Bierman and Caffee,

2001; Granger and others, 2001; Bierman and Caffee, 2002; Belton and others, 2004).

Bedrock erosion rates in tectonically stable regions are generally low, despite the varying

climatic environments, which supports Riebe and others (2001a) conclusion from the

Sierra Nevada Mountains that climate only weakly influences erosion rates.

71

Why does the Blue Ridge of the Shenandoah National Park area look the way it does?

The lack of significant and pervasive lithologic and slope relationships with basin-scale erosion rates appears to contradict the long-standing observation that structure and lithology control the large-scale geomorphology of the Shenandoah region. Cosmogenic data suggest that although there are small variances in basin-scale erosion rate by lithology (quartzite eroding more slowly than granite), there is no correlation between erosion rate and basin average slope, except for siliciclastic ($R^2 = 0.49$) and quartzite basins ($R^2 = 0.45$) (fig. 5C, tables 4 and 5), with only siliciclastic basins being statistically significant ($p \leq 0.05$). This lack of correlation stands in stark contrast to other areas in the Appalachians such as the Great Smoky Mountains (Matmon and others, 2003a; Matmon and others, 2003b), the Blue Ridge Escarpment (Sullivan and others, 2006; Sullivan and others, accepted), and the Susquehanna Drainage Basin (Reuter, 2005) where erosion rate and slope are positively and significantly correlated.

One can consider the slope/erosion rate relationship in the context of two long-standing but contrasting qualititative models of landscape behavior, those of Davis and Hack. Davis' *Geographic Cycle* (1899), developed from observations in the Susquehanna River and the Appalachian Mountains, describes how topography changes

over time. Davis' model is based on the peneplain concept where in an unperturbed landscape, topography will diminish over time, until only the flat, low relief peneplain exists. Alternatively, Hack's (1960) model of *dynamic equilibrium* describes where landscape morphology is adjusted to the erosional resistance of the underlying rock over the long-term.

The independence of erosion rate from slope, lithology, and basin area in the Shenandoah region dataset supports Hack's model of *dynamic equilibrium.* In Hack's schema, differences in erosional resistance or rock strength are compensated for by slope; less resistant lithologies have low slopes, and more resistant lithologies have steeper slopes yet all erode at similar rates, as the Shenandoah region data suggests. Hack's model in particular can be used as a framework within which to assess the landscape evolution of the Blue Ridge Province in the Shenandoah National Park region.

In a modern adaptation of Hack's theme, Riebe and others (2000) cosmogenic data from very small basins in the Sierra Nevada Mountains, suggest that slope and erosion rate co-vary only when base-level has lowered and the landscape upstream has not adjusted. If Riebe and others (2000) supposition is correct, the base-level to which the regions' streams are graded has been stable, with the exception of basins underlain by

quartzite. Perhaps the time scale of adjustment for resistant quartzite is longer than that

for other lithologies? Stream profiles in the Shenandoah region, did not reveal distinct

features associated with stream adjustment such as knickpoints, but this does not

necessarily rule out the possibility that the quartzite streams are in a period of adjustment.

Broader application of this line of reasoning suggests that base-level fall and consequent

landscape adjustment is still occurring in the Susquehanna River Basin, the Great Smoky

Mountains, and the Blue Ridge Escarpment areas, and also perhaps within the quartzite

basins of the Shenandoah region. Of the high-relief areas examined so far in the

Appalachians, only the area around Shenandoah National Park area appears to meet

Hack's definition of *dynamic equilibrium*.

If quartzite is the most resistant rock in this region why isn't it holding up the

highlands? To answer this question it is necessary to examine the geologic controls

operating within the Park. Quartzites underlie Massanutten Mountain (west of Blue

Ridge) and low hills along the west flank of the Blue Ridge. These low hills are in the

footwall of Late Paleozoic thrust faults, which decapitated the folded quartzite strata, i.e.,

they never cropped out at a much higher elevation. North of the Stanley Fault at Thornton

Gap (Bailey and others, 2006), flat-lying quartzite does underlie a highland area.

Reconstructions of cross-sections show that the current morphology of the Blue Ridge is

a function of the erosion level on faulted and folded strata that plunge to the northeast.

Structurally higher areas have been eroded down to Mesoproterozoic granite (Bailey and

others, 2006). Locally, the near flat-lying metabasalt overlies the granite and caps the

highlands along the ridgeline, and at lower elevations, the flat-lying quartzite overlies the

metabasalt.

All things being constant, the cap rocks will continue to erode, exposing the

underlying strata and rocks as the landscape is lowered (Bailey and others, 2006).

Perhaps this juxtaposition of the local stratigraphy gets to the essence of what Hack's

model of *dynamic equilibrium* espouses? It appears that structure in part controls

landscape morphology and erosion has yet to exert control on a scale sufficient to alter

these structurally controlled mega geomorphic patterns.

Conclusion

The metamorphic rocks of the Shenandoah National Park region do not fit into the

simple landscape model of ridge-capping resistant rocks that has been applied to other

areas of the Appalachian Mountains (Matmon and others, 2003a; Matmon and others,

2003b; Reuter, 2005). In the Park highlands, metabasalt and metagranites, rather than the

more erosion-resistant quartzite, form the ridgeline. The lack of significant lithologic and

slope relationships with basin-scale erosion rates supports Hack's (1960) model of

dynamic equilibrium where landscape morphology is adjusted to the erosional resistance

of the underlying rock over the long-term. The landscape of the Blue Ridge Province is a

product of slow erosion, with millennial scale erosion rates averaging ~11 m/My, similar

to post-orogenic denudation rates integrated over times periods 1 to 2 orders of

magnitude longer. This steady erosion over time suggests that the region's landscape

may well have remained grossly similar for millions of years. Slow denudation of ancient

rocks is most likely driving slow but continual isostatic uplift that maintains self-similar

topography (Pavich, 1985) controlled by rock competence and structure.

References

Badger, R. L., and Sinha, A. K., 1988, Age and Sr isotopic signature of the Catoctin
volcanic province; implications for subcrustal mantle evolution: Geology, v. 16,
p. 692-695.

Bailey, C. M., Southworth, S., and Tollo, R. P., 2006, Tectonic history of the Blue Ridge,
north-central Virginia, *in* Pazzaglia, F. J., editor, Excursions in Geology and
History: Field Trips in the Middle Atlantic States: Boulder, The Geological
Society of America, p. 22.

Bard, E., 2003, North-Atlantic sea surface temperature reconstruction: IGBP
PAGES/World Data Center for Paleoclimatology Data Contribution Series, v. 26.

Barron, E. J., 1989, Climate variations and the Appalachians from the Late Paleozoic to
the present: Results from Model Simulations: Geomorphology, v. 2, p. 99-118.

Belmont, P., Pazzaglia, F. J., and Gosse, J., 2006, Using the 10-Be grain size dependency
in alluvial sediments to investigate hillslope and channel processes: American
Geophysical Union, Fall Meeting 2006, abstract# H21H-06.

Belton, D. X., Brown, R. W., Kohn, B. P., Fink, D., and Farley, K. A., 2004, Quantitative
resolution of the debate over antiquity of the central Australian landscape:
implications for the tectonic and geomorphic stability of cratonic interiors: Earth
and Planetary Science Letters, v. 219, p. 21-34.

Bierman, P., and Nichols, K., 2004, Rock to sediment - Slope to sea with 10-Be - Rates
of landscape change: Annual Review of Earth and Planetary Sciences, v. 32, p.
215-255.

Bierman, P., and Turner, J., 1995, [10]Be and [26]Al evidence for exceptionally low rates of
Australian bedrock erosion and the likely existence of pre-Pleistocene landscapes:
Quaternary Research, v. 44, p. 378-382.

Bierman, P. R., 1993, In situ produced cosmogenic isotopes and the evolution of granitic
landforms: Ph.D. Thesis, University of Washington, Seattle, WA, p. 289.

—, 1994, Using in situ produced cosmogenic isotopes to estimate rates of landscape evolution; a review from the geomorphic perspective: Journal of Geophysical Research, B, Solid Earth and Planets, v. 99, p. 13885-13896.

Bierman, P. R., and Caffee, M., 2002, Cosmogenic exposure and erosion history of ancient Australian bedrock landforms: Geological Society of America Bulletin, v. 114, p. 787-803.

Bierman, P. R., and Caffee, M. W., 2001, Slow rates of rock surface erosion and sediment production across the Namib Desert and escarpment, Southern Africa: American Journal of Science, v. 301, p. 326-358.

Bierman, P. R., Caffee, M. W., Davis, P. T., Marsella, K., Pavich, M., Colgan, P., Mickelson, D., and Larsen, J., 2002a, Rates and timing of Earth surface processes from in situ-produced cosmogenic Be-10, *in* Grew, E. S., editor, Reviews in Mineralogy and Geochemistry: Beryllium; mineralogy, petrology, and geochemistry: Washington, DC, United States, Mineralogical Society of America and Geochemical Society, Washington, DC, p. 147-205.

Bierman, P. R., Neis, S., Zehfuss, P., Burke, R., Gillespie, A., and Caffee, M., 1998, 10-Be and 26-Al age estimates for five tectonically offset fan surfaces, Owens Valley, CA: Geological Society of America, 1998 annual meeting Abstracts with Programs - Geological Society of America, v. 30, p. 141.

Bierman, P. R., Pavich, M., Eaton, L. S., Finkel, R., and Larsen, J., 2002b, The Boulders of Madison County, Geological Society of America Abstracts with Programs, 2002 Denver Annual Meeting.

Bierman, P. R., and Steig, E., 1996, Estimating rates of denudation and sediment transport using cosmogenic isotope abundances in sediment: Earth Surface Processes and Landforms, v. 21, p. 125-139.

Bishop, P., 2007, Long-term landscape evolution: linking tectonics and surface processes: Earth Surface Processes and Landforms, v. 32, p. 329-365.

Braun, D. D., 1989, Glacial and periglacial erosion of the Appalachians: Geomorphology, v. 2, p. 233–256.

Brown, E. T., Stallard, R. F., Larsen, M. C., Raisbeck, G. M., and Yiou, F., 1995, Denudation rates determined from the accumulation of in situ-produced [10]Be in the Luquillo Experimental Forest, Puerto Rico: Earth and Planetary Science Letters, v. 129, p. 193-202.

Child, D., Elliott, G., Mifsud, C., Smith, A. M., and Fink, D., 2000, Sample processing for earth science studies at ANTARES: Nuclear Inst. and Methods in Physics Research, B, v. 172, p. 856-860.

Chirico, P., and Tanner, S., 2004, Shaded relief image map of topogrid derived 10 meter resolution digital elevation model of the Shenandoah National Park and surrounding region, Virginia, U.S: United States Geological Survey Open-File Report 04-1321.

Clapp, E., Bierman, P. R., and Caffee, M., 2002, Using ^{10}Be and ^{26}Al to determine sediment generation rates and identify sediment source areas in an arid region drainage basin: Geomorphology, v. 45, p. 89-104.

Clapp, E. M., Bierman, P. B., and Caffee, M. W., 1998, Estimating long-term erosion rates in a hyper-arid region using in situ produced cosmogenic 10-Be and 26-Al in sediment and bedrock: Geological Society of America, 1998 annual meeting Abstracts with Programs - Geological Society of America, v. 30, p. 361.

Clapp, E. M., Bierman, P. R., and Caffee, M., 1997, Rates of erosion determined using in situ produced cosmogenic isotopes in a small arroyo basin, northwestern New Mexico: Geological Society of America, 1997 annual meeting Abstracts with Programs - Geological Society of America, v. 29, p. 371-372.

Clapp, E. M., Bierman, P. R., and Caffee, M. W., 1999, Sediment generation and export rates in the Nahal Yael drainage basin, determined from cosmogenic ^{10}Be and ^{26}Al, Negev Desert, southern Israel: Geological Society of America, 1999 annual meeting Abstracts with Programs - Geological Society of America, v. 31, p. 256.

Clapp, E. M., Bierman, P. R., Nichols, K. K., Pavich, M., and Caffee, M., 2001, Rates of sediment supply to arroyos from upland erosion determined using in situ produced cosmogenic ^{10}Be and ^{26}Al: Quaternary Research (New York), v. 55, p. 235-245.

Clapp, E. M., Bierman, P. R., Schick, A. P., Lekach, J., Enzel, Y., and Caffee, M., 2000, Sediment yield exceeds sediment production in arid region drainage basins: Geology, v. 28, p. 995-998.

Clark, G. M., and Ciolkosz, E. J., 1988, Periglacial geomorphology of the Appalachian Highlands and Interior Highlands south of the glacial border: a review: Geomorphology (Amsterdam), v. 1, p. 191-200.

Cockburn, H. A. P., Seidl, M. A., and Summerfield, M. A., 1999, Quantifying denudation rates on inselbergs in the central Namib Desert using in situ-produced cosmogenic ^{10}Be and ^{26}Al: Geology, v. 27, p. 399-402.

Davis, W. M., 1899, The geographical cycle: Geographical Journal, v. 14, p. 481-504.

Desilets, D., and Zreda, M., 2000, Scaling production rates of terrestrial cosmogenic nuclides for altitude and geomagnetic effects: Geological Society of America Abstracts with Programs, v. 31, p. A-400.

Driese, S. G., Li, Z.-H., and Horn, S. P., 2005, Late Pleistocene and Holocene climate and geomorphic histories as interpreted from a 23,000 ^{14}C yr B.P. paleosol and floodplain soils, southeastern West Virginia, USA: Quaternary Research, v. 63, p. 136-149.

Dunai, T. J., 2000, Scaling factors for production rates of in situ produced cosmogenic nuclides: a critical reevaluation: Earth and Planetary Science Letters, v. 176, p. 157-169.

Duxbury, J., Bierman, P. R., Pavich, M. J., Larsen, J., and Finkel, R. C., 2006, Be Monitoring of Erosion Rates in the Appalachian Mountains, Shenandoah National Park, Virginia, Geological Society of America Abstracts with Programs, 2006 Philadelphia Annual Meeting, p. 278.

Eaton, L. S., Morgan, B. A., Kochel, C., R., and Howard, A. D., 2003a, Quaternary deposits and landscape evolution of the central Blue Ridge of Virginia: Geomorphology, v. 56, p. 139-154.

—, 2003b, Role of debris flows in long-term landscape denudation in the central Appalachians of Virginia: Geology, v. 31, p. 339-342.

Galloway, R. W., 1961, Periglacial Phenomena in Scotland: Geografiska Annaler, v. 43, p. 348-353.

Gathright, T. M., 1976, Geology of the Shenandoah National Park, Virginia: Virginia Division of Mineral Resources Bulletin, v. 86, p. 93.

Gosse, J. C., and Phillips, F. M., 2001, Terrestrial in situ cosmogenic nuclides: theory and application: Quaternary Science Reviews, v. 20, p. 1475-1560.

Goudie, A., 1995, The Changing Earth: Rates of Geomorphological Processes: Oxford, Blackwell, 352 p.

Granger, D. E., Fabel, D., and Palmer, A. N., 2001, Pliocene-Pleistocene incision of the Green River, Kentucky, determined from radioactive decay of cosmogenic ^{26}Al

and [10]Be in Mammoth Cave sediments: Geological Society of America Bulletin, v. 113, p. 825-836.

Granger, D. E., Kirchner, J. W., and Finkel, R., 1996, Spatially averaged long-term erosion rates measured from in situ-produced cosmogenic nuclides in alluvial sediments: Journal of Geology, v. 104, p. 249-257.

Granger, D. E., Kirchner, J. W., and Finkel, R. C., 1997, Quaternary downcutting rate of the New River, Virginia, measured from differential decay of cosmogenic [26]Al and [10]Be in cave-deposited alluvium: Geology, v. 25, p. 107-110.

Hack, J. T., 1960, Interpretation of erosional topography in humid temperate regions: American Journal of Science, v. 258A, p. 80-97.

—, 1965, Geomorphology of the Shenandoah Valley, Virginia and West Virginia, and origin of the residual ore deposits: US Geological Survey Professional Paper, v. 484, p. 84.

—, 1982, Physiographic divisions and differential uplift in the Piedmont and Blue Ridge: US Geological Survey Professional Paper, v. 1265, p. 49.

Hancock, G., and Kirwan, M., 2007, Summit erosion rates deduced from [10]Be: Implications for relief production in the central Appalachians: Geology, v. 35, p. 89-92.

Harris, S. E., and Mix, A. C., 2002, Climate and tectonic influences on continental erosion of tropical South America, 0-13 Ma: Geology (Boulder), v. 30, p. 447-450.

Heimsath, A. M., Chappell, J., Dietrich, W. E., Nishiizumi, K., and Finkel, R. C., 2000, Soil production on a retreating escarpment in southeastern Australia: Geology, v. 28, p. 787-790.

Heimsath, A. M., Dietrich, W. E., Nishiizumi, K., and Finkel, R. C., 1999, Cosmogenic nuclides, topography, and the spatial variation of soil depth: Geomorphology, v. 27, p. 151-172.

—, 2001, Stochastic processes of soil production and transport; erosion rates, topographic variation and cosmogenic nuclides in the Oregon Coast Range: Earth Surface Processes and Landforms, v. 26, p. 531-552.

Hills, R. C., 1969, Comparative weathering of granite and quartzite in a periglacial environment: Geografiska Annaler. Series A, Physical Geography, v. 51, p. 46-47.

King, P. B., 1950, Geology of the Elkton area: Virginia: US Geological Survey Professional Paper, v. 230, p. 82.

Kirwan, M. L., 2002, Upland periglacial features and bare bedrock erosion rates inferred from 10Be, Dolly Sods, West Virginia, Southeastern Geological Society of America Annual Meeting.

Kirwan, M. L., Hancock, G. S., and Small, E. E., 2002, Erosion rates on central Appalachian upland bedrock surfaces deduced from in-situ ^{10}Be: evidence for increasing relief?, EOS Trans. American Geophysical Union Fall Meeting Supplement, Abstract H222B-0896, 2002.

Kiver, E. P., Harris, D. V., and Harris, D. V., 1999, Geology of U.S. parklands: New York, John Wiley.

Kochel, R. C., and Johnson, R. A., 1984, Geomorphology and sedimentology of humid-temperate alluvial fans, central Virginia: Sedimentology of gravels and conglomerates: Canadian Society of Petroleum Geologists Memoir, v. 10, p. 109–122.

Kohl, C. P., and Nishiizumi, K., 1992, Chemical isolation of quartz for measurement of *in-situ*-produced cosmogenic nuclides: Geochimica et Cosmochimica Acta, v. 56, p. 3583-3587.

Kurz, M., 1986, In situ production of terrestrial cosmogenic helium and some applications to geochronology: Geochimica et Cosmochimica Acta, v. 50, p. 2855-2862.

Kutzbach, J., Gallimore, R., Harrison, S., Behling, P., Selin, R., and Laarif, F., 1998, Climate and biome simulations for the past 21,000 years: Quaternary Science Reviews, v. 17, p. 473-506.

Lal, D., 1988, In situ-produced cosmogenic isotopes in terrestrial rocks: Annual Reviews of Earth and Planetary Science, v. 16, p. 355-388.

—, 1991, Cosmic ray labeling of erosion surfaces; in situ nuclide production rates and erosion models: Earth and Planetary Science Letters, v. 104, p. 424-439.

—, 1998, Cosmic ray produced isotopes in terrestrial systems: Journal of Earth System Science, v. 107, p. 241-249.

Lal, D., and Peters, B., 1967, Cosmic ray produced radioactivity on the earth, *in* Sitte, K., editor, Handbuch der Physik: New York, Springer-Verlag, p. 551-612.

Leigh, D. S., and Webb, P. A., 2006, Holocene erosion, sedimentation, and stratigraphy at Raven Fork, Southern Blue Ridge Mountains, USA: Geomorphology, v. 78, p. 161-177.

Lifton, N. A., 2000, A robust scaling model for in situ cosmogenic nuclide production rates: Geological Society of America Abstracts with Programs, v. 31.

Litwin, R. J., Morgan, B., Eaton, S., Wieczorek, G., and Smoot, J. P., 2001, Proxy climate evidence from Late Pleistocene Deposits in the Blue Ridge of Virginia: US Geological Survey Open File Report, p. 01-406.

Matmon, A., Bierman, P. R., Larsen, J., Southworth, S., Pavich, M., and Caffee, M., 2003a, Temporally and spatially uniform rates of erosion in the southern Appalachian Great Smoky Mountains: Geology, v. 31, p. 155–158.

Matmon, A. S., Bierman, P., Larsen, J., Southworth, S., Pavich, M., Finkel, R., and Caffee, M., 2003b, Erosion of an ancient mountain range, the Great Smoky Mountains, North Carolina and Tennessee: American Journal of Science, v. 303, p. 817-855.

Merschat, C. E., 1997, Geology of Yancy County: Raleigh, North Carolina Geological Survey, Division of Land Resources, p. 22.

Morgan, B. A., Eaton, L. S., and Wieczorek, G. F., 2004, Pleistocene and Holocene colluvial fans and terraces in Shenandoah National Park, Virginia, Open-File Report 03-410, U.S. Geological Survey.

Morgan, B. A., Wieczorek, G. F., and Campbell, R. H., 1999, Map of rainfall, debris flows, and flood effects of the June 27, 1995, storm in Madison County, Virginia: United States Geological Survey Geologic Investigation Series Map I-2623A, 1:24,000.

Naeser, C. W., Naeser, N. D., Kunk, M. J., Morgan Iii, B. A., Schultz, A. P., Southworth, C. S., and Weems, R. E., 2001, Paleozoic through Cenozoic uplift, erosion, stream capture, and deposition history in the Valley and Ridge, Blue Ridge, Piedmont, and Coastal Plain provinces of Tennessee, North Carolina, Virginia, Maryland, and District of Columbia, GSA Annual Meeting, November 5-8, 2001.

Naeser, C. W., Naeser, N. D., and Southworth, C. S., 2005, Tracking Across the southern Appalachians *in* Blue Ridge Geology Geotraverse East of the Great Smoky Mountains National Park, Western North Carolina: Carolina Geological Society.

—, 2006a, Tracking Across the Southern Appalachians: Eastern Tennessee and Western Carolinas Geological Society of America Abstracts with Programs, p. 67.

Naeser, N. D., Naeser, C. W., Newell, W. L., Southworth, S., Weems, R. E., and Edwards, L. E., 2006b, Provenance studies in the Atlantic Coastal Plain: What fission-track ages of detrital zircons can tell us about the erosion history of the Appalachians: Geological Society of America Abstracts with Programs, 2006 Philadelphia Annual Meeting, p. 503.

Naeser, N. D., Naeser, C. W., Southworth, C. S., Morgan, B. A., and Schultz, A. P., 2004, Paleozoic to recent tectonic and denudation history of rocks in the Blue Ridge province, central and southern Appalachians - evidence from fission-track thermochronology Geological Society of America Abstracts with Programs, p. 114.

Nishiizumi, K., Imamura, M., Caffee, M. W., Southon, J. R., Finkel, R. C., and McAninch, J., 2007, Absolute calibration of ^{10}Be AMS standards: Nuclear Instruments and Methods in Physics Research Section B: Beam Interactions with Materials and Atoms, v. 258, p. 403-413.

Nishiizumi, K., Lal, D., Klein, J., Middleton, R., and Arnold, J. R., 1986, Production of ^{10}Be and ^{26}Al by cosmic rays in terrestrial quartz in situ and implications for erosion rates: Nature, v. 319, p. 134-136.

Pavich, M., 1985, Appalachian piedmont morphogenesis: weathering, erosion, and Cenozoic uplift, *in* Morisaura, M., and Hack, J., editors, "Tectonic Geomorphology", Proceedings of the 15th Annual Geomorphology Symposium Series: Binghampton, p. 299-319.

Pavich, M. J., 1990, Characteristics, origin, and residence time of saprolite and soil of the Piedmont upland, Virginia, U.S.A., and model testing using cosmogenic ^{10}Be, Geochemistry of the Earth's Surface and of Mineral Formation, 2nd International Symposium: Aix en Provence, France, p. 2.

Pazzaglia, F. J., 1993, Stratigraphy, petrography, and correlation of late Cenozoic middle Atlantic Coastal Plain deposits: Implications for late-stage passive-margin geologic evolution: Geological Society of America Bulletin, v. 105, p. 1617-1634.

Pazzaglia, F. J., Braun, D. D., Pavich, M., Bierman, P., Potter Jr, N., Merritts, D., Walter, R., and Germanoski, D., 2006, Rivers, glaciers, landscape evolution, and active tectonics of the central Appalachians, Pennsylvania and Maryland, *in* Pazzaglia, F. J., editor, Excursions in Geology and History: Field Trips in the Middle Atlantic States: Boulder, The Geological Society of America, p. 247.

Pazzaglia, F. J., and Brandon, M. T., 1996, Macrogeomorphic evolution of the post-Triassic Appalachian mountains determined by deconvolution of the offshore basin sedimentary record: Basin Research, v. 8.

Pazzaglia, F. J., Braun, D. D., Pavich, M., Bierman, P., Potter Jr, N., Merritts, D., Walter, R., and Germanoski, D., 2006, Rivers, glaciers, landscape evolution, and active tectonics of the central Appalachians, Pennsylvania and Maryland, *in* Pazzaglia, F. J., editor, Excursions in Geology and History: Field Trips in the Middle Atlantic States: Boulder, The Geological Society of America, p. 247.

Pazzaglia, F. J., and Gardner, T. W., 1994, Late Cenozoic flexural deformation of the middle U. S. Atlantic passive margin: Journal of Geophysical Research, B, Solid Earth and Planets, v. 99, p. 12,143-12,157.

Pazzaglia, F. J., and Gardner, T. W., 2000, Late Cenozoic large-scale landscape evolution of the US Atlantic passive margin: Geomorphology and Global Tectonics: New York, John Wiley, p. 283–302.

Phillips, W. M., Hall, A. M., Mottram, R., Fifield, L. K., and Sugden, D. E., 2006, Cosmogenic [10]Be and [26]Al exposure ages of tors and erratics, Cairngorm Mountains, Scotland: Timescales for the development of a classic landscape of selective linear glacial erosion: Geomorphology, v. 73, p. 222-245.

Pierce, K. L., 1965, Geomorphic significance of Cretaceous deposits in the Great Valley of southern Pennsylvania: US Geological Survey, Professional Paper 525C, p. 152–156.

Reed Jr, J. C., 1955, Catoctin Formation near Luray: Virginia: Geological Society of America Bulletin, v. 66, p. 871-896.

Reiners, P. W., and Brandon, M. T., 2006, Using thermochronology to understand orogenic erosion: Annual Review of Earth and Planetary Sciences, v. 34, p. 419-66.

Reusser, L. J., Bierman, P. R., Pavich, M. J., Zen, E.-a., Larsen, J., and Finkel, R., 2004, Rapid Late Pleistocene incision of Atlantic passive-margin river gorges: Science, v. 305, p. 499-502.

Reuter, J. M., 2005, Erosion rates and patterns inferred from cosmogenic [10]Be in the Susquehanna River Basin: Masters Thesis, University of Vermont, Burlington, VT, p. 172.

Riebe, C. S., Kirchner, J. W., and Finkel, R. C., 2003, Long-term rates of chemical weathering and physical erosion from cosmogenic nuclides and geochemical mass balance: Geochimica et Cosmochimica Acta, v. 67, p. 4411-4427.

—, 2004, Erosional and climatic effects on long-term chemical weathering rates in granitic landscapes spanning diverse climate regimes: Earth and Planetary Science Letters, v. 224, p. 547-562.

Riebe, C. S., Kirchner, J. W., Granger, D. E., and Finkel, R. C., 2000, Erosional equilibrium and disequilibrium in the Sierra Nevada, inferred from cosmogenic ^{26}Al and ^{10}Be in alluvial sediment: Geology, v. 28, p. 803-806.

— 2001a, Minimal climatic control on erosion rates in the Sierra Nevada, California: Geology, v. 29, p. 447-450.

— 2001b, Strong tectonic and weak climatic control of long-term chemical weathering rates: Geology, v. 29, p. 511–514.

Rodgers, J., 1970, The Tectonics of the Appalachians: New York, Wiley-Interscience, 271 p.

Shepard, M. K., Arvidson, R. E., Caffee, M., Finkel, R., and Harris, L., 1995, Cosmogenic exposure ages of basalt flows; Lunar Crater volcanic field, Nevada: Geology (Boulder), v. 23, p. 21-24.

Small, E. E., Anderson, R. S., Repka, J. L., and Finkel, R., 1997, Erosion rates of alpine bedrock summit surfaces deduced from in situ ^{10}Be and ^{26}Al: Earth and Planetary Science Letters, v. 150, p. 413-425.

Smoot, J. P., 2004, Sedimentary fabrics of stratified slope deposits at a site near Hoover's Camp, Shenandoah National Park, Virginia: US Geological Survey Open-File Report, v. 2004, p. 1059.

Southworth, S., 2008, Geologic map of the Shenandoah National Park area, Virginia: U.S. Geological Survey, Open File Report 2008-XXXX, scale 1:100,000.

Southworth, S., Drake Jr, A. A., Brezinski, D. K., Wintsch, R. P., Kunk, M. J., Aleinikoff, J. N., Naeser, C. W., and Naeser, N. D., 2006, Central Appalachian Piedmont and Blue Ridge tectonic transect, Potomac River corridor: Excursions in Geology and History: Field Trips in the Middle Atlantic States.

Spotila, J. A., Bank, G. C., Reiners, P. W., Naeser, C. W., Naeser, N. D., and Henika, B. S., 2004, Origin of the Blue Ridge escarpment along the passive margin of Eastern North America: Basin Research, v. 16, p. 41-63.

Stanford, S. D., Ashley, G. M., Russell, E. W. B., and Brenner, G. J., 2002, Rates and patterns of late Cenozoic denudation in the northernmost Atlantic Coastal Plain and Piedmont: Bulletin of the Geological Society of America, v. 114, p. 1422-1437.

Stose, G. W., Miser, H. D., Katz, F. J., and Hewett, D. F., 1919, Manganese deposits of the west foot of the Blue Ridge, Virginia: Virginia Geological Survey Bulletin v. 17, p. 166.

Sullivan, C. L., Bierman, P., Pavich, M., Larsen, J., and Finkel, R., 2006, Cosmogenically derived erosion rates for the Blue Ridge Escarpment, Southern Appalachian Mountains, Geological Society of America Abstracts with Programs, 2006 Philadelphia Annual Meeting, p. 279.

Sullivan, C. L., Bierman, P. R., Reusser, L. J., Larsen, J., Pavich, M. J., and Finkel, R. C., accepted, Erosion and landscape evolution of the Blue Ridge escarpment, southern Appalachian Mountains: Earth Surface Processes and Landforms.

Tollo, R. P., Aleinikoff, J. N., Borduas, E. A., Dickin, A. P., McNutt, R. H., and Fanning, C. M., 2006, Grenvillian magmatism in the northern Virginia Blue Ridge: Petrologic implications of episodic granitic magma production and the significance of postorogenic A-type charnockite: Precambrian Research, v. 151, p. 224-264.

von Blanckenburg, F., 2005, The control mechanisms of erosion and weathering at basin scale from cosmogenic nuclides in river sediment: Earth and Planetary Science Letters, v. 237, p. 462-479.

Ward, D. J., Spotila, J. A., Hancock, G. S., and Galbraith, J. M., 2005, New constraints on the late Cenozoic incision history of the New River, Virginia: Geomorphology, v. 72, p. 54-72.

Washburn, A. L., 1973, Periglacial processes and environments, Edward Arnold, London, p. 320.

—, 1980, Geocryology: a survey of periglacial processes and environments, New York: Wiley, p. 406.

White, W. B., 1984, Rate processes: chemical kinetics and karst landform development: Groundwater as a Geomorphic Agent, p. 227-248.

—, 2000, Dissolution of limestone from field observations, *in* Klimchouk, A. B., Ford, D. C., Palmer, A. N., and Dreybrodt, W., editors, Speleogenesis: Evolution of Karst Aquifers: Huntsville, Alabama, National Speleological Society, p. 527.

White, W. B., and White, E. L., 1991, Karst erosion surfaces in the Appalachian
     highlands: Appalachian Karst: Proceedings of the Appalachian Karst Symposium.
     1991.

Whittecar, G. R., 1992, Alluvial fans and boulder streams of the Blue Ridge Mountains,
     west-central Virginia, Southeastern Friends of the Pleistocene, 1992 Field Trip, p.
     128.

Tables

TABLE 1

Fluvial Sample Characteristics

Lithology	Number of Samples	Basin Area (km²)	Slope °
Granite	17 + 3 grain-size splits	~0.4-40	11-23
Metabasalt*	9 + 3 grain-size splits	~1-25	11-19
Quartzite**	9 + 3 grain-size splits	~0.1-9	12-23
Siliciclastic	8 + 3 grain-size splits	~0.3-13	18-26
Multilithology	9	~9-22	12-22
Shenandoah River	1	~3351	7
Rappahannock River	1	~13	11

*Includes SH-18 (temporal replicate of SH-02)

**Includes SH-41 (temporal replicate of SH-36)

TABLE 3

Bedrock Samples ^{10}Be concentrations and ^{10}Be erosion rates

Sample ID	Lithology	SUERC[1] ID #[2]	^{10}Be Concentration (x 10⁵ atoms/gram)[3]	^{10}Be Model Erosion Rate (m/My)[4]
SH-53	Sandstone	B2268	8.12 ± 0.22	3.6 ± 0.5
SH-55	Quartzite	B2272	11.80 ± 0.31	2.4 ± 0.3
SH-57	Siliciclastic	B2260	2.43 ± 0.07	12.8 ± 1.6
SH-58	Metabasalt	B2273	2.40 ± 0.09	13.0 ± 1.7
SH-59	Granite	B2274	3.93 ± 0.10	7.8 ± 1.0

[1]SUERC - Scottish Universities Environmental Research Centre, Accelerator Mass Spectrometry Laboratory. [2]SUERC ID # - a unique number that identifies each individual sample. [3]Normalized to SUERC standards prepared, including blank corrections; error is counting statistics with uncertainty in carrier concentration (Be 2%) added quadratically. Standard used for normalization for samples : NIST (SRM4325). [10/9]Be ratio for standard = 3.06 x 10¹¹. [4]Normalized to sea level and high latitude using data of Lal (1991) including only spallation production and elevation and latitude of the sample site, normalized to the surface using an attenuation coefficient of 165 g/cm². * one σ analytical error.

TABLE 2

Sample Locations

Sample ID	Lithology	Sample Type	Easting[1]	Northing[1]	Sample Collection Elevation (m)	USGS[2] 7.5-minute, 1:24,000-scale Quadrangles	Stream/River/Bedrock
SH-01 (0.25-0.85 mm)	Granite	fluvial sediment	736324	4272684	283	Old Rag Mountain	Hughes
SH-01 (0.85-2 mm)	Granite	fluvial sediment	736324	4272684	283	Old Rag Mountain	Hughes
SH-01 (2-10 mm)	Granite	fluvial sediment	736324	4272684	283	Old Rag Mountain	Hughes
SH-01 (>10 mm)	Granite	fluvial sediment	736324	4272684	283	Old Rag Mountain	Hughes
SH-07	Granite	fluvial sediment	725233	4273513	475	Big Meadows	Buracker Hollow
SH-08	Granite	fluvial sediment	727035	4279401	354	Luray	South Fork Dry Run
SH-10	Granite	fluvial sediment	736495	4282213	375	Thornton Gap	Thornton
SH-11	Granite	fluvial sediment	739752	4281853	226	Washington	Thornton
SH-12	Granite	fluvial sediment	738857	4277575	293	Old Rag Mountain	Hazel
SH-13	Granite	fluvial sediment	737679	4269600	223	Old Rag Mountain	Rosson Hollow Run
SH-14	Granite	fluvial sediment	737188	4267845	218	Old Rag Mountain	Ragged Run
SH-15	Granite	fluvial sediment	736216	4267136	232	Old Rag Mountain	Popham Run
SH-21	Granite	fluvial sediment	728957	4280649	402	Thornton Gap	North Fork Dry Run
SH-22	Granite	fluvial sediment	724850	4276706	329	Big Meadows	Tributary of East Hawksbill
SH-45	Granite	fluvial sediment	738472	4267440	195	Old Rag Mountain	Dulaney Hollow
SH-46	Granite	fluvial sediment	739697	4280609	232	Washington	Jenkins Hollow
SH-47	Granite	fluvial sediment	742935	4281305	183	Washington	Beaverdam Creek
SH-50	Granite	fluvial sediment	742376	4300370	354	Chester Gap	Lands Run Tributary
SH-51	Granite	fluvial sediment	739767	4297760	317	Chester Gap	Phils Arm Run
SH-52	Granite	fluvial sediment	740175	4299449	287	Chester Gap	Gooney Run
SH-59	Granite	bedrock	734720	4280010	835	Thornton Gap	bedrock
SH-02 (0.25-0.85 mm)	Metabasalt	fluvial sediment	730091	4282755	390	Thornton Gap	Pass Run
SH-02 (0.85-2 mm)	Metabasalt	fluvial sediment	730091	4282755	390	Thornton Gap	Pass Run
SH-02 (2-10 mm)	Metabasalt	fluvial sediment	730091	4282755	390	Thornton Gap	Pass Run
SH-02 (>10 mm)	Metabasalt	fluvial sediment	730091	4282755	390	Thornton Gap	Pass Run
SH-05	Metabasalt	fluvial sediment	734721	4293571	762	Bentonville	Jeremys Run
SH-09	Metabasalt	fluvial sediment	732865	4286590	695	Thornton Gap	Rocky Branch
SH-16	Metabasalt	fluvial sediment	730811	4269239	360	Old Rag Mountain	White Oak Run
SH-18*	Metabasalt	fluvial sediment	730088	4282767	384	Thornton Gap	Pass Run - Shenks Hollow
SH-19	Metabasalt	fluvial sediment	718300	4261025	451	Fletcher	East Branch Naked Creek
SH-25	Metabasalt	fluvial sediment	697272	4224629	341	Browns Cove	North Fork Moormans River
SH-26	Metabasalt	fluvial sediment	708069	4241014	610	Swift Run	Ivy Creek - Fork Hollow
SH-40	Metabasalt	fluvial sediment	702060	4234803	512	Browns Cove	Doyles
SH-58	Metabasalt	bedrock	732667	4287143	860	Thornton Gap	bedrock

90

Sample	Lithology	Type	Easting	Northing	Elev	Quadrangle	Location
SH-03 (0.25-0.85 mm)	Quartzite	fluvial sediment	704974	4248555	344	McGaheysville	Gap Run
SH-03 (0.85-2 mm)	Quartzite	fluvial sediment	704974	4248555	344	McGaheysville	Gap Run
SH-03 (2-10 mm)	Quartzite	fluvial sediment	704974	4248555	344	McGaheysville	Gap Run
SH-03 (>10 mm)	Quartzite	fluvial sediment	704974	4248555	344	McGaheysville	Gap Run
SH-20	Quartzite	fluvial sediment	704275	4247989	341	McGaheysville	Walls Run
SH-29	Quartzite	fluvial sediment	690397	4220154	469	Waynesboro East	unnamed
SH-30	Quartzite	fluvial sediment	693633	4227895	604	Crimora	Meadow Run - Rip Rap Hollow
SH-32	Quartzite	fluvial sediment	698743	4242670	378	McGaheysville	Hangmans Run Tributary
SH-34	Quartzite	fluvial sediment	691885	4227255	488	Crimora	Meadow Run Tributary
SH-35	Quartzite	fluvial sediment	692083	4227608	524	Crimora	Meadow Run Tributary
SH-36	Quartzite	fluvial sediment	692204	4227789	536	Crimora	Meadow Run Tributary
SH-41**	Quartzite	fluvial sediment	692180	4227796	564	Crimora	Meadow Run Tributary
SH-55	Quartzite	bedrock	698684	4241401	518	McGaheysville	bedrock
SH-04 (0.25-0.85 mm)	Siliciclastic	fluvial sediment	693189	4230180	427	Crimora	Paine Run
SH-04 (0.85-2 mm)	Siliciclastic	fluvial sediment	693189	4230180	427	Crimora	Paine Run
SH-04 (2-10 mm)	Siliciclastic	fluvial sediment	693189	4230180	427	Crimora	Paine Run
SH-04 (>10 mm)	Siliciclastic	fluvial sediment	693189	4230180	427	Crimora	Paine Run
SH-06	Siliciclastic	fluvial sediment	727619	4284094	299	Luray	Britton Hollow (tributary of Pass
SH-27	Siliciclastic	fluvial sediment	692551	4219150	475	Waynesboro East	Tributary of Saw Mill Run
SH-28	Siliciclastic	fluvial sediment	692528	4219091	457	Waynesboro East	Saw Mill Run
SH-37	Siliciclastic	fluvial sediment	697182	4236207	463	McGaheysville	Madison Run
SH-39	Siliciclastic	fluvial sediment	694228	4232723	512	Crimora	Stull Run
SH-42	Siliciclastic	fluvial sediment	694064	4225856	640	Crimora	unnamed
SH-54	Siliciclastic	fluvial sediment	699057	4240410	503	McGaheysville	Lower Lewis Run
SH-57	Siliciclastic	bedrock	732036	4287176	811	Thornton Gap	bedrock
SH-17	Multilithology	fluvial sediment	728841	4295614	195	Bentonville	Dry Run
SH-31	Multilithology	fluvial sediment	692472	4225882	469	Crimora	Meadow Run
SH-33	Multilithology	fluvial sediment	698786	4242809	360	McGaheysville	Hangmans Run
SH-38	Multilithology	fluvial sediment	695213	4236654	415	Grottoes	Madison Run
SH-43	Multilithology	fluvial sediment	711967	4248830	472	Swift Run	Swift Run
SH-44	Multilithology	fluvial sediment	722245	4246727	259	Stannardsville	unnamed
SH-48	Multilithology	fluvial sediment	751201	4302777	213	Flint Hill	Rappahanock
SH-49	Multilithology	fluvial sediment	744849	4312419	165	Front Royal	Leach Run
SH-56	Multilithology	fluvial sediment	708939	4267556	256	Stanley	Shenandoah
SH-53	Sandstone	bedrock	708568	4280726	692	Hamburg	Massanutten Ridge

[1]Coordinate System - NAD 83, UTM 17 using a Garmin 12 GPS unit. [2]United States Geological Survey. *Temporal replication of SH-02. **Temporal replication of SH-36.

TABLE 4

Fluvial Samples ^{10}Be concentrations and erosion rates

Sample ID	Lithology	CAMS #[1]/ SUERC ID #[2]	Slope °	Basin Area (km²)	Correction Factor[3]	^{10}Be Concentration (x10⁵ atoms/gram)[4]	^{10}Be Model Erosion Rate (m/My)[5]
SH-01 (0.25-0.85 mm)	Granite	BE22557	18	39.6	1.64	2.13 ± 0.06	14.7 ± 1.9
SH-01 (0.85-2 mm)	Granite	BE22558	18	39.6	1.64	2.09 ± 0.08	14.9 ± 2.0
SH-01 (2-10 mm)	Granite	BE22559	18	39.6	1.64	1.87 ± 0.09	16.7 ± 2.2
SH-01 (>10 mm)	Granite	BE22560	18	39.6	1.64	1.39 ± 0.04	22.5 ± 2.9
SH-07	Granite	B2189	23	10.6	1.84	2.10 ± 0.06	14.8 ± 1.9
SH-08	Granite	B2190	20	4.3	1.74	1.44 ± 0.04	21.8 ± 2.8
SH-10	Granite	B2241	18	9.5	1.45	1.92 ± 0.06	16.3 ± 2.1
SH-11	Granite	B2194	18	24.1	1.50	1.84 ± 0.06	17.0 ± 2.2
SH-12	Granite	B2195	17	14	1.67	1.97 ± 0.06	15.8 ± 2.0
SH-13	Granite	B2242	17	4.7	1.42	2.47 ± 0.07	12.6 ± 1.6
SH-14	Granite	B2196	17	4.6	1.49	1.74 ± 0.08	18.0 ± 2.4
SH-15	Granite	B2198	18	5.8	1.35	2.41 ± 0.07	12.9 ± 1.7
SH-21	Granite	B2202	22	5.6	1.68	2.08 ± 0.06	15.0 ± 1.9
SH-22	Granite	B2244	21	4.3	1.62	3.08 ± 0.08	10.0 ± 1.3
SH-45	Granite	B2235	11	3.7	1.16	3.17 ± 0.09	9.7 ± 1.3
SH-46	Granite	B2236	19	1.7	1.34	1.59 ± 0.05	19.7 ± 2.5
SH-47	Granite	B2254	13	12.2	1.15	2.62 ± 0.08	11.9 ± 1.5
SH-50	Granite	B2265	16	0.4	1.41	3.88 ± 0.10	7.9 ± 1.0
SH-51	Granite	B2266	16	12.8	1.50	2.66 ± 0.07	11.7 ± 1.5
SH-52	Granite	B2267	16	21.6	1.48	2.53 ± 0.07	12.3 ± 1.6
SH-02 (0.25-0.85 mm)	Metabasalt	BE22589	14	1.0	1.42	7.21 ± 0.20	4.1 ± 0.6
SH-02 (0.85-2 mm)	Metabasalt	BE22590	14	1.0	1.42	6.15 ± 0.19	4.9 ± 0.7
SH-02 (2-10 mm)	Metabasalt	BE22591	14	1.0	1.42	5.57 ± 0.15	5.4 ± 0.7
SH-02 (>10 mm)	Metabasalt	BE22592	14	1.0	1.42	5.56 ± 0.17	5.4 ± 0.7
SH-05	Metabasalt	B2188	11	1.5	1.98	5.87 ± 0.14	5.1 ± 0.7
SH-09	Metabasalt	B2193	13	6.4	1.80	3.75 ± 0.11	8.2 ± 1.1
SH-16	Metabasalt	B2199	15	13.9	1.93	1.33 ± 0.04	23.6 ± 3.0
SH-18*	Metabasalt	B2200	13	4.6	1.54	5.47 ± 0.15	5.5 ± 0.7
SH-19	Metabasalt	B2201	17	11.7	1.85	2.21 ± 0.06	14.1 ± 1.8
SH-25	Metabasalt	B2205	19	25.3	1.68	3.31 ± 0.16	9.3 ± 1.3
SH-26	Metabasalt	B2264	15	2.6	1.80	2.66 ± 0.07	11.7 ± 1.5
SH-40	Metabasalt	B2231	16	3.3	1.83	3.40 ± 0.09	9.1 ± 1.2

SH-03 (0.25-0.85 mm)	Quartzite	BE21899	18	9.3	1.41	5.7 ± 0.7	5.7 ± 0.7
SH-03 (0.85-2 mm)	Quartzite	BE21900	18	9.3	1.41	7.3 ± 1.0	7.3 ± 1.0
SH-03 (2-10 mm)	Quartzite	BE21901	18	9.3	1.41	8.5 ± 1.1	8.5 ± 1.1
SH-03 (>10 mm)	Quartzite	BE22593	18	9.3	1.41	7.2 ± 0.9	7.2 ± 0.9
SH-20	Quartzite	B2243	20	1.7	1.46	7.0 ± 0.9	7.0 ± 0.9
SH-29	Quartzite	B2207	16	0.7	1.52	4.7 ± 0.6	4.7 ± 0.6
SH-30	Quartzite	B2211	18	0.8	1.76	7.5 ± 1.0	7.5 ± 1.0
SH-32	Quartzite	B2213	12	1.1	1.39	5.0 ± 0.7	5.0 ± 0.7
SH-34	Quartzite	B2224	21	0.5	1.56	16.8 ± 2.1	16.8 ± 2.1
SH-35	Quartzite	B2225	13	0.1	1.46	6.3 ± 0.8	6.3 ± 0.8
SH-36	Quartzite	B2226	23	0.2	1.61	10.8 ± 1.4	10.8 ± 1.4
SH-41**	Quartzite	B2250	22	0.2	1.59	8.9 ± 1.2	8.9 ± 1.2
SH-04 (0.25-0.85 mm)	Siliciclastic	BE22525	23	12.7	1.6	12.3 ± 1.6	12.3 ± 1.6
SH-04 (0.85-2 mm)	Siliciclastic	BE22526	23	12.7	1.6	13.5 ± 1.7	13.5 ± 1.7
SH-04 (2-10 mm)	Siliciclastic	BE22527	23	12.7	1.6	12.1 ± 1.6	12.1 ± 1.6
SH-04 (>10 mm)	Siliciclastic	BE22528	23	12.7	1.6	8.8 ± 1.2	8.8 ± 1.2
SH-06	Siliciclastic	B2240	21	1.5	1.37	6.9 ± 0.9	6.9 ± 0.9
SH-27	Siliciclastic	B2249	21	0.3	1.57	6.2 ± 0.8	6.2 ± 0.8
SH-28	Siliciclastic	B2206	18	5.9	1.57	6.7 ± 0.9	6.7 ± 0.9
SH-37	Siliciclastic	B2228	23	1.5	1.55	9.0 ± 1.2	9.0 ± 1.2
SH-39	Siliciclastic	B2230	26	3.0	1.73	10.2 ± 1.4	10.2 ± 1.4
SH-42	Siliciclastic	B2252	23	0.5	1.77	16.2 ± 2.1	16.2 ± 2.1
SH-54	Siliciclastic	B2492	26	1.9	1.63	16.7 ± 2.1	16.7 ± 2.1
SH-17	Multilithology	B2262	17	20.0	1.38	5.2 ± 0.7	5.2 ± 0.7
SH-23	Multilithology	B2247	14	18.7	1.43	17.6 ± 2.2	17.6 ± 2.2
SH-24	Multilithology	B2248	21	3.6	1.73	13.5 ± 1.7	13.5 ± 1.7
SH-31	Multilithology	B2212	21	8.6	1.70	8.4 ± 1.1	8.4 ± 1.1
SH-33	Multilithology	B2214	12	1.2	1.39	5.3 ± 0.7	5.3 ± 0.7
SH-38	Multilithology	B2229	22	15.0	1.60	9.7 ± 1.3	9.7 ± 1.3
SH-43	Multilithology	B2253	16	2.2	1.57	15.1 ± 1.9	15.1 ± 1.9
SH-44	Multilithology	B2232	17	35.0	1.59	12.9 ± 1.7	12.9 ± 1.7
SH-48	Multilithology	B2255	11	13.4	1.28	13.8 ± 1.8	13.8 ± 1.8
SH-49	Multilithology	B2237	9	9.4	1.18	3.8 ± 0.5	3.8 ± 0.5
SH-56	Multilithology	B2256	7	1.2	1.47	7.3 ± 0.9	7.3 ± 0.9

[1]CAMS (Center for Accelerator Mass Spectrometry) # - (samples SH-01-SH-04) unique numbers that identify each indvidual sample.

[2]SUERC (Scottish Universities Environmental Research Centre, Accelerator Mass Spectrometry Laboratory) - (samples SH-05-SH-59) unique numbers that identify each indvidual sample.

[3]The correction factor used to model 10Be erosion rates. The weighted elevation correction was calculated by subdividing each basin into 100 elevation to give the area (km2) per bin. Using the nucleon data of Lal (1991) with linear interpolation between latitudes, effective production drainage basins are generated bin by bin.

[4]Normalized to standards prepared by K. Nishizumi at Lawrence Livermore National Laboratory and SUERC, including blank corrections; err statistics with uncertainty in carrier concentration (Be 2%) added quadratically. Standard used for normalization for samples : CAMS - KNSTI $^{10}Be/^9Be$ ratio for standard = 3.11 x 10^{12}; SUERC AMS - NIST (SRM4325), $^{10}Be/^9Be$ ratio for standard = 3.06 x 10^{11}.

[5]Normalized to sea level and high latitude using data of Lal (1991), including only spallation production and elevation and latitude of the samp normalized to the surface using an attenuation coefficient of 165 g/cm². Assumed sea-level, high latitude production rate of 5.2 atoms g^{-1} y^{-1}.

†one σ analytical error.   *Temporal replication of SH-02. **Temporal replication of SH-36.

TABLE 5

P-Values - Fluvial Samples

	Granite	Metabasalt	Quartzite	Siliciclastic	Multilithology	All Data
Erosion Rate vs Slope	0.08 −	0.65 +	0.07 +	0.05 +	0.37 +	0.02 +
Erosion Rate vs Basin Area	0.72 −	0.29 +	0.52 −	0.88 −	0.52 +	0.05 +
Slope vs Basin Area	0.89 −	0.030 +	0.94 −	0.81 −	0.49 +	0.53 −

+ Positive correlation - Negative correlation

TABLE 6

Erosion Rate Dependence on Aspect

Lithology	East - Average Erosion Rate (m/My)	Number of Samples	West - Average Erosion Rate (m/My)	Number of Samples
Granite	14.9 ± 3.1	10	13.4 ± 1.7	7
Metabasalt*	12.4 ± 6.4	5	8.0 ± 1.1	3
Quartzite**	n/a ± n/a	0	9.0 ± 1.2	8
Siliciclastic	n/a ± n/a	0	10.5 ± 1.4	8
Multilithology	13.4 ± 0.5	3	9.3 ± 1.2	8
Average	13.9 ± 4.0	18	10.0 ± 4.7	34

*Samples SH-02 and SH-18 (temporal replicate) have been averaged.

** Samples SH-36 and SH-41 (temporal replicate) have been averaged.

Figure Captions

Figure 1. Shaded digital elevation model* of north-central Virginia showing the Shenandoah Region and adjacent physiographic provinces. White line is the Park boundary. Inset shows the location of the Shenandoah National Park region in Virginia. FR = Front Royal, W = Waynesboro. (*USGS digital data, http://pubs.usgs.gov/of/2003/0f03-410/).

Figure 2A. Shaded digital elevation model* of north-central Virginia showing the northern section of the Shenandoah Region with geologic units**,sample sites and sampled drainage basins are outlined. Inset shows location of close-up. (*USGS digital data, http://pubs.usgs.gov/of/2003/0f03-410/, ** Southworth, 2008).

Figure 2B. Shaded digital elevation model* of north-central Virginia showing the southern section of the Shenandoah Region with geologic units**, sample sites and sampled drainage basins are outlined. Inset shows location of close-up. (*USGS digital data, http://pubs.usgs.gov/of/2003/0f03-410/, ** Southworth, 2008).

Figure 3A. Upstream view of Leach Run, Shenandoah National Park (SH-49).

Figure 3B. Looking west from Shenandoah National Park to the Valley and Ridge Province.

Figure 4. Latitude normalized and altitude corrected ^{10}Be concentrations by grain-size (10^5 atoms/ gram quartz). (A) Granite, (B) Metabasalt, (C) Quartzite, (D) Siliciclastic Rocks. Error bars are one standard deviation analytical error.

Figure 5. Erosion rate (m/My) vs. slope (degrees) relationships. (A) Granite, (B) Metabasalt, (C) Quartzite, (D) Siliciclastic rocks, (E) Multilithology, (F) All fluvial samples. Slope and erosion rate are significantly related ($p \leq 0.02$) for siliciclastic rocks and all fluvial samples (F). For all other lithologies the relationship is not significant (Table 2). Error bars are one standard deviation analytical error.

Figure 6. Basin area (km^2) vs. ^{10}Be erosion rate. (A) Granite, (B) Metabasalt, (C) Quartzite, (D) Siliciclastic Rocks, (E) Multilithology, SH-56, Shenandoah River basin not shown, (F) All fluvial samples. Error bars are one standard deviation analytical error.

Figure 7. Basin area and slope are only significantly related for metabasalt (B) ($p \leq 0.03$). (A) Granite, (B) Metabasalt, (C) Quartzite, (D) Siliciclastic rocks, (E) Multilithology, SH-56, Shenandoah River basin not shown, (F) All fluvial samples. Error bars are one standard deviation.

Figure 8. Boxplot of fluvial and bedrock erosion rates by lithology. Lower line of the box is the 25th percentile, middle line is the median, and the upper line is the 75th

percentile. Whiskers are minimum and maximum data values. Diamond symbols are the mean fluvial erosion rates; star symbols are the bedrock erosion rates.

Figure 9. Map showing erosion rate dependence on aspect by lithology. The numbers are [10]Be model erosion rates for basins. Figure 10. Histogram of erosion rate dependence on aspect by lithology. Numbers in the bars are the number of samples collected in each lithology.
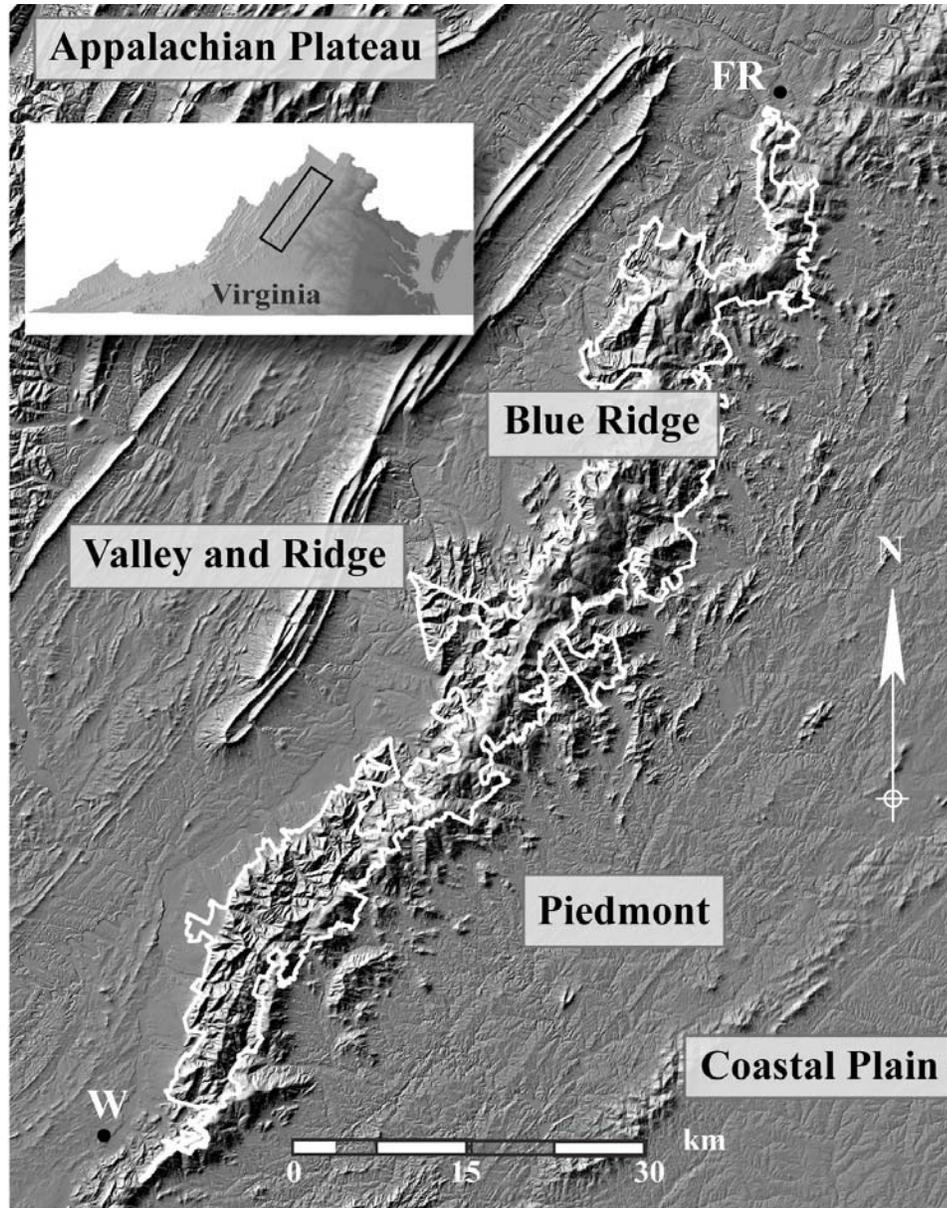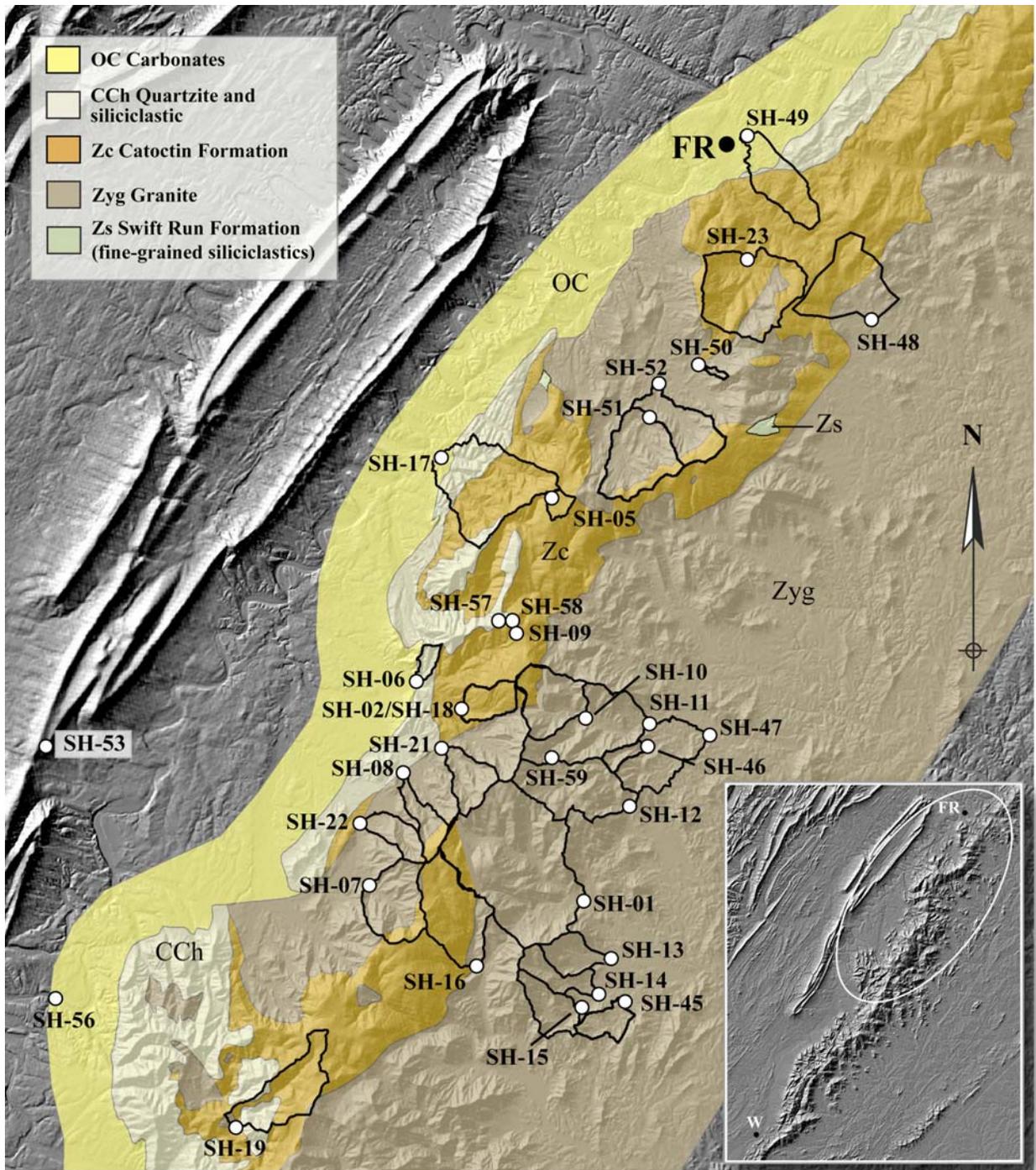
Figure 10. Histogram of erosion rate dependence on aspect by lithology. Numbers in the bars are the number of samples collected in each lithology.
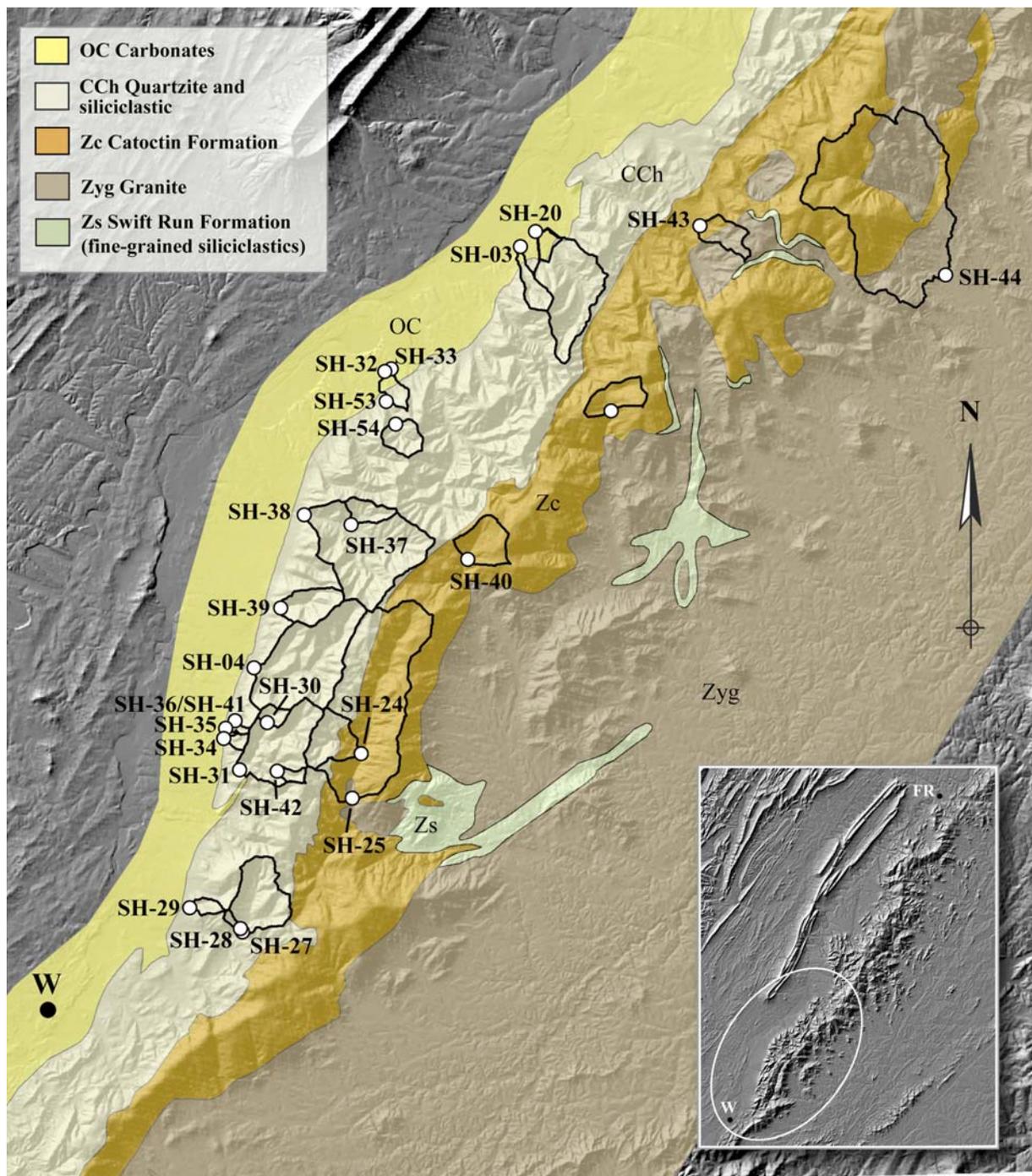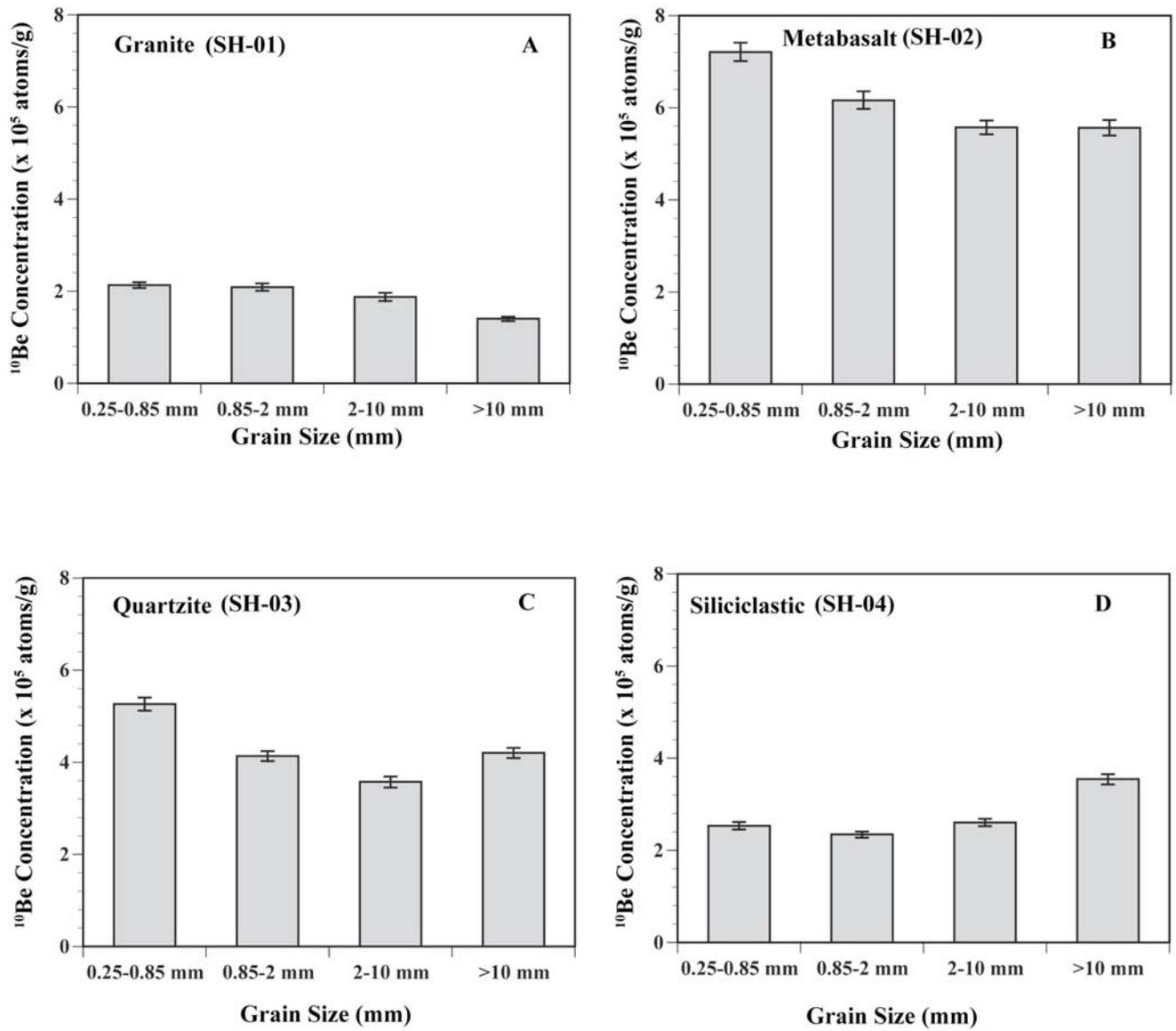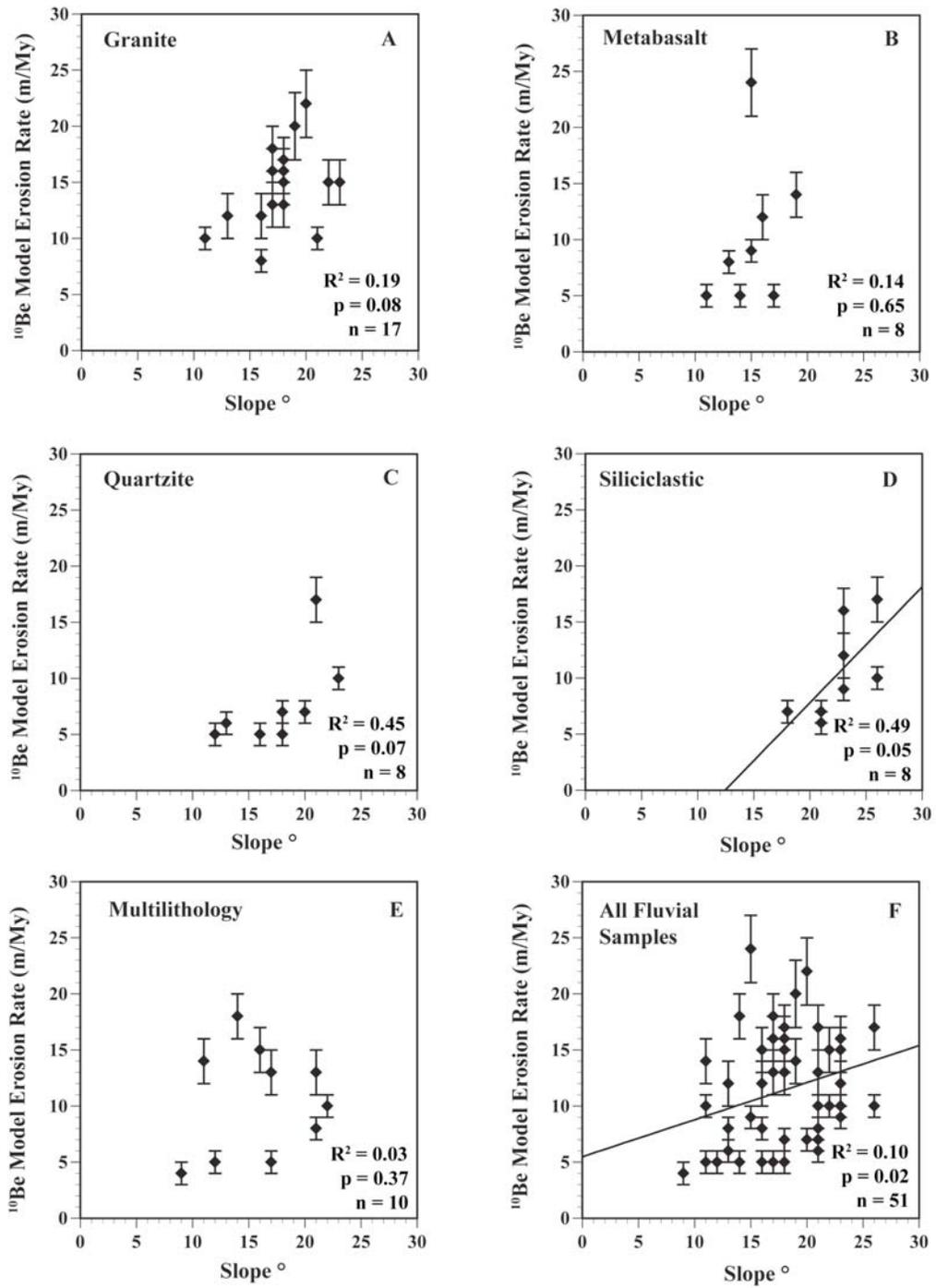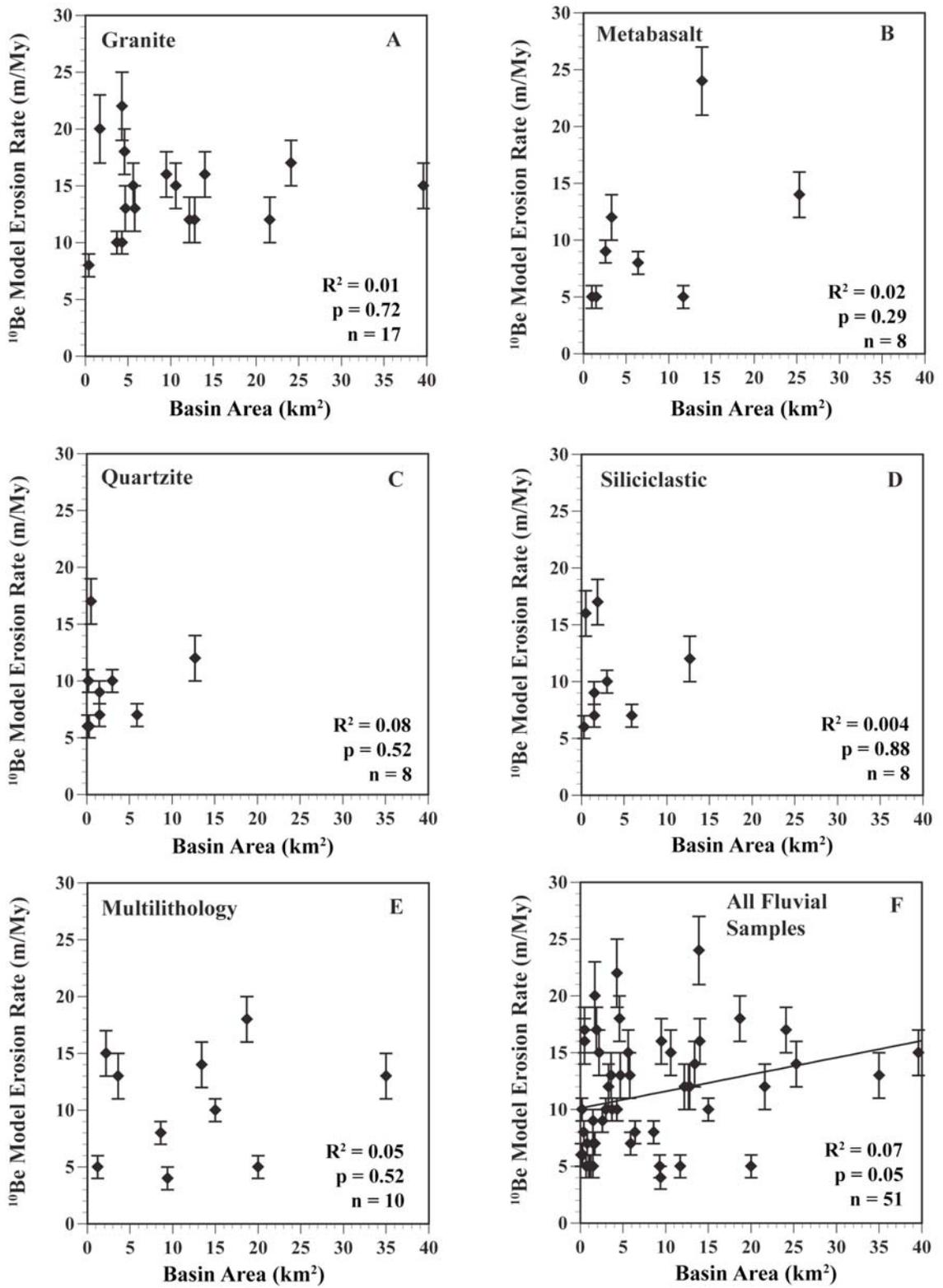
Figures

Fig. 1.

Fig. 2A.

Fig. 2B.
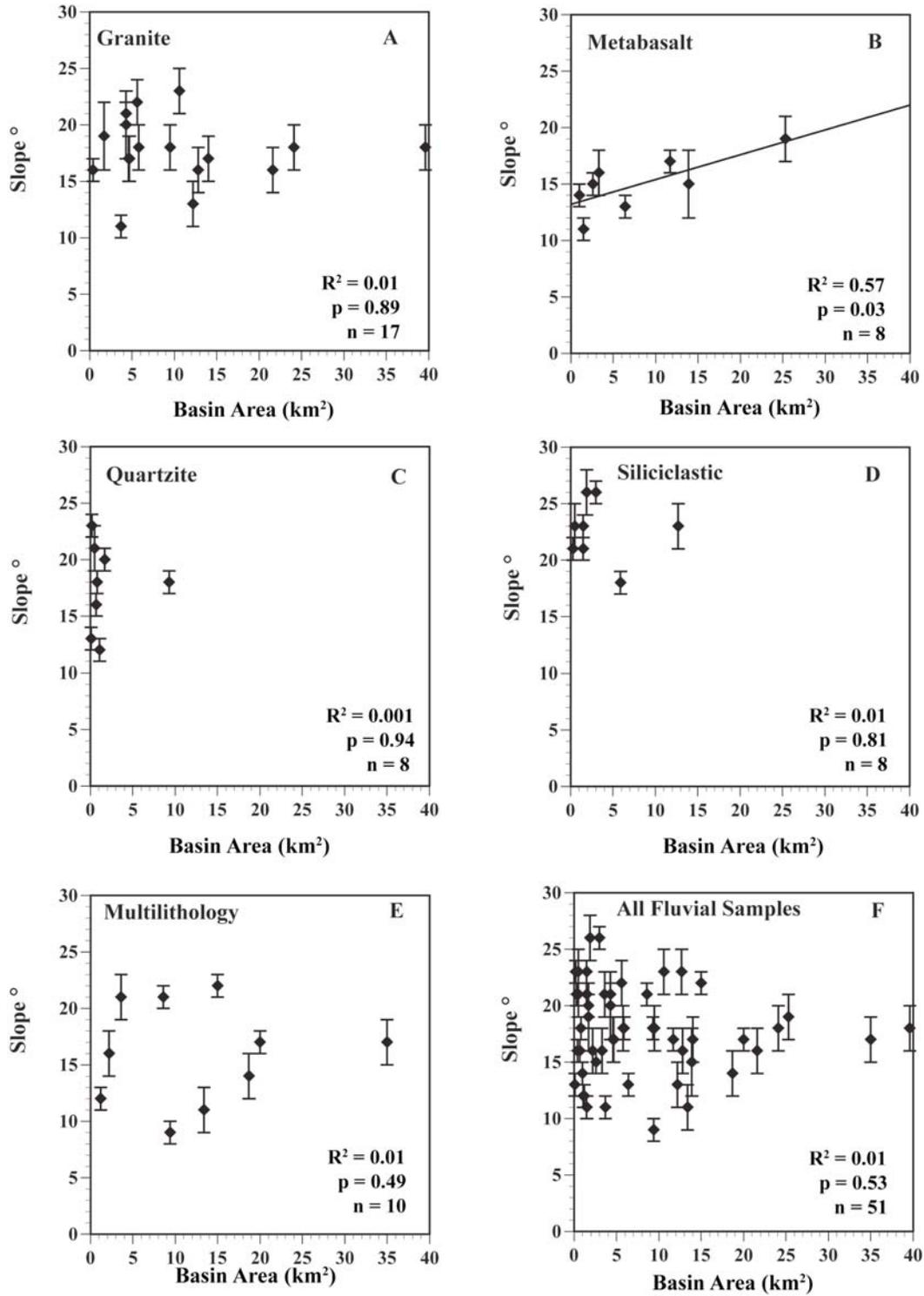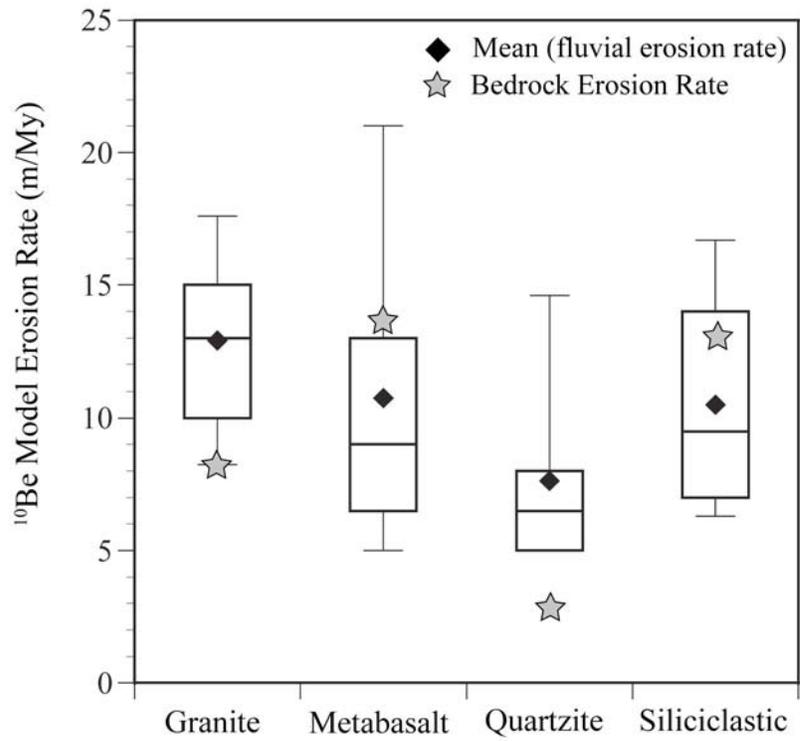
Fig. 3A.

Fig. 3B.

100

Fig. 4.

Fig. 5.

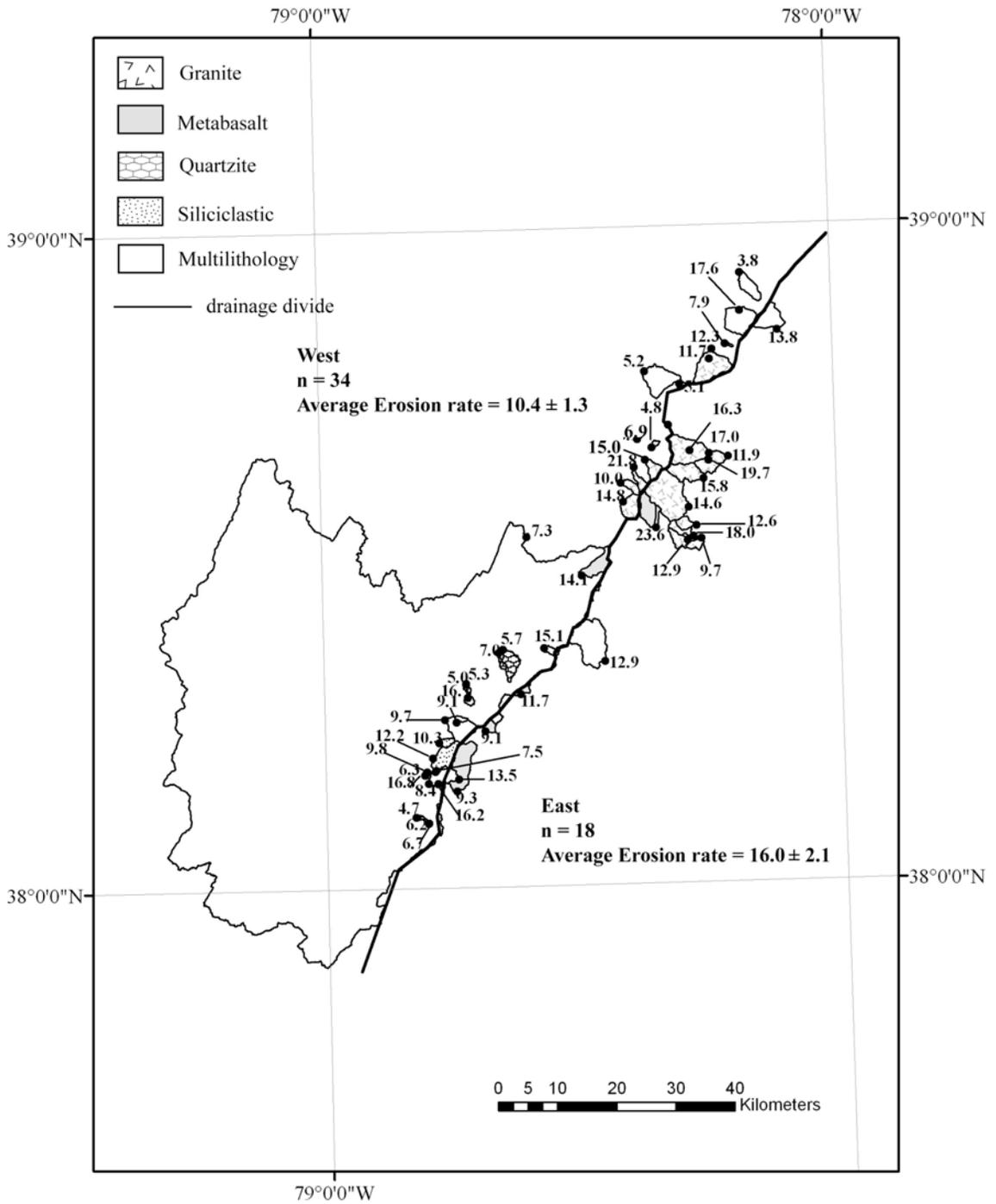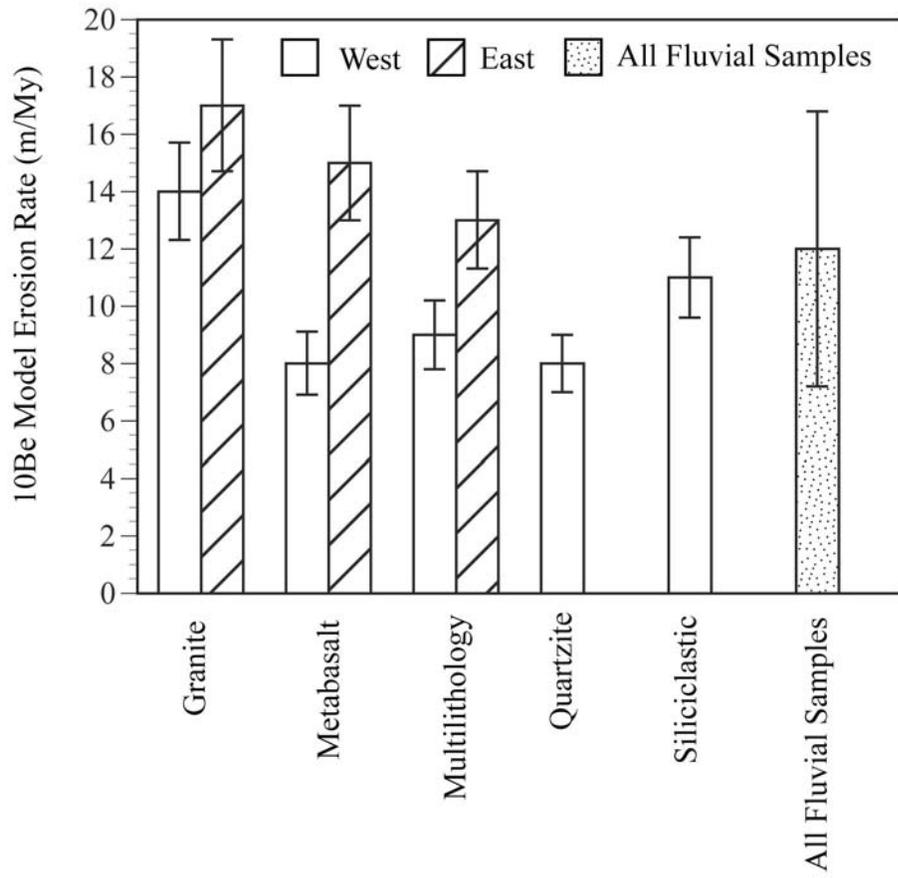**Fig. 6**

103

Fig. 7.

Fig. 8.

Fig. 9.

Fig. 10.

Chapter 5 – Conclusions and Recommendations

Erosion rates measured from ^{10}Be concentrations in fluvial sediment in the Shenandoah Park region range from 4.4 to 26 m/My, with a mean erosion rate for single-lithology basins of 12.2 ± 5.7 m/My. Bedrock erosion rates range from 0.9-11 m/My across all lithologies, with a mean erosion rate of 4.9 ± 4.3 m/My. Samples collected from the two main rivers draining the western and eastern slopes of the Park are 3.1 m/My, North Fork of the Shenandoah River, and 11m/My, Rappahannock River. Erosion rates appear to be different on either side of the drainage divide. Single-lithology basin erosion rates on the eastern side of the divide are faster ($\mu = 16.5 \pm 5.0$ m/My) than those on the west ($\mu = 10.2 \pm 5.1$ m/My) ($p = 0.00$). These east-west variations in erosion rates are mirrored by the erosion rates obtained from two of the major rivers draining the Park, the Rappahannock River to the east (11 m/My) and the Shenandoah River to the west (3.1 m/My). This east-west dichotomy may be a function of rock type, where weathered metagranites have more rapid erosion rates to the east, and to the west, resistant members of the Chilhowee Group rocks largely underlie the Page Valley. Miocene drainage capture diverted drainages from the west to the east, which may have promoted rapid incision of Atlantic slope drainages and the removal of much of the Piedmont regolith. Grain-size specific cosmogenic analysis of four sediment samples showed no consistent trend of concentration.

The metamorphic rocks of the Shenandoah National Park region do not fit into the simple landscape model of ridge-capping resistant rocks that has been applied to other areas of the Appalachian Mountains (Matmon and others, 2003a; Matmon and others,

2003b; Reuter, 2005). In the Park highlands, metabasalt and metagranites, rather than the more erosion-resistant quartzite, form the ridgeline. The lack of significant lithologic and slope relationships with basin-scale erosion rates supports Hack's (1960) model of *dynamic equilibrium* where landscape morphology is adjusted to the erosional resistance of the underlying rock over the long-term.

Cosmogenically determined bedrock and basin-scale erosion rates for the Shenandoah National Park region are in general consistent with those estimated elsewhere in the Appalachian Mountains (Matmon and others, 2003a; Matmon and others, 2003b; Reuter, 2005b; Ward and others, 2005; Hancock and others, 2007; Sullivan and others, accepted). Erosion rates for Shenandoah National Park region with its mixed lithologies (12.9 m/My) are indistinguishable from basin-scale erosion rates measured in schist and gneiss (12.5 m/My) for the Blue Ridge just above the Blue Ridge Escarpment (Sullivan and others, accepted), ~300 km to the south.

The data generated from this study indicate that the landscape of the Blue Ridge Province is a product of slow erosion over a $10^3 – 10^6$ year timescale. Millennial scale erosion rates averaging ~11.6 m/My are similar to post-orogenic denudation rates integrated over times periods 1 to 2 orders of magnitude longer. This steady erosion over time suggests that the region's landscape may well have remained grossly similar for millions of years. Slow denudation of ancient rocks is most likely driving slow but continual isostatic uplift that maintains self-similar topography (Pavich, 1985) controlled by rock competence and structure.

Recommendations for Future Work

Data from this study provides a baseline for erosion rates measured using cosmogenic isotope analysis for the Blue Ridge region in the vicinity of the Shenandoah National Park. The lower erosion rates of quartzite rocks and the presence of less resistant rocks on the ridgeline such as granite and metabasalt requires further investigation to tease out the relationships between these lithologies. This may include deeper integration of ongoing structural studies, where a greater understanding of the geologic controls in the region may help to elucidate the relationships between erosion rates and the tested parameters for each lithology. This study did not have enough samples in order to ascertain whether erosional resistance varies more among lithologies or between them. Further sampling may aid in understanding of rock resistance through examining the importance of local variations in rock structure in the lithologies cropping out in the park.

In terms of the broader picture and improving the understanding of the geomorphic processes involved in the evolution of the Appalachian Mountains, a collaborative study that integrates all the cosmogenic data and thermochronologic data gathered thus far will be useful. It may provide opportunities to pull together the disparate pieces of the Appalachian Mountain evolution story, answer some outstanding questions, and also provide a jumping off point for future research.

Comprehensive Bibliography

Ahnert, F., 1970, Functional relationships between denudation, relief, and uplift in large mid-latitude drainage basins: American Journal of Science, v. 268, p. 243-263.

Badger, R. L., and Sinha, A. K., 1988, Age and Sr isotopic signature of the Catoctin volcanic province; implications for subcrustal mantle evolution: Geology, v. 16, p. 692-695.

Bailey, C. M., Southworth, S., and Tollo, R. P., 2006, Tectonic history of the Blue Ridge, north-central Virginia, *in* Pazzaglia, F. J., editor, Excursions in Geology And History: Field Trips in the Middle Atlantic States: Boulder, The Geological Society of America, p. 22.

Baldwin, J. A., Whipple, K. X., and Tucker, G. E., 2003, Implications of the shear stress river incision model for the timescale of postorogenic decay of topography: Journal of Geophysical Research, v. 108.

Bard, E., 2003, North-Atlantic Sea Surface Temperature Reconstruction: IGBP PAGES/World Data Center for Paleoclimatology Data Contribution Series, v. 26.

Barron, E. J., 1989, Climate Variations and the Appalachians from the Late Paleozoic to the Present: Results from Model Simulations: Geomorphology, v. 2, p. 99-118.

Barron, E. J., and Washington, W. M., 1982, Cretaceous climate: a comparison of atmospheric simulations with the geologic record: Palaeogeography, Palaeoclimatology, Palaeoecology, v. 40, p. 103–133.

—, 1984, The role of geographic variables in explaining paleoclimates: Results from Cretaceous climate model sensitivity studies: Journal of Geophysical Research, v. 89, p. 1267-1279.

Beeson, D. C., 1984, Relative significance of tectonics, sea level fluctuations, and paleoclimate to Cretaceous coal distribution in North America. Cooperative thesis, PB-85-180412/XAB, National Center for Atmospheric Research, Boulder, CO (USA); Colorado Univ., Boulder (USA).

Belmont, P., Pazzaglia, F. J., and Gosse, J., 2006, Using the 10-Be Grain Size Dependency in Alluvial Sediments to Investigate Hillslope and Channel Processes: American Geophysical Union, Fall Meeting 2006, abstract# H21H-06.

Belton, D. X., Brown, R. W., Kohn, B. P., Fink, D., and Farley, K. A., 2004, Quantitative resolution of the debate over antiquity of the central Australian landscape: implications for the tectonic and geomorphic stability of cratonic interiors: Earth and Planetary Science Letters, v. 219, p. 21-34.

Berner, R. A., Lasaga, A. C., and Garrels, R. M., 1983, The carbonate-silicate geochemical cycle and its effect on atmospheric carbon dioxide over the past 100 million years: American Journal of Science, v. 283, p. 641.

Bierman, P., Caffee, M., and Matmon, A., 1999, Rates of rock surface erosion and sediment production across the hyperarid Namib Desert and the great Namibian escarpment: Geological Society of America Abstracts with Programs, v. 31, p. A-297.

Bierman, P., and Nichols, K., 2004, Rock to sediment - Slope to sea with 10-Be - Rates of landscape change: Annual review of Earth and Planetary Sciences, v. 32, p. 215-255.

Bierman, P., and Turner, J., 1995, [10]Be and [26]Al evidence for exceptionally low rates of Australian bedrock erosion and the likely existence of pre-Pleistocene landscapes: Quaternary Research, v. 44, p. 378-382.

Bierman, P. R., 1993, In situ produced cosmogenic isotopes and the evolution of granitic landforms: Ph.D. Thesis, University of Washington, Seattle, WA, p. 289.

—, 1994, Using in situ produced cosmogenic isotopes to estimate rates of landscape evolution; a review from the geomorphic perspective: Journal of Geophysical Research, B, Solid Earth and Planets, v. 99, p. 13885-13896.

—, 1995, A new method of estimating basin scale erosion rates -- measurement of in situ produced [10]Be and [26]Al in sediments: EOS, v. 76, p. S143.

—, 2002, The Boulders of Madison County, Geological Society of America Abstracts with Programs, 2002 Denver Annual Meeting.

Bierman, P. R., and Caffee, M., 2002a, Cosmogenic exposure and erosion history of ancient Australian bedrock landforms: Geological Society of America Bulletin, v. 114, p. 787-803.

Bierman, P. R., and Caffee, M. W., 2001, Slow rates of rock surface erosion and sediment production across the Namib Desert and escarpment, Southern Africa: American Journal of Science, v. 301, p. 326-358.

Bierman, P. R., Caffee, M. W., Davis, P. T., Marsella, K., Pavich, M., Colgan, P., Mickelson, D., and Larsen, J., 2002b, Rates and timing of Earth surface processes from in situ-produced cosmogenic Be-10, in Grew, E. S., editor, Reviews in Mineralogy and Geochemistry: Beryllium; mineralogy, petrology, and geochemistry: Washington, DC, United States, Mineralogical Society of America and Geochemical Society, Washington, DC, p. 147-205.

Bierman, P. R., Neis, S., Zehfuss, P., Burke, R., Gillespie, A., and Caffee, M., 1998, 10-Be and 26-Al age estimates for five tectonically offset fan surfaces, Owens Valley, CA: Geological Society of America, 1998 annual meeting Abstracts with Programs - Geological Society of America, v. 30, p. 141.

Bierman, P. R., Reuter, J. M., Pavich, M., Gellis, A. C., Caffee, M. W., and Larsen, J., 2005, Using cosmogenic nuclides to contrast rates of erosion and sediment yield in a semi-arid, arroyo-dominated landscape, Rio Puerco Basin, New Mexico: Earth Surface Processes and Landforms, v. 30, p. 935-953.

Bierman, P. R., and Steig, E., 1996, Estimating rates of denudation and sediment transport using cosmogenic isotope abundances in sediment: Earth Surface Processes and Landforms, v. 21, p. 125-139.

Bishop, P., 2007, Long-term landscape evolution: linking tectonics and surface processes: Earth Surface Processes and Landforms, v. 32, p. 329-365.

Bluth, G. J. S., and Kump, L. R., 1994, Lithologic and climatologic controls of river chemistry: Geochimica et Cosmochimica Acta, v. 58, p. 2341-2359.

Bookhagen, B., Thiede, R. C., and Strecker, M. R., 2005, Late Quaternary intensified monsoon phases control landscape evolution in the northwest Himalaya: Geology, v. 33, p. 149-152.

Braun, D. D., 1989, Glacial and periglacial erosion of the Appalachians: Geomorphology, v. 2, p. 233–256.

Brown, E. T., Stallard, R. F., Larsen, M. C., Raisbeck, G. M., and Yiou, F., 1995, Denudation rates determined from the accumulation of in situ-produced [10]Be in the Luquillo Experimental Forest, Puerto Rico: Earth and Planetary Science Letters, v. 129, p. 193-202.

Chamley, H., 1979, North Atlantic clay sedimentation and paleoenvironment since the late Jurassic: Deep Drilling Results in the Atlantic Ocean: Continental Margins and Paleoenvironment. Am. Geophys. Union, Maurice Ewing Ser, v. 3, p. 342-361.

Child, D., Elliott, G., Mifsud, C., Smith, A. M., and Fink, D., 2000, Sample processing for earth science studies at ANTARES: Nuclear Inst. and Methods in Physics Research, B, v. 172, p. 856-860.

Chirico, P., and Tanner, S., 2004, Shaded Relief Image Map of Topogrid Derived 10 Meter Resolution Digital Elevation Model of the Shenandoah National Park and Surrounding Region, Virginia, U.S: United States Geological Survey Open-File Report 04-1321.

Chorley, R. J., 1971, 3. ll. The Role of Water in Rock Disintegration: Introduction to Fluvial Processes.

Clapp, E., Bierman, P. R., and Caffee, M., 2002, Using [10]Be and [26]Al to determine sediment generation rates and identify sediment source areas in an arid region drainage basin: Geomorphology, v. 45, p. 89-104.

Clapp, E. M., Bierman, P. B., and Caffee, M. W., 1998, Estimating long-term erosion rates in a hyper-arid region using in situ produced cosmogenic 10-Be and 26-Al in sediment and bedrock: Geological Society of America, 1998 annual meeting Abstracts with Programs - Geological Society of America, v. 30, p. 361.

Clapp, E. M., Bierman, P. R., and Caffee, M., 1997, Rates of erosion determined using in situ produced cosmogenic isotopes in a small arroyo basin, northwestern New Mexico: Geological Society of America, 1997 annual meeting Abstracts with Programs - Geological Society of America, v. 29, p. 371-372.

Clapp, E. M., Bierman, P. R., and Caffee, M. W., 1999, Sediment generation and export rates in the Nahal Yael drainage basin, determined from cosmogenic 10Be and 26Al, Negev Desert, southern Israel: Geological Society of America, 1999 annual meeting Abstracts with Programs - Geological Society of America, v. 31, p. 256.

Clapp, E. M., Bierman, P. R., Nichols, K. K., Pavich, M., and Caffee, M., 2001, Rates of sediment supply to arroyos from upland erosion determined using in situ produced cosmogenic [10]Be and [26]Al: Quaternary Research (New York), v. 55, p. 235-245.

Clapp, E. M., Bierman, P. R., Schick, A. P., Lekach, J., Enzel, Y., and Caffee, M., 2000, Sediment yield exceeds sediment production in arid region drainage basins: Geology, v. 28, p. 995-998.

Clark, G. M., and Ciolkosz, E. J., 1988, Periglacial geomorphology of the Appalachian Highlands and Interior Highlands south of the glacial border: a review: Geomorphology (Amsterdam), v. 1, p. 191-200.

Clayton, K., and Shamoon, N., 1998, A new approach to the relief of Great Britain: I. The machine-readable database: Geomorphology, v. 25, p. 31-42.

Cockburn, H. A. P., Seidl, M. A., and Summerfield, M. A., 1999, Quantifying denudation rates on inselbergs in the central Namib Desert using in situ-produced cosmogenic ^{10}Be and ^{26}Al: Geology, v. 27, p. 399-402.

Davis, W. M., 1899, The geographical cycle: Geographical Journal, v. 14, p. 481-504.

Delcourt, P. A., and Delcourt, H. R., 1984, Late Quaternary paleoclimates and biotic responses in eastern North America and the western North Atlantic Ocean: Paleogeography, Paleoclimatology, Paleoecology, v. 48, p. 263-284.

Desilets, D., and Zreda, M., 2000, Scaling production rates of terrestrial cosmogenic nuclides for altitude and geomagnetic effects: Geological Society of America Abstracts with Programs, v. 31, p. A-400.

Driese, S. G., Li, Z.-H., and Horn, S. P., 2005, Late Pleistocene and Holocene climate and geomorphic histories as interpreted from a 23,000 14C yr B.P. paleosol and floodplain soils, southeastern West Virginia, USA: Quaternary Research, v. 63, p. 136-149.

Dunai, T. J., 2000, Scaling factors for production rates of in situ produced cosmogenic nuclides: a critical reevaluation: Earth and Planetary Science Letters, v. 176, p. 157-169.

Durgin, P. B., 1977, Landslides and the weathering of granitic rocks: Reviews in Engineering Geology, v. 3, p. 127-131.

Duxbury, J., Bierman, P. R., Pavich, M. J., Larsen, J., and Finkel, R. C., 2006, Be Monitoring of Erosion Rates in the Appalachian Mountains, Shenandoah National Park, Virginia, Geological Society of America Abstracts with Programs, 2006 Philadelphia Annual Meeting, p. 278.

Eaton, L. S., Morgan, B. A., Kochel, C., R., and Howard, A. D., 2003a, Quaternary deposits and landscape evolution of the central Blue Ridge of Virginia: Geomorphology, v. 56, p. 139-154.

—, 2003b, Role of debris flows in long-term landscape denudation in the central Appalachians of Virginia: Geology, v. 31, p. 339-342.

Etienne, S., 2002, The role of biological weathering in periglacial areas: a study of weathering rinds in south Iceland: Geomorphology, v. 47, p. 75-86.

Evans, M. A., 1989, The structural geometry and evolution of foreland thrust systems, northern Virginia: Bulletin of the Geological Society of America, v. 101, p. 339-354.

Gaillardet, J., Dupré, B., Louvat, P., and Allègre, C. J., 1999, Global silicate weathering and CO2 consumption rates deduced from the chemistry of large rivers: Chemical Geology, v. 159, p. 3-30.

Galloway, R. W., 1961, Periglacial Phenomena in Scotland: Geografiska Annaler, v. 43, p. 348-353.

Gardner, T. W., 1989, Neotectonism along the Atlantic Passive Continental Margin: A Review: Geomorphology, v. 2, p. 71-97.

Gathright, T. M., 1976, Geology of the Shenandoah National Park, Virginia: Virginia Division of Mineral Resources Bulletin, v. 86, p. 93.

Gellis, A. C., Pavich, M. J., Bierman, P. R., Clapp, E. M., Ellevein, A., and Aby, S., 2004, Modern sediment yield compared to geologic rates of sediment production in a semi-arid basin, New Mexico: assessing the human impact: Earth Surface Processes and Landforms, v. 29.

Gilchrist, A. R., and Summerfield, M. A., 1990, Tectonic models of passive margin evolution and their implications for theories of long-term landscape development, *in* Kirkby, M. J., editor, Process Models and Theoretical Geomorphology: Wiley, Chichester, p. 55-84.

Gíslason, S. R., Arnorsson, S., and Armannsson, H., 1996, Chemical weathering of basalt in Southwest Iceland; effects of runoff, age of rocks and vegetative/glacial cover: Am J Sci, v. 296, p. 837-907.

Gosse, J. C., Evenson, E. B., Klein, J., Lawn, B., and Middleton, R., 1995, Precise cosmogenic 10Be measurements in western North America; support for a global Younger Dryas cooling event: Geology, v. 23, p. 877-880.

Gosse, J. C., and Phillips, F. M., 2001, Terrestrial in situ cosmogenic nuclides: theory and application: Quaternary Science Reviews, v. 20, p. 1475-1560.

Goudie, A., 1995, The Changing Earth: Rates of Geomorphological Processes: Oxford, Blackwell, 352 p.

Granger, D. E., Fabel, D., and Palmer, A. N., 2001, Pliocene-Pleistocene incision of the Green River, Kentucky, determined from radioactive decay of cosmogenic ^{26}Al and ^{10}Be in Mammoth Cave sediments: Geological Society of America Bulletin, v. 113, p. 825-836.

Granger, D. E., Kirchner, J. W., and Finkel, R., 1996, Spatially averaged long-term erosion rates measured from in situ-produced cosmogenic nuclides in alluvial sediments: Journal of Geology, v. 104, p. 249-257.

Granger, D. E., Kirchner, J. W., and Finkel, R. C., 1997, Quaternary downcutting rate of the New River, Virginia, measured from differential decay of cosmogenic ^{26}Al and ^{10}Be in cave-deposited alluvium: Geology, v. 25, p. 107-110.

Grender, G. C., 1973, Slope distribution and relationship to bedrock in Appalachian ridges near Roanoke, Virginia: The American Journal of Science, v. 273A, p. 391-395.

Hack, J. T., 1960, Interpretation of erosional topography in humid temperate regions: American Journal of Science, v. 258A, p. 80-97.

—, 1965, Geomorphology of the Shenandoah Valley, Virginia and West Virginia, and origin of the residual ore deposits: US Geological Survey Professional Paper, v. 484, p. 84.

—, 1975, Dynamic equilibrium and landscape evolution, *in* Melhorn, W. N., and Flemal, R. C., editors, Theories of landform development: Binghamton, N.Y., SUNY Binghamton, p. 87-102.

—, 1982, Physiographic divisions and differential uplift in the Piedmont and Blue Ridge: US Geological Survey Professional Paper, v. 1265, p. 49.

Hallam, A., 1985, A review of Mesozoic climate: Journal of the Geological Society, v. 142, p. 433-445.

Hancock, G., and Kirwan, M., 2007, Summit erosion rates deduced from 10Be: Implications for relief production in the central Appalachians: Geology, v. 35, p. 89-92.

Harris, A. G., Tuttle, E., and Tuttle, S. D., 1990, Geology of national parks: Dubuque, Iowa, Kendall/Hunt Pub. Co.

Harris, S. E., and Mix, A. C., 2002, Climate and tectonic influences on continental erosion of tropical South America, 0-13 Ma: Geology (Boulder), v. 30, p. 447-450.

Hebbeln, D., Lamy, F., Mohtadi, M., and Echtler, H., 2007, Tracing the impact of glacial-interglacial climate variability on erosion of the southern Andes: Geology, v. 35, p. 131-134.

Heimsath, A. M., Chappell, J., Dietrich, W. E., Nishiizumi, K., and Finkel, R. C., 2000, Soil production on a retreating escarpment in southeastern Australia: Geology, v. 28, p. 787-790.

Heimsath, A. M., Dietrich, W. E., Nishiizumi, K., and Finkel, R. C., 1999, Cosmogenic nuclides, topography, and the spatial variation of soil depth: Geomorphology, v. 27, p. 151-172.

—, 2001, Stochastic processes of soil production and transport; erosion rates, topographic variation and cosmogenic nuclides in the Oregon Coast Range: Earth Surface Processes and Landforms, v. 26, p. 531-552.

Hills, R. C., 1969, Comparative Weathering of Granite and Quartzite in a Periglacial Environment: Geografiska Annaler. Series A, Physical Geography, v. 51, p. 46-47.

King, P. B., 1950, Geology of the Elkton area: Virginia: US Geological Survey Professional Paper, v. 230, p. 82.

Kirchner, J. W., Finkel, R. C., Riebe, C. S., Granger, D. E., Clayton, J. L., King, J. G., and Megahan, W. F., 2001, Mountain erosion over 10 yr, 10 k.y., and 10 m.y. time scales: Geology, v. 29, p. 591-594.

Kirwan, M. L., 2002, Upland periglacial features and bare bedrock erosion rates inferred from 10Be, Dolly Sods, West Virginia, Southeastern Geological Society of America Annual Meeting.

Kirwan, M. L., Hancock, G. S., and Small, E. E., 2002, Erosion rates on central Appalachian upland bedrock surfaces deduced from in-situ 10Be: evidence for increasing relief?, EOS Trans. American Geophysical Union Fall Meeting Supplement, Abstract H222B-0896, 2002.

Kiver, E. P., Harris, D. V., and Harris, D. V., 1999, Geology of U.S. parklands: New York, John Wiley.

Kneller, M., and Peteet, D., 1999, Late-Glacial to Early Holocene Climate Changes from a Central Appalachian Pollen and Macrofossil Record: Quaternary Research, v. 51, p. 133-147.

Kochel, R. C., and Johnson, R. A., 1984, Geomorphology and sedimentology of humid-temperate alluvial fans, central Virginia: Sedimentology of gravels and conglomerates: Canadian Society of Petroleum Geologists Memoir, v. 10, p. 109–122.

Kohl, C. P., and Nishiizumi, K., 1992, Chemical isolation of quartz for measurement of *in-situ*-produced cosmogenic nuclides: Geochimica et Cosmochimica Acta, v. 56, p. 3583-3587.

Kurz, M., 1986, In situ production of terrestrial cosmogenic helium and some applications to geochronology: Geochimica et Cosmochimica Acta, v. 50, p. 2855-2862.

Kutzbach, J., Gallimore, R., Harrison, S., Behling, P., Selin, R., and Laarif, F., 1998, Climate and biome simulations for the past 21,000 years: Quaternary Science Reviews, v. 17, p. 473-506.

Lal, D., 1988, In situ-produced cosmogenic isotopes in terrestrial rocks: Annual Reviews of Earth and Planetary Science, v. 16, p. 355-388.

—, 1991, Cosmic ray labeling of erosion surfaces; in situ nuclide production rates and erosion models: Earth and Planetary Science Letters, v. 104, p. 424-439.

—, 1998, Cosmic ray produced isotopes in terrestrial systems: Journal of Earth System Science, v. 107, p. 241-249.

Lal, D., and Peters, B., 1967, Cosmic ray produced radioactivity on the earth, *in* Sitte, K., editor, Handbuch der Physik: New York, Springer-Verlag, p. 551-612.

Lasaga, A. C., Berner, R. A., and Garrels, R. M., 1985, An improved geochemical model of atmospheric CO2 fluctuations over the past 100 million years: IN: The carbon cycle and atmospheric CO2: Natural variations archean to present; Proceedings of the Chapman Conference on Natural Variations in Carbon Dioxide and the Carbon Cycle, Tarpon Springs, FL, January 9-13, 1984 (A86-39426 18-46). Washington, DC, American Geophysical Union, 1985, p. 397-411.

Leigh, D. S., and Webb, P. A., 2006, Holocene erosion, sedimentation, and stratigraphy at Raven Fork, Southern Blue Ridge Mountains, USA: Geomorphology, v. 78, p. 161-177.

Lifton, N. A., 2000, A robust scaling model for in situ cosmogenic nuclide production rates: Geological Society of America Abstracts with Programs, v. 31.

Litwin, R. J., Morgan, B., Eaton, S., Wieczorek, G., and Smoot, J. P., 2001, Proxy climate evidence from Late Pleistocene Deposits in the Blue Ridge of Virginia: US Geological Survey Open File Report, p. 01-406.

Matmon, A., Bierman, P. R., Larsen, J., Southworth, S., Pavich, M., and Caffee, M., 2003a, Temporally and spatially uniform rates of erosion in the southern Appalachian Great Smoky Mountains: Geology, v. 31, p. 155–158.

Matmon, A. S., Bierman, P., Larsen, J., Southworth, S., Pavich, M., Finkel, R., and Caffee, M., 2003b, Erosion of an ancient mountain range, the Great Smoky Mountains, North Carolina and Tennessee: American Journal of Science, v. 303, p. 817-855.

McDougall, I., and Harrison, T. M., 1988, Geochronology and thermochronology by the 40Ar/39Ar method: Oxford monographs on geology and geophysics; no. 9: New York, Oxford University Press.

Merschat, C. E., 1997, Geology of Yancy County: Raleigh, North Carolina Geological Survey, Division of Land Resources, p. 22.

Miller, D. S., and Duddy, I. R., 1989, Early Cretaceous uplift and erosion of the northern Appalachian Basin, New York, based on apatite fission track analysis: Earth and Planetary Science Letters, v. 93, p. 35-49.

Millot, R., Gaillardet, J., Dupré, B., and Allègre, C. J., 2002, The global control of silicate weathering rates and the coupling with physical erosion: new insights from rivers of the Canadian Shield: Earth and Planetary Science Letters, v. 196, p. 83-98.

Mills, H. H., 2003, Inferring erosional resistance of bedrock units in the east Tennessee mountains from digital elevation data: Geomorphology, v. 55, p. 263-281.

Morgan, B. A., Eaton, L. S., and Wieczorek, G. F., 2004, Pleistocene and Holocene colluvial fans and terraces in Shenandoah National Park, Virginia, Open-File Report 03-410, U.S. Geological Survey.

Morgan, B. A., Wieczorek, G. F., and Campbell, R. H., 1999, Map of rainfall, debris flows, and flood effects of the June 27, 1995, storm in Madison County, Virginia: United States Geological Survey Geologic Investigation Series Map I-2623A, 1:24,000.

Moulton, K. L., and Berner, R. A., 1998, Quantification of the effect of plants on weathering: Studies in Iceland: Geology, v. 26, p. 895-898.

Naeser, C. W., Naeser, N. D., Kunk, M. J., Morgan Iii, B. A., Schultz, A. P., Southworth, C. S., and Weems, R. E., 2001, Paleozoic through Cenozoic uplift, erosion, stream capture, and deposition history in the Valley and Ridge, Blue Ridge, Piedmont, and Coastal Plain provinces of Tennessee, North Carolina, Virginia, Maryland, and District of Columbia, GSA Annual Meeting, November 5-8, 2001.

Naeser, C. W., Naeser, N. D., and Southworth, C. S., 2005, Tracking Across the southern Appalachians *in* Blue Ridge Geology Geotraverse East of the Great Smoky Mountains National Park, Western North Carolina: Carolina Geological Society.

—, 2006a, Tracking Across the Southern Appalachians: Eastern Tennessee and Western Carolinas Geological Society of America Abstracts with Programs, p. 67.

Naeser, N. D., Naeser, C. W., Newell, W. L., Southworth, S., Weems, R. E., and Edwards, L. E., 2006b, Provenance Studies In The Atlantic Coastal Plain: What Fission-Track Ages Of Detrital Zircons Can Tell Us About The Erosion History Of The Appalachians: 2006 Philadelphia Annual Meeting.

Naeser, N. D., Naeser, C. W., Southworth, C. S., Morgan, B. A., and Schultz, A. P., 2004, Paleozoic to recent tectonic and denudation history of rocks in the Blue Ridge province, central and southern Appalachians - evidence from fission-track thermochronology Geological Society of America Abstracts with Programs, p. 114.

Nishiizumi, K., Imamura, M., Caffee, M. W., Southon, J. R., Finkel, R. C., and McAninch, J., 2007, Absolute calibration of 10Be AMS standards: Nuclear

Instruments and Methods in Physics Research Section B: Beam Interactions with Materials and Atoms, v. 258, p. 403-413.

Nishiizumi, K., Lal, D., Klein, J., Middleton, R., and Arnold, J. R., 1986, Production of [10]Be and [26]Al by cosmic rays in terrestrial quartz in situ and implications for erosion rates: Nature, v. 319, p. 134-136.

Nishiizumi, K., Winterer, E. L., Kohl, C. P., Klein, J., Middleton, R., Lal, D., and Arnold, J. R., 1989, Cosmic ray production rates of [10]Be and [26]Al in quartz from glacially polished rocks: Journal of Geophysical Research, B, Solid Earth and Planets, v. 94, p. 17,907-17,915.

Ollier, C. D., 1971, Causes of spheroidal weathering: Earth-Sci. Rev, v. 7, p. 127–141.

Parrish, J. T., and Curtis, R. L., 1982a, Atmospheric circulation, upwelling, and organic-rich rocks in the Mesozoic and Cenozoic eras: Palaeogeography, Palaeoclimatology, Palaeoecology, v. 40, p. 3.

Parrish, J. T., Ziegler, A. M., and Scotese, C. R., 1982b, Rainfall patterns and the distribution of coals and evaporites in the Mesozoic and Cenozoic: Palaeogeography, Palaeoclimatology, Palaeoecology, v. 40, p. 67-101.

Pavich, M., 1985, Appalachian piedmont morphogenesis: weathering, erosion, and Cenozoic uplift, *in* Morisaura, M., and Hack, J., editors, "Tectonic Geomorphology", Proceedings of the 15th Annual Geomorphology Symposium Series: Binghampton, p. 299-319.

Pavich, M. J., 1990, Characteristics, origin, and residence time of saprolite and soil of the Piedmont upland, Virginia, U.S.A., and model testing using cosmogenic 10Be, Geochemistry of the Earth's Surface and of Mineral Formation, 2nd International Symposium: Aix en Provence, France, p. 2.

Pavlides, L., Boucot, A. J., and Skidmore, W. B., 1968, Stratigraphic evidence for the Taconic Orogeny in the northern Appalachians, *in* Zen, E., White, W. S., Hadley, J. B., and Thompson, J. B. Jr., editor, Studies of Appalachian geology: Northern and Maritime New York, Interscience Publishers (John Wiley & Sons) p. 61-83.

Pazzaglia, F. J., 1993, Stratigraphy, petrography, and correlation of late Cenozoic middle Atlantic Coastal Plain deposits: Implications for late-stage passive-margin geologic evolution: Geological Society of America Bulletin, v. 105, p. 1617-1634.

—, 2006, Excursions in Geology and History: Field Trips in the Middle Atlantic States: Boulder, The Geological Society of America, p. 247.

Pazzaglia, F. J., and Brandon, M. T., 1996, Macrogeomorphic evolution of the post-Triassic Appalachian mountains determined by deconvolution of the offshore basin sedimentary record: Basin Research, v. 8.

Pazzaglia, F. J., and Gardner, T. W., 1994, Late Cenozoic flexural deformation of the middle U. S. Atlantic passive margin: Journal of Geophysical Research, B, Solid Earth and Planets, v. 99, p. 12,143-12,157.

—, 2000, Late Cenozoic large-scale landscape evolution of the US Atlantic passive margin: Geomorphology and Global Tectonics: New York, John Wiley, p. 283–302.

Phillips, W. M., Hall, A. M., Mottram, R., Fifield, L. K., and Sugden, D. E., 2006, Cosmogenic 10Be and 26Al exposure ages of tors and erratics, Cairngorm

Mountains, Scotland: Timescales for the development of a classic landscape of selective linear glacial erosion: Geomorphology, v. 73, p. 222-245.

Poag, C. W., and Sevon, W. D., 1989, A record of Appalachian denudation in postrift Mesozoic and Cenozoic sedimentary deposits of the U.S. middle Atlantic continental margin: Geomorphology, v. 2, p. 119-157.

Raymo, M. E., and Ruddiman, W. F., 1988, Influence of late Cenozoic mountain building on ocean geochemical cycles: Geology, v. 16, p. 649-653.

Reed Jr, J. C., 1955, Catoctin Formation near Luray: Virginia: Geological Society of America Bulletin, v. 66, p. 871-896.

Reiners, P. W., 2002, (U-Th)/He chronometry experiences a renaissance: Eos, Transactions, American Geophysical Union, v. 83, p. 21-27.

Reiners, P. W., and Brandon, M. T., 2006, Using Thermochronology to Understand Orogenic Erosion: Annual Review of Earth and Planetary Sciences, v. 34, p. 419-66.

Reiners, P. W., Ehlers, T. A., Mitchell, S. G., and Montgomery, D. R., 2003, Coupled spatial variations in precipitation and long-term erosion rates across the Washington Cascades: Nature, v. 426, p. 645-647.

Reusser, L. J., Bierman, P. R., Pavich, M. J., Zen, E.-a., Larsen, J., and Finkel, R., 2004, Rapid Late Pleistocene Incision of Atlantic Passive-Margin River Gorges: Science, v. 305, p. 499-502.

Reuter, J., Bierman, P. R., Pavich, M., Gellis, A., Larsen, J., and Finkel, R., 2003, Long-term sediment generation rates derived from 10Be in river sediment of the Susquehanna River Basin, in "channeling through time: Landscape evolution, land use change, and stream restoration in the lower Susquehanna Basin", *in* Merritts, D., Walter, R., and de Wet, A., editors, Southeastern Friends of the Pleistocene Fall 2003 Guidebook, p. 48-55.

Reuter, J., Bierman, P. R., Pavich, M., Larsen, J., and Finkel, R., 2004, Linking 10Be estimates of erosion rates with landscape variables: compilation and consideration of multiple data sets from around the world, International Geological Conference: Florence.

Reuter, J. M., 2005, Erosion rates and patterns inferred from cosmogenic 10Be in the Susquehanna River Basin: Masters Thesis, University of Vermont, Burlington, VT, p. 172.

Riebe, C. S., Kirchner, J. W., and Finkel, R. C., 2003, Long-term rates of chemical weathering and physical erosion from cosmogenic nuclides and geochemical mass balance: Geochimica et Cosmochimica Acta, v. 67, p. 4411-4427.

—, 2004, Erosional and climatic effects on long-term chemical weathering rates in granitic landscapes spanning diverse climate regimes: Earth and Planetary Science Letters, v. 224, p. 547-562.

Riebe, C. S., Kirchner, J. W., Granger, D. E., and Finkel, R. C., 2000, Erosional equilibrium and disequilibrium in the Sierra Nevada, inferred from cosmogenic ^{26}Al and ^{10}Be in alluvial sediment: Geology, v. 28, p. 803-806.

—, 2001a, Minimal climatic control on erosion rates in the Sierra Nevada, California: Geology, v. 29, p. 447-450.

—, 2001b, Strong tectonic and weak climatic control of long-term chemical weathering rates: Geology, v. 29, p. 511–514.

Rodgers, J., 1970, The Tectonics of the Appalachians: New York, Wiley-Interscience, 271 p.

Ruddiman, W. F., and McIntyre, A., 1982, Severity and speed of Northern Hemisphere glaciation pulses; the limiting case?: Bulletin of the Geological Society of America, v. 93, p. 1273-1279.

Shepard, M. K., Arvidson, R. E., Caffee, M., Finkel, R., and Harris, L., 1995, Cosmogenic exposure ages of basalt flows; Lunar Crater volcanic field, Nevada: Geology (Boulder), v. 23, p. 21-24.

Slingerland, R., and Furlong, K. P., 1989, Geodynamic and Geomorphic Evolution of the Permo-Triassic Appalachian Mountains: Geomorphology, v. 2, p. 23-27.

Small, E. E., Anderson, R. S., Repka, J. L., and Finkel, R., 1997, Erosion rates of alpine bedrock summit surfaces deduced from in situ 10Be and 26Al: Earth and Planetary Science Letters, v. 150, p. 413-425.

Smoot, J. P., 2004, Sedimentary Fabrics of Stratified Slope Deposits at a Site near Hoover's Camp, Shenandoah National Park, Virginia: US Geological Survey Open-File Report, v. 2004, p. 1059.

Southworth, S., 2008, Geologic map of the Shenandoah National Park area, Virginia: U.S. Geological Survey, Open File Report 2008-XXXX, scale 1:100,000.

Southworth, S., Drake Jr, A. A., Brezinski, D. K., Wintsch, R. P., Kunk, M. J., Aleinikoff, J. N., Naeser, C. W., and Naeser, N. D., 2006, Central Appalachian Piedmont and Blue Ridge tectonic transect, Potomac River corridor: Excursions in Geology and History: Field Trips in the Middle Atlantic States.

Spotila, J. A., Bank, G. C., Reiners, P. W., Naeser, C. W., Naeser, N. D., and Henika, B. S., 2004, Origin of the Blue Ridge escarpment along the passive margin of Eastern North America: Basin Research, v. 16, p. 41-63.

Stallard, R. F., 1988, Weathering and Erosion in the Humid Tropics: Physical and Chemical Weathering in Geochemical Cycles.

Stanford, S. D., Ashley, G. M., Russell, E. W. B., and Brenner, G. J., 2002, Rates and patterns of late Cenozoic denudation in the northernmost Atlantic Coastal Plain and Piedmont: Bulletin of the Geological Society of America, v. 114, p. 1422-1437.

Stefánsson, A., and Gíslason, S. R., 2001, Chemical weathering of basalts, southwest Iceland: Effect of rock crystallinity and secondary minerals on chemical fluxes to the ocean: American Journal of Science, v. 301, p. 513.

Stewart, B. W., Capo, R. C., and Chadwick, O. A., 2001, Effects of rainfall on weathering rate, base cation provenance, and Sr isotope composition of Hawaiian soils: Geochimica et Cosmochimica Acta, v. 65, p. 1087-1099.

Stose, G. W., Miser, H. D., Katz, F. J., and Hewett, D. F., 1919, Manganese deposits of the west foot of the Blue Ridge, Virginia: Virginia Geological Survey Bulletin v. 17, p. 166.

Sullivan, C. L., Bierman, P. R., Reusser, L. J., Larsen, J., Pavich, M. J., and Finkel, R. C., accepted, Erosion and landscape evolution of the Blue Ridge escarpment, southern Appalachian Mountains: Earth Surface Processes and Landforms.

Tollo, R. P., Aleinikoff, J. N., Borduas, E. A., Dickin, A. P., McNutt, R. H., and Fanning, C. M., 2006, Grenvillian magmatism in the northern Virginia Blue Ridge: Petrologic implications of episodic granitic magma production and the significance of postorogenic A-type charnockite: Precambrian Research, v. 151, p. 224-264.

Tollo, R. P., Bailey, C. M., Borduas, E. A., and Aleinikoff, J. N., 2004, 2. Mesoproterozoic Geology of the Blue Ridge Province in North-Central Virginia: Petrologic and Structural Perspectives on Grenvillian Orogenesis and Paleozoic Tectonic Processes.

Tourtelot, H. A., 1883, Continental aluminous weathering sequences and their climatic implications in the United States, *in* Cronin, T. M., Cannon, W. F., and Poore, R. Z., editors, Paleoclimate and Mineral Deposits, U.S. Geol. Survey Circular 822: 1-5.

Trimble, S. W., 1977, The fallacy of stream equilibrium in contemporary denudation studies: American Journal of Science, v. 277, p. 876-887.

Turner, B. F., Stallard, R. F., and Brantley, S. L., 2003, Investigation of in situ weathering of quartz diorite bedrock in the Rio Icacos basin, Luquillo Experimental Forest, Puerto Rico: Chemical Geology, v. 202, p. 313-341.

von Blanckenburg, F., 2005, The control mechanisms of erosion and weathering at basin scale from cosmogenic nuclides in river sediment: Earth and Planetary Science Letters, v. 237, p. 462-479.

Ward, D. J., Spotila, J. A., Hancock, G. S., and Galbraith, J. M., 2005, New constraints on the late Cenozoic incision history of the New River, Virginia: Geomorphology, v. 72, p. 54-72.

Washburn, A. L., 1973, Periglacial processes and environments, Edward Arnold, London.

Washburn, A. L., and Lincoln, A., 1980, Geocryology: a survey of periglacial processes and environments, New York: Wiley.

West, A. J., Galy, A., and Bickle, M., 2005, Tectonic and climatic controls on silicate weathering: Earth and Planetary Science Letters, v. 235, p. 211-228.

White, A. F., and Blum, A. E., 1995, Effects of climate on chemical weathering in watersheds: Geochimica et Cosmochimica Acta, v. 59, p. 1729-1747.

White, A. F., Bullen, T. D., Schulz, M. S., Blum, A. E., Huntington, T. G., and Peters, N. E., 2001, Differential rates of feldspar weathering in granitic regoliths: Geochimica et Cosmochimica Acta, v. 65, p. 847-869.

White, W. B., 1984, Rate processes: chemical kinetics and karst landform development: Groundwater as a Geomorphic Agent, p. 227-248.

—, 2000, Dissolution of limestone from field observations, *in* Klimchouk, A. B., Ford, D. C., Palmer, A. N., and Dreybrodt, W., editors, Speleogenesis: Evolution of Karst Aquifers: Huntsville, Alabama, National Speleological Society, p. 527.

White, W. B., and White, E. L., 1991, Karst erosion surfaces in the Appalachian highlands: Appalachian Karst: Proceedings of the Appalachian Karst Symposium. 1991.

Whittecar, G. R., 1992, Alluvial Fans and Boulder streams of the Blue Ridge Mountains, west-central Virginia, Southeastern Friends of the Pleistocene, 1992 Field Trip, p. 128.

Zimmerman, H. B., Shackleton, N. J., Backman, J., Kent, D. V., Baldauf, J. G., Kaltenback, A. J., and Morton, A. C., 1984, History of Plio-Pleistocene climate in the northeastern Atlantic, Deep Sea Drilling Project Hole 552A: Roberts, DG, Schnitker, D., et al., Init. Repts. DSDP, v. 81, p. 861-875.